International Telecommunication Union

ITU-R

Radiocommunication Sector of ITU

Report ITU-R BT.2142-2

(07/2015)

The effect of the scattering of digital television signals from wind turbines

BT Series

Broadcasting service (television)

Foreword

The role of the Radiocommunication Sector is to ensure the rational, equitable, efficient and economical use of the radio-frequency spectrum by all radiocommunication services, including satellite services, and carry out studies without limit of frequency range on the basis of which Recommendations are adopted.

The regulatory and policy functions of the Radiocommunication Sector are performed by World and Regional Radiocommunication Conferences and Radiocommunication Assemblies supported by Study Groups.

Policy on Intellectual Property Right (IPR)

ITU-R policy on IPR is described in the Common Patent Policy for ITU-T/ITU-R/ISO/IEC referenced in Annex 1 of Resolution ITU-R 1. Forms to be used for the submission of patent statements and licensing declarations by patent holders are available from http://www.itu.int/ITU-R/go/patents/en where the Guidelines for Implementation of the Common Patent Policy for ITU-T/ITU-R/ISO/IEC and the ITU-R patent information database can also be found.

Series of ITU-R Reports

(Also available online at http://www.itu.int/publ/R-REP/en)

Series	Title
BO	Satellite delivery
BR	Recording for production, archival and play-out; film for television
BS	Broadcasting service (sound)
BT	**Broadcasting service (television)**
F	Fixed service
M	Mobile, radiodetermination, amateur and related satellite services
P	Radiowave propagation
RA	Radio astronomy
RS	Remote sensing systems
S	Fixed-satellite service
SA	Space applications and meteorology
SF	Frequency sharing and coordination between fixed-satellite and fixed service systems
SM	Spectrum management

***Note**: This ITU-R Report was approved in English by the Study Group under the procedure detailed in Resolution ITU-R 1.*

Electronic Publication
Geneva, 2015

REPORT ITU-R BT.2142-2

The effect of the scattering of digital television signals from wind turbines

(2009-2010-2015)

TABLE OF CONTENTS

1 Introduction

This Report is on the topic of performance of television reception in the presence of reflected signals, specifically those from wind turbines as identified in Recommendation ITU-R BT.1893 – Assessment of impairment caused to digital television reception by one or more wind turbines.

Results from studies in Australia, in Spain and Italy are presented in three Parts A, B and C respectively. The first Part relating to the effect of the scattering of digital television signals from a wind turbine. The second Part relating to effect of the scattering of digital television signals from multiple wind turbines and the development of a propagation channel model due to the presence of a wind farm. The third Part relating to results of actual application of the analysis of scattering from windfarms.

2 Background

Wind turbine farms are proving to be a popular energy source. Due to this growth many administrations are now experiencing interest from developers in constructing wind farms. This has raised concerns about the potential impact of wind farms on the reception of broadcasting services.

In considering the planning for digital television services within the VHF and UHF broadcasting bands traditionally used for analogue television services, some administrations have sought to reference Recommendation ITU-R BT.805 – Assessment of impairment caused to television reception by a wind turbine. Recommendation ITU-R BT.805 – was approved in 1992 in response to Question ITU-R 6/11. Recommendation ITU-R BT.1893-0 – Assessment of impairment caused to digital television reception by a wind turbine –was developed to address the emergence of digital television and it retains the reference to the Question ITU-R 6/11. Question ITU-R 69/6 –

Conditions for a satisfactory television service in the presence of reflected signals – deals with reflections affecting analogue television systems.

In 2004 a modification to Question ITU-R 69/6 was approved that extended studies to include digital television. The purpose was to encourage eventual modifications to Recommendation ITU-R BT.805 as a result of further study as to whether impairment is caused by wind turbines to digital television, as well as the development of further Recommendations, should they be required, relating to reflections from other objects.

In 2006 a modification of Recommendation ITU-R BT.805 was approved. The study used theoretical modelling to identify that Recommendation ITU-R BT.805 was not adequate for predicting interference from wind farms for analogue and digital TV signals.

In 2007 a further study indicated that the methods to assist in quality assessment of the coverage and service area for digital television broadcasting in System B in Recommendation ITU-R BT.1735 were not satisfactory for the type of dynamic signal variations from rotating wind turbine blades.

From these studies, it was agreed that Recommendation ITU-R BT.805 does not provide adequate advice for predicting interference from wind farms for analogue and digital TV signals. Subsequently Working Party 6A approved Recommendation ITU-R BT.1893 Assessment of impairment caused to digital television reception by a wind turbine.

Working Party 6A also observed that further study was required to review the relationship between the mean MER, slow MER variations, short deep MER notches and the receiver performance.

In 2009 and 2010, the preliminary results obtained from a measurement campaign carried out in the vicinity of a wind farm in Spain were presented in the ITU.

Further theoretical and empirical studies in Spain have obtained significant results in response to Question ITU-R 69-1/6 that may advance Recommendation ITU-R BT.1893 further. More precisely:

– A channel model to characterize signal propagation in the presence of a wind farm has been developed. This channel model includes a novel scattering model and the effect of the variability of scattered signals due to the movement of the wind turbines in operation.

– A simplified method has been developed in order to obtain the potential increment in the *C/N* threshold ratio of the DVB-T system as a function of the propagation channel characteristics.

This Report is organized in three parts.

Part A includes the contents related to Recommendations ITU-R BT.805 and BT.1893, which describe the scattering effect of one wind turbine due to its metallic blades.

Part B includes the new contents contributed to Recommendation ITU-R BT.1893-1, which describe a complete channel model to characterize signal propagation in the presence of a whole wind farm, with contributions from a metallic pylon and fibreglass blades of each wind turbine.

Part C includes a complete set of results of the application of the methodologies of analysis proposed in an actual scenario of potential affection.

The Attachments to Part A of this Report contain the results of studies in Australia up to 2010:

Attachment 1 – Scattering model calculations.

Attachment 2 – The effect of the scattering of digital television signals from wind turbines.

The Attachments to Part B of this Report contain the results of studies in Spain from 2009 to 2014:

Attachment 1 – Field trials

Attachment 2 – Empirical analysis of the scattering signals from wind turbines

Attachment 3 – Summary of measurements and analysis of the results

Attachment 4 – Wind turbines impact to terrestrial DTV services in the UHF band

Attachment 5 – Example of use

The Attachment to Part C contains the results of a study in Italy carried out in 2014:

Attachment 1 – Results of actual use case

PART A

Results of studies in Australia

TABLE OF CONTENTS

Attachment 1
to
Part A

Scattering model calculations

1 Introduction

This Attachment analyses the scattering model used in Recommendation ITU-R BT.805, describes its limitations and weaknesses, and suggests improvements. The analysis is extended to include the scattering from rotating triangular shaped blades and the wind turbine pylon.

2 Analysis

2.1 Overview

The basis for the scattering model in Recommendation ITU-R BT.805 is somewhat unclear, as it apparently calculates backscattering from the turbine blades, although it is referred to as forward scattering. The model in the Recommendation assumes perfect conductors for the blades, although they are typically fibreglass or other composite materials, and a scattering pattern based on vertical blade orientation only.

The following analysis assumes that the dimensions of the scattering object are much greater than a wavelength, which then allows a semi-rigorous analysis based on the physical optics approximation. For the low frequency Band III channels, the wavelength is of the order of 2 m. The maximum blade width is about 3 m for typical turbines, but the blades taper to a point, so the assumption that the dimensions are greater than a wavelength is clearly invalid for such low frequencies.

2.2 Analysis of Recommendation ITU-R BT.805 mathematics

Recommendation ITU-R BT.805 is based on the scattering from a rectangular, metallic wind turbine blade in a vertical orientation, as shown in Fig. A-1.

FIGURE A-1

Geometry of wind turbine blade (rectangular, vertical) and incident and scattered signals

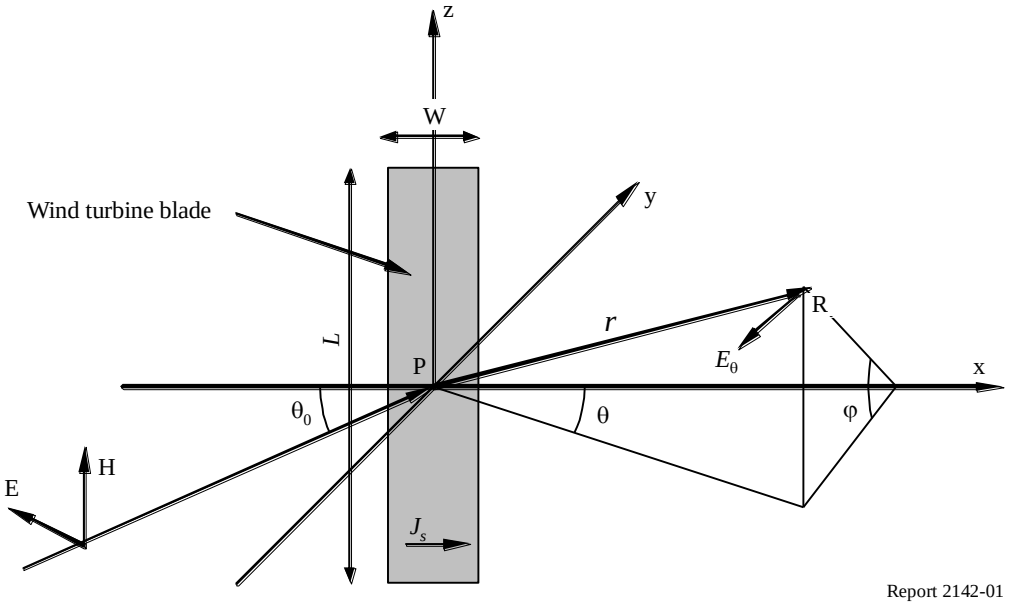

It is assumed the incident signal is horizontally polarized and arrives horizontally at the turbine, as the transmitter is assumed to be a long distance from the wind turbine. The signal scattered from the blade is received at point R with signal strength E_θ at distance r from the blade. Because the blade is assumed to be metallic (infinite conductivity), the surface current density J_s is given by:

$$J_s(x, z) = 2\hat{n} \times H = \frac{2E_0}{\eta} \, \mathrm{e}^{-jk \cos\theta_0 x} \, \hat{x} \tag{A-1}$$

where θ_0 is the incident angle relative to the plane of the blade and E_0 is the incident electric field strength (assumed to be a plane wave). The surface currents re-radiate, resulting in the far field E_θ given by the surface integral:

$$E_\theta = jk\eta \sin\theta \left(\frac{\mathrm{e}^{-jkr}}{4\pi r} \right) \int_{-\frac{W}{2}}^{\frac{W}{2}} \int_{-\frac{L}{2}}^{\frac{L}{2}} J_s(x', z') \, \mathrm{e}^{jk(nx' + mz')} \, \mathrm{d}x' \, \mathrm{d}z' \tag{A-2}$$

where $k = 2\pi/\lambda$ and $n = \cos\theta$, $m = \sin\theta \sin\varphi$. See Fig. A-1 for the definition of the angles.

Upon substituting equation (A-1) into equation (A-2) the resulting field at the receiver is given by:

$$\begin{aligned} E_\theta &= \frac{jE_0 \sin\theta}{\lambda} \left(\frac{\mathrm{e}^{-jkr}}{r} \right) \int_{-\frac{W}{2}}^{\frac{W}{2}} \mathrm{e}^{jk(n-n_0)x'} \mathrm{d}x' \int_{-\frac{L}{2}}^{\frac{L}{2}} \mathrm{e}^{jkmz''} \, \mathrm{d}z' \\ &= \frac{j \, AE_0 \sin\theta}{\lambda} \left(\frac{\mathrm{e}^{-jkr}}{r} \right) \mathrm{sinc}\left((n - n_0) \frac{W}{\lambda} \right) \mathrm{sinc}\left(m \frac{L}{\lambda} \right) \end{aligned} \tag{A-3}$$

where the blade area $A = WL$, $n_0 = \cos\theta_0$ and $\text{sinc}(x) = \sin(\pi x)/\pi x$. Therefore the scattering coefficient, ρ, is given by:

$$\rho = \frac{|E_\theta|}{E_0} = \frac{A}{\lambda r} g(\theta, \varphi)$$
$$g(\theta, \varphi) = \text{sinc}\left(\frac{W}{\lambda}(\cos\theta - \cos\theta_0)\right) \text{sinc}\left(\frac{L}{\lambda}\sin\theta\sin\varphi\right)\sin\theta \quad \text{(A-4)}$$

In this application, the scattered signal of interest will be close to the horizon, so $\varphi \approx 0$, and the scattering function can be approximated by $g(\theta, \varphi) \approx g(\theta) = \text{sinc}\left(\frac{W}{\lambda}(\cos\theta - \cos\theta_0)\right)\sin\theta$.

For specular reflections $\theta_0 = \theta$, and the scattering function reduces to $g(\theta) = \sin\theta = \sin\theta_0$.

The maximum of the scattering coefficient is given by $\rho_{max} = \frac{A}{\lambda r}$. Recommendation ITU-R BT.805 defines this maximum coefficient at a range of 1 000 m (dB), so that:

$$\Gamma = 20\ \log(\rho_{max}) = 20\ \log(A/\lambda) - 60 \quad \text{dB} \quad \text{(A-5)}$$

However, the scattering spatial function $g(\theta)$ is different from the Recommendation by the incorporation of the additional $\sin\theta$ term, and the additional term associated with the incident angle, which is assumed to be 90° in Recommendation ITU-R BT.805. Note that the Recommendation uses a different definition of angles, namely relative to the normal to the blade, so that the associated Recommendation ITU-R BT.805 expression is:

$$g(\alpha) = \text{sinc}\left(\frac{W}{\lambda}(\sin\alpha - \sin\alpha_0)\right)\cos\alpha \qquad \alpha \approx 0 \quad \text{(A-6)}$$

Therefore Recommendation ITU-R BT.805 applies only when the incident signal is near normal to the blade, whereas equation (A-4) is valid for all geometries of incident and scattering angles.

2.3 Numerical example

The application of Recommendation ITU-R BT.805 can be illustrated with a numerical example. A wind turbine scatters to a point 1 km from the turbine, as shown in Fig. A-2. The wind turbine has three blades, 33 m in length, triangular in shape, and having a base width of 3.3 m. As the model assumes a rectangular blade, it will be assumed that the average width is 1.65 m, so the total area is about 160 m^2. Additional (static) scattering from the tower is ignored in this example.

The wind direction is aligned with the vector between the transmitter and the wind turbine, so the incident signal on the turbine blade is close to normal (the worst case). The frequency is 600 MHz. As the transmitter is assumed to be remote, the direction of the signal at the receiving site and at the wind turbine is assumed to be the same.

FIGURE A-2

Geometry for the example. The transmitter is remote, so the drawing is not to scale

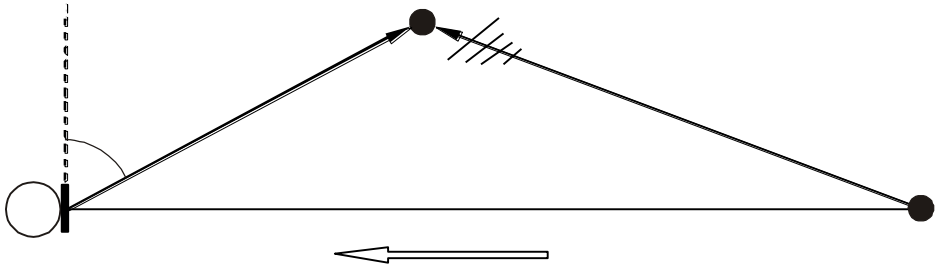

Report 2142-02

The reflection coefficient based on the Recommendation ITU-R BT.805 model is thus:

$$\Gamma = 20 \log(\rho_{max}) = 20 \log\left(\frac{A}{\lambda r}\right) = -10 \quad \text{dB} \tag{A-7}$$

With an omnidirectional antenna, the signal-to-interference ratio (SIR) will therefore be 10 dB. For DTV, the SIR can be equated approximately to the receiver *C*/*N* due to the randomization processing in the receiver, and so the *C*/*N* is well below the typical 20 dB required for DTV planning. It should be noted that this example assumes flat metal blades, which is not typical. Additionally, a directional antenna were pointed at the DTV transmitter and away from the reflected signal, the directivity of the antenna would be added to the 10 dB; for a typical television antenna with directivity of 12 to 20 dB, this would provide sufficient margin.

It is important to note that the interference signal is due to backscattering, rather than forward scattering as stated in Recommendation ITU-R BT.805. The practical significance is that the directivity of a correctly oriented antenna reduces the observed effects of the scattering from the wind turbine. This is considered in more detail in § 2.4.5.

2.4 Extension of the analysis

This section suggests the issues that should be addressed in modifying Recommendation ITU-R BT.805 model to improve the accuracy of the predictions of the scattered signals. These corrections would apply equally to both analogue and digital television signals.

The issues in the following subsections are components that affect the prediction of the scattered signal. The individual examples are not necessarily related, and the combination of these individual effects is not discussed here. The examples are intended only to illustrate the particular aspects, and are not intended as a comprehensive statement of potential interference from wind farms in general.

2.4.1 Non-metallic turbine blades

Recommendation ITU-R BT.805 assumes metallic (perfectly conducting) wind turbine blades, but actual blades are typically made of fibreglass. As a consequence the Recommendation ITU-R BT.805 model over predicts the level of the scattered signal.

The rigorous calculation of scattering from a non-conducting material can be simplified by an extension of the physical optics principle used in calculating the scattering from a metallic surface. As the surface becomes large relative to the wavelength, the physical optics solution approaches the simple ray optics solution, with the angle of incidence equal to the angle of reflection. For an infinite non-conducting surface with a relative dielectric constant ε_r, the reflection coefficient can be calculated as a function of the angle of incidence. Therefore the scattering from a finite dielectric surface can be obtained by multiplying the solution from a metallic surface by the reflection coefficient calculated for an infinite surface.

The reflection coefficient from a non-conductor depends on the polarization of the signal. For these calculations it is assumed that the polarization is horizontal. The reflection coefficient for horizontal polarization is given by:

$$\rho_E = \frac{\varepsilon_r \cos\theta - \sqrt{\varepsilon_r - \sin^2\theta}}{\varepsilon_r \cos\theta + \sqrt{\varepsilon_r - \sin^2\theta}} \tag{A-8}$$

where θ is the incident angle relative to the normal to the surface, and ε_r is the relative dielectric constant and is greater than 1. For fibreglass typically used in wind turbine blades the relative dielectric constant is about 4. The main practical interest when the incident angle is near the normal (θ is small), so that equation (A-8) becomes:

$$\rho_E \approx \frac{\varepsilon_r - \sqrt{\varepsilon_r}}{\varepsilon_r + \sqrt{\varepsilon_r}} \tag{A-9}$$

For $\varepsilon_r = 4$, this gives a reflection coefficient of 1/3, or –10 dB. The reflection coefficient is not very sensitive to the exact value of the dielectric; for a value of $\varepsilon_r = 9$, which results in $\rho_E = 1/2$ or –6 dB. Thus the inclusion of this electric field reflection coefficient is important in assessing the overall scattered signal from wind turbines. In particular, based on the above analysis, Recommendation ITU-R BT.805 overestimates the scattered signal by about 6 to 10 dB.

2.4.2 Triangular turbine blades

Recommendation ITU-R BT.805 assumes that the wind turbine blades are rectangular, while actual turbine blades are close to triangular. Therefore the calculations need to use a triangular shape for the surface integral in equation (A-3). The only modification is that the limits in the x-coordinate are replaced by:

$$w(z) = \frac{W}{2}\left(1 - \frac{z}{L}\right) \tag{A-10}$$

so that surface integral becomes:

$$E_\theta = \frac{jE_0 \sin\theta}{\lambda}\left(\frac{e^{-jkr}}{r}\right)\int_{-w(z)}^{w(z)}\int_{-\frac{L}{2}}^{\frac{L}{2}} e^{jk(n-n_0)x'} e^{jkmz''}\, dx'dz' \tag{A-11}$$

Again the assumption is made that the signal is measured near the horizon, so that $m = 0$ in equation (A-11). With this simplification the integral can be evaluated to give:

$$E_\theta = \frac{j\,\Delta E_0 \sin\theta}{\lambda}\left(\frac{e^{-jkr}}{r}\right)\mathrm{sinc}^2\left((n-n_0)\frac{W/2}{\lambda}\right) \tag{A-12}$$

where $\Delta = LW/2$ is the area of the triangular blade. The scattering coefficient ρ is therefore:

$$\rho = \frac{|E_\theta|}{E_0} = \frac{A}{\lambda r}\, g(\theta)$$
$$g(\theta) = \mathrm{sinc}^2\left(\frac{\overline{W}}{\lambda}(\cos\theta - \cos\theta_0)\right)\sin\theta \tag{A-13}$$

where A is the area of the blade, and $\overline{W}$ is the mean width of the blade. The form of this expression is the same as for the rectangular blade (with the appropriate definitions of the area and the mean width), but with a different scattering pattern $g(\theta)$.

Because on average the triangular blade is narrower than a rectangular blade with the same width at the base, the scattering pattern will be broader. The relative scattering coefficient as a function of θ is illustrated in Fig. A-3. It is clear that the scattering pattern for the triangular blade is broader and has smaller side-lobes. Note also that Recommendation ITU-R BT.805 suggests that scattering away from the main direction has a magnitude of about –10 dB (or 0.32 on the scale in the figure below). It is not clear how this value was derived.

FIGURE A-3

Relative scattering patterns (as a ratio) for rectangular and triangular blades. The blade base width is 2.35 m with the incident signal normal to the blade.
Frequency = 600 MHz

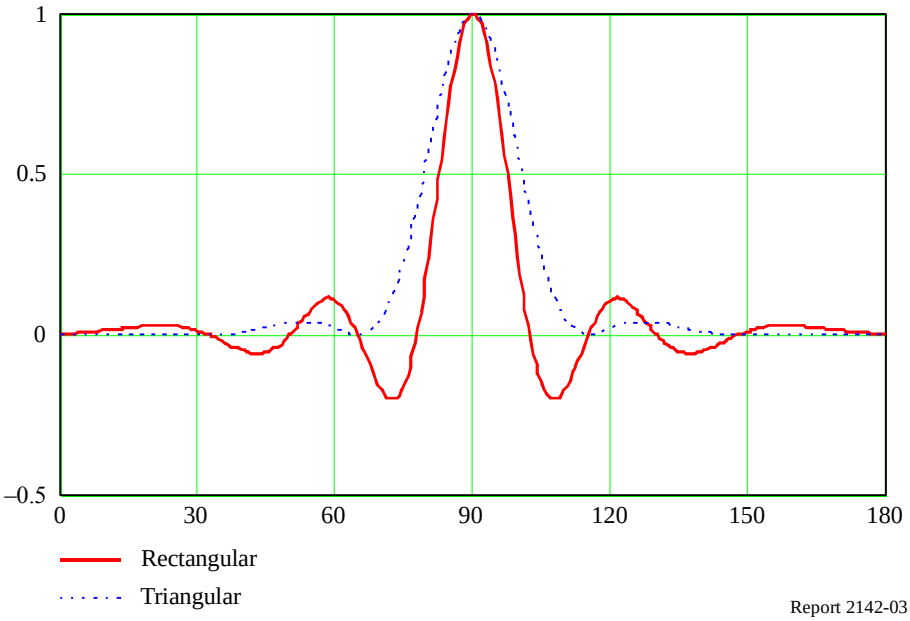

Figure A-4 shows the polar pattern of scattering from the turbine blades (as pictured in Fig. A-5). The scattering is largely confined to the backscattering and forward scattering directions, with the backscattering about 13 dB greater than the forward scattering. This result is similar to that obtained for the turbine pylon described below. In contrast, Recommendation ITU-R BT.805 states that the dominant scattering is in the forward scattering direction.

FIGURE A-4

Polar pattern of the scattering (dB) from the turbine blades, showing the backscattering (right) and the forward scattering (left). The backscattering level is about 13 dB greater than forward-scattering. One blade is vertical, so scattering is symmetric about the horizontal axis

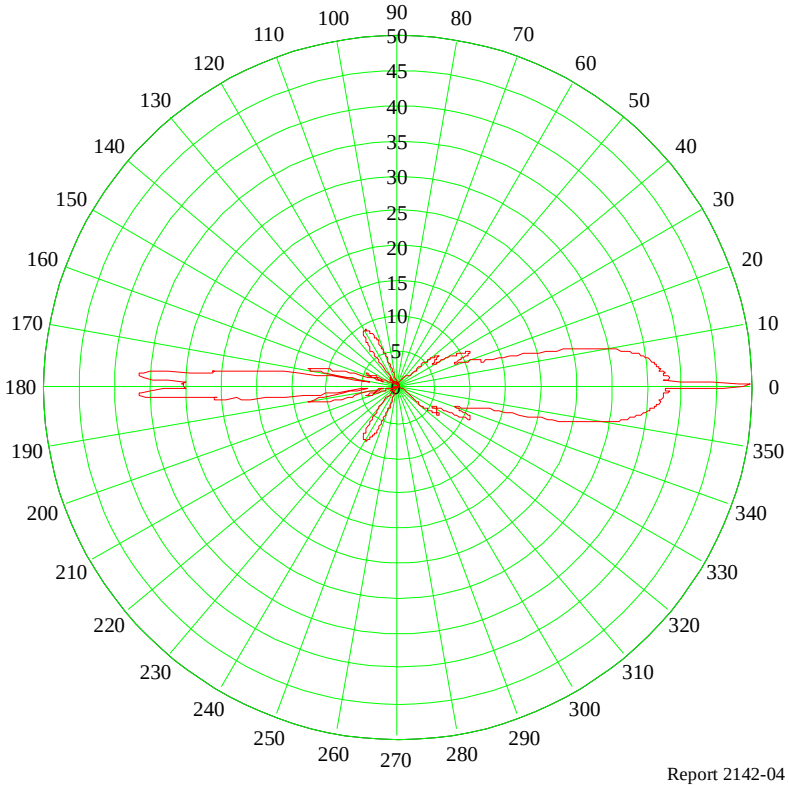

FIGURE A-5

Geometry of wind turbine surfaces. Total rotor area is 160 m^2. Diagram not to scale

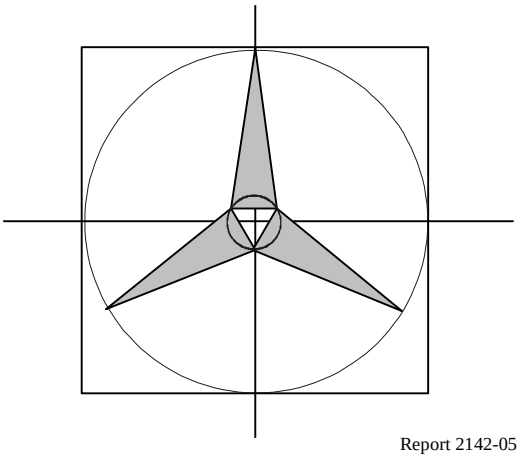

2.4.3 Arbitrary orientation of turbine blades

The calculations in the previous sections were based on the assumption that the wind turbine blade is vertical. However, with rotating blades the orientation is constantly changing and this must be taken into account.

The analysis of the scattering from a blade at an arbitrary orientation is similar to the vertical case with an adjustment to the surface integral. For the far-field case, the surface integral can be interpreted as a two-dimensional Fourier transform. However, at 600 MHz with a 30 m blade (diameter 45 m for

three blades) the far-field range, given by $R = 2D^2/\lambda$, is 8 km. Therefore a near-field analysis is required. This is done by approximating the phase variation by a second-order function using Fresnel zone analysis. Although the following computations are complicated, they are much faster to implement than a numerical method for the same situation.

Using the geometry in Fig. A-6, the receiver at range r from the coordinate reference point is at:

$$P(x, y, z) = r(\cos\theta, -\sin\theta\cos\varphi, \sin\theta\sin\varphi) \tag{A-14}$$

Thus the range R to a point $Q(x, z)$ on the blade (in the x-z plane) is given by:

$$\begin{aligned} R &= \sqrt{(r\cos\theta - x)^2 + (r\sin\theta\cos\varphi)^2 + (r\sin\theta\sin\varphi - z)^2} \\ &= \sqrt{r^2 + x^2 + z^2 - 2rx\cos\theta - 2rz\sin\theta\sin\varphi} \end{aligned} \tag{A-15}$$

FIGURE A-6

Geometry of the propagation path from a point (x, z) on the blade to the receiver

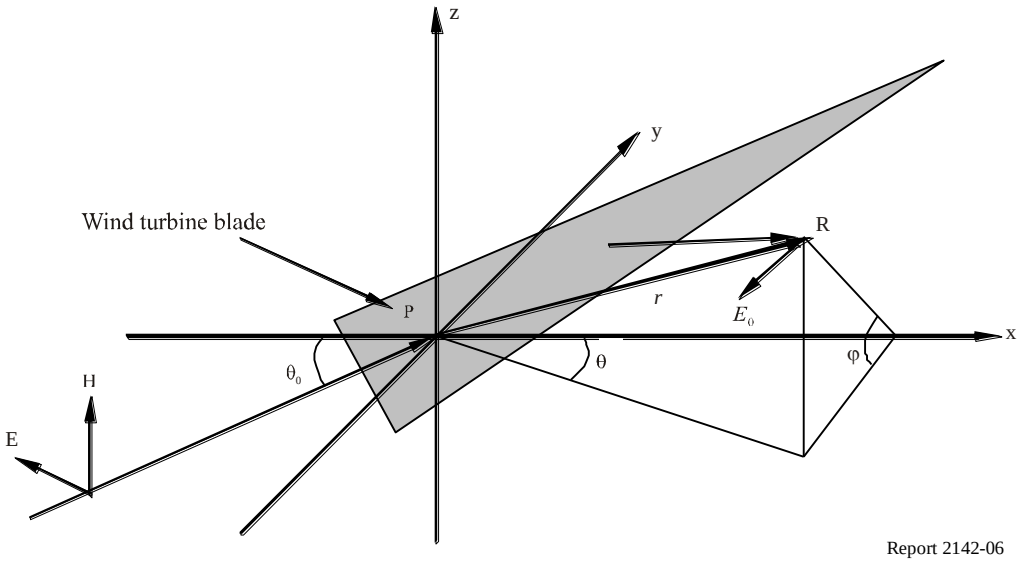

The Fresnel (second order) approximation to the range R is:

$$R(x, z) \approx r - x\cos\theta - z\sin\theta\sin\varphi + \frac{x^2}{2r}\sin^2\theta + \frac{z^2}{2r}\left(1 - \sin^2\theta\sin^2\varphi\right) \tag{A-16}$$

To evaluate the surface integral over the triangular blade for an arbitrary rotation (ψ) of the blade, a new coordinate system (u, y, v) is used to conserve the symmetry of the blade:

$$\begin{aligned} x &= u\cos\psi - v\sin\psi \\ z &= u\sin\psi + v\cos\psi \end{aligned} \tag{A-17}$$

Equation (16) can then be approximated as:

$$R(u,v) \approx r - \left(\cos\theta\cos\psi + \sin\theta\sin\varphi\sin\psi\right)u - \left(\sin\theta\sin\varphi\cos\psi - \cos\theta\sin\psi\right)v + \frac{u^2}{2r}\left[1 - \left(\cos\psi\cos\theta + \sin\theta\sin\varphi\sin\psi\right)^2\right] + \frac{v^2}{2r}\left[1 - \left(\sin\theta\sin\varphi\cos\psi - \cos\theta\sin\psi\right)^2\right] \quad \text{(A-18)}$$

A similar expression can be derived for the incident path ($R_0(u, v)$) from the transmitter, but as the transmitter is in the far field, only the first order (linear) terms in (u, v) need to be included to give the required accuracy. The phase from transmitter to blade to the receiver can be expressed as:

$$\Phi(u,v) = \exp\left[-jk\left(R_0(u,v) + R(u,v)\right)\right] \quad \text{(A-19)}$$

By substituting, the signal phase is given approximately by:

$$\begin{aligned}
&\Phi(u,v) \approx \exp\left[-jk\left(r_0 + r\right)\right]\exp\left[j\left(\alpha u + \beta v - \gamma u^2\right)\right] \\
&\alpha = k\left[\left(\cos\theta - \cos\theta_0\right)\cos\psi - \left(\sin\theta\sin\varphi - \sin\theta_0\sin\varphi_0\right)\sin\psi\right] \\
&\beta = k\left[\left(\sin\theta\sin\varphi - \sin\theta_0\sin\varphi_0\right) + \left(\cos\theta - \cos\theta_0\sin\psi\right)\right] \\
&\gamma = \frac{k}{2r}\left[1 - \left(\cos\theta\cos\psi + \sin\theta\sin\varphi\sin\psi\right)^2\right]
\end{aligned} \quad \text{(A-20)}$$

With these approximations to the phase, and assuming that for the calculation of amplitude, the range from points on the blade to the receiver are the same, the scattered field can be evaluated as:

$$\begin{aligned}
&E_\theta = \frac{jE_0\sin\theta}{\lambda}\left(\frac{e^{-jkr}}{r}\right)\left\{\int_{L_0}^{L+L_0} e^{j\left(\alpha u - \gamma u^2\right)}\left[\int_{-w(u)}^{w(u)} e^{j\beta v}\,dv\right]\,du\right\} \\
&w(u) = \frac{W}{2}\left(1 - \frac{u - L_0}{L}\right)
\end{aligned} \quad \text{(A-21)}$$

where W is the width of the blade at its base, L is the length of the blade, and L_0 is the distance from the axis of the rotor to the base of the blade.

This can ultimately be solved to give the following expression:

$$E_\theta = \frac{jE_0\sin\theta}{\lambda}\left(\frac{e^{-jkr}}{r}\right)\left\{I(a,b,c,1) - I(a,b,c,0)\right\} \quad \text{(A-22)}$$

where:

$$a = \frac{\beta W}{2} \qquad b = L\left(\alpha - 2\gamma\left(L_0 + L\right)\right) \qquad c = \gamma L^2 \quad \text{(A-23)}$$

and $I(a,b,c,x)$ is given by the following equations, depending on β.

For $\beta \neq 0$:

$$I(a,b,c,x) = \frac{1}{4\sqrt{c}}\left[M\sqrt{\pi}\,\exp\left(j\frac{(a-b)^2}{4c}\right)\left\{ f(-a,b,c,x) - \exp\left(j\frac{ab}{c}\right) f(a,b,c,x)\right\}\right]$$

$$f(a,b,c,x) = \text{erfi}\left[\frac{M}{2\sqrt{c}}(a+b+2cx)\right] \qquad \text{(A-24)}$$

$$\text{erfi}(z) = -j\,\text{erf}(jz) \qquad M = \frac{j-1}{\sqrt{2}}$$

and for $\beta \to 0$:

$$I(a,b,c,x) = \frac{1}{2c}\left[\frac{b}{2}\sqrt{\frac{j\pi}{c}}\,\exp\left(j\frac{b^2}{4c}\right) f(b,c,x) + j\exp\left(-jx(b+cx)\right)\right]$$

$$f(a,b,c,x) = \text{erfi}\left(M\left(\frac{b+2cx}{2\sqrt{c}}\right)\right) \qquad \text{(A-25)}$$

This solution is demonstrated for three cases, using the near-field formula derived above, a far-field solution, and a numerical approximation with a pixel size of 1/8 of a wavelength. Note that, for simplicity, these examples use perfectly conducting blades, and that in real analysis, the effect of the non-metallic structure would have to be included.

Figure A-7 shows the scattering from a three-blade rotor with one blade vertical, giving a symmetric horizontal pattern. As the rotor consists of vertically and horizontally large dimensions the scattering pattern has both broad and narrow components. The far-field solution overestimates the scattering coefficient, and there is good agreement between the numerical and near-field solutions.

Figure A-8 shows the scattering with the rotor rotated 90º anti-clockwise, giving an asymmetric scattering pattern. The scattering pattern is similar to the previous case, but the main beam is wider and the broad beam less prominent. These two examples illustrate the changing scattering pattern as the wind turbine rotates.

Figure A-9 shows the scattering coefficient from a three-blade rotor as the blades rotate through 360º. The far-field and near-field solutions have broadly similar characteristics, but the far-field solution is shifter slightly by about 10º relative to the near-field (true) position. The scattering pattern has six peaks within the 360º; as the three blades and mirror image patterns result in similar scattering. However, overall the pattern repeats three times as expected for a three-blade rotor.

FIGURE A-7

Scattering coefficient from three-blade rotor with one blade vertical. Range 1 km, pylon height 67 m, receiver height 67 m. Incident signal normal to blade

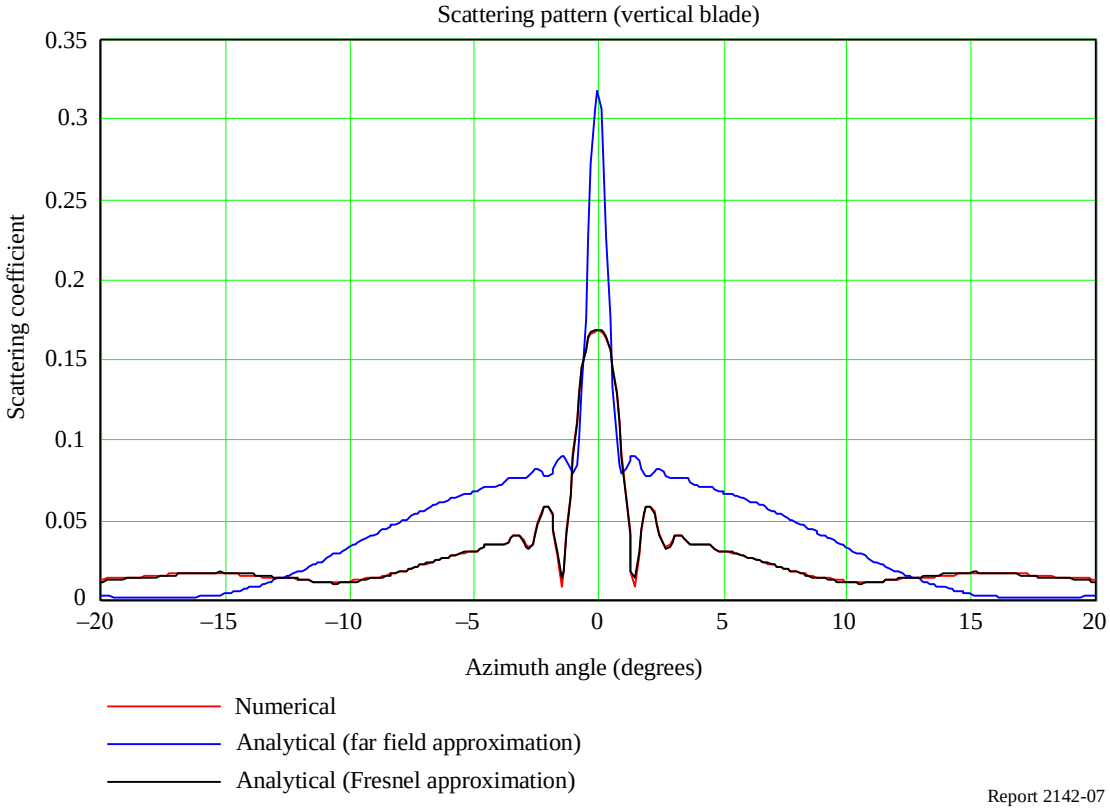

Report 2142-07

FIGURE A-8

As in Fig. A-7 but with one blade horizontal. The far-field solution is (erroneously) symmetric, but the numerical and Fresnel solutions are asymmetric

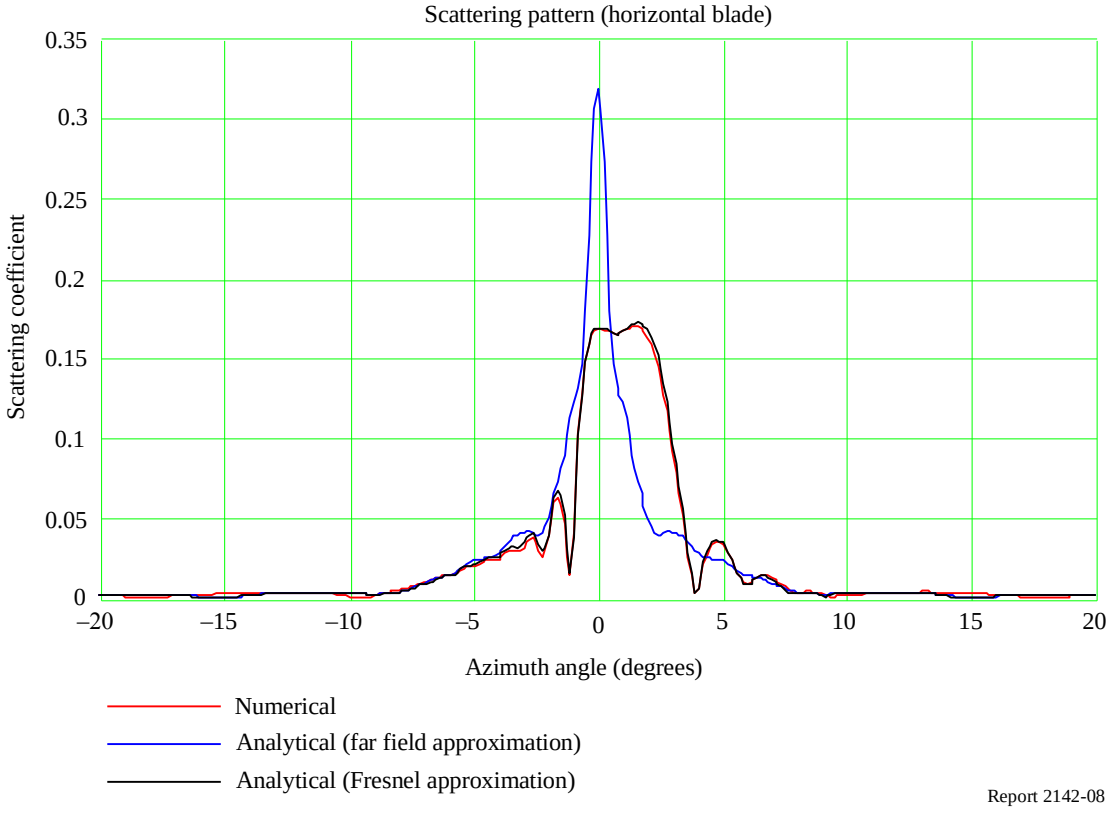

Report 2142-08

FIGURE A-9

Scattering coefficient from a three blade rotor. Pylon height 67 m. Incident signal normal to blade. Receiver is 1 km from the blade, 10 m above ground, and at an azimuth angle of 85° relative to the plane of the blade. The far field solution is shifted by about 10° relative to the Fresnel zone (true) position

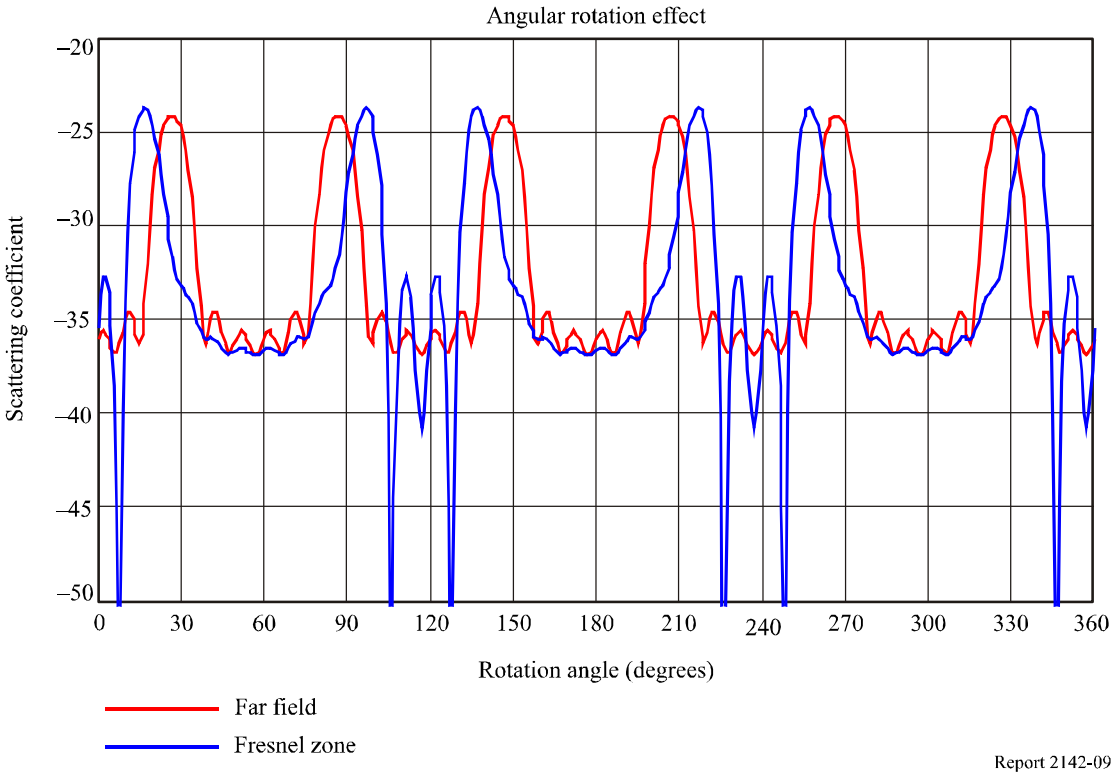

The main conclusion is that at positions of practical interest, the scattering pattern will vary by at least 10 dB, with (for a three-bladed turbine) a dominant frequency component of six times the rotation rate or about 3 Hz for a typical rotation rate of 20 rpm.

2.4.4 Scattering from pylon

As the support pylon of the wind turbine is a large metallic structure, the scattering from the pylon must also be considered. Wind turbine pylons are typically tapered (typically 0.5° to 1°) cylindrical structures, and scattering calculations can be based on a conducting cylinder with a diameter equal to the mean of the actual pylon. The pylons used in the following example have a base diameter of 4.2 m and a top diameter of 2.3 m, giving a mean diameter of 3.25 m. The height is 68 m and the taper is 0.8°.

The rigorous expression for the scattering coefficient from an infinite conducting cylinder for a vertically polarized plane wave is given by:

$$\Gamma_v = \frac{E_s}{E_0} = \sum_{n=0}^{\infty} \varepsilon_n (-j)^n J_n(ka) \frac{H_n^{(2)}(kr)}{H_n^{(2)}(ka)} \cos(n\varphi) \qquad \text{(A-26)}$$

where ε_n is the Neumann's number ($\varepsilon_n = 1$ when $n = 0$ and $\varepsilon_n = 2$ when $n \neq 0$), a is the radius of the cylinder, and φ is the horizontal scattering angle relative to the incident propagation direction.

The corresponding expression for horizontal polarization is given by:

$$\Gamma_h = \frac{E_s}{E_0} = -j \sum_{n=0}^{\infty} \varepsilon_n (-j)^n J'_n(ka) \frac{H_n^{(2)}(kr)}{H_n'^{(2)}(ka)} \cos(n\varphi) \qquad \text{(A-27)}$$

where the "dash" on the Bessel and Hankel functions represents the derivative of the function. While these two expressions are different, as the diameter of the cylinder becomes large relative to wavelength, the two expressions approach the same solution. For example, in Fig. A-10 the diameter is 6.6 wavelengths, and the shape of the two curves is very similar.

The computed scattering coefficient from an infinite cylinder with a diameter of 3.3 m is shown in Fig. A-10. The scattering pattern consists of a strong backscatter (scattering coefficient 0.158 or –16 dB for vertical polarization, 0.139 or –17 dB for horizontal polarization), and an approximately constant value in the range to 0.02 to 0.03 (–34 dB to –30 dB) at angles greater than 10° from the peak reflection. Thus the scattering in the horizontal plane is confined to a narrow 3 dB beamwidth of ±3.5°.

FIGURE A-10

Computed scattering coefficient in the horizontal plane from an infinite cylinder, diameter 3.3 m, range 1 km.

Frequency = 600 MHz

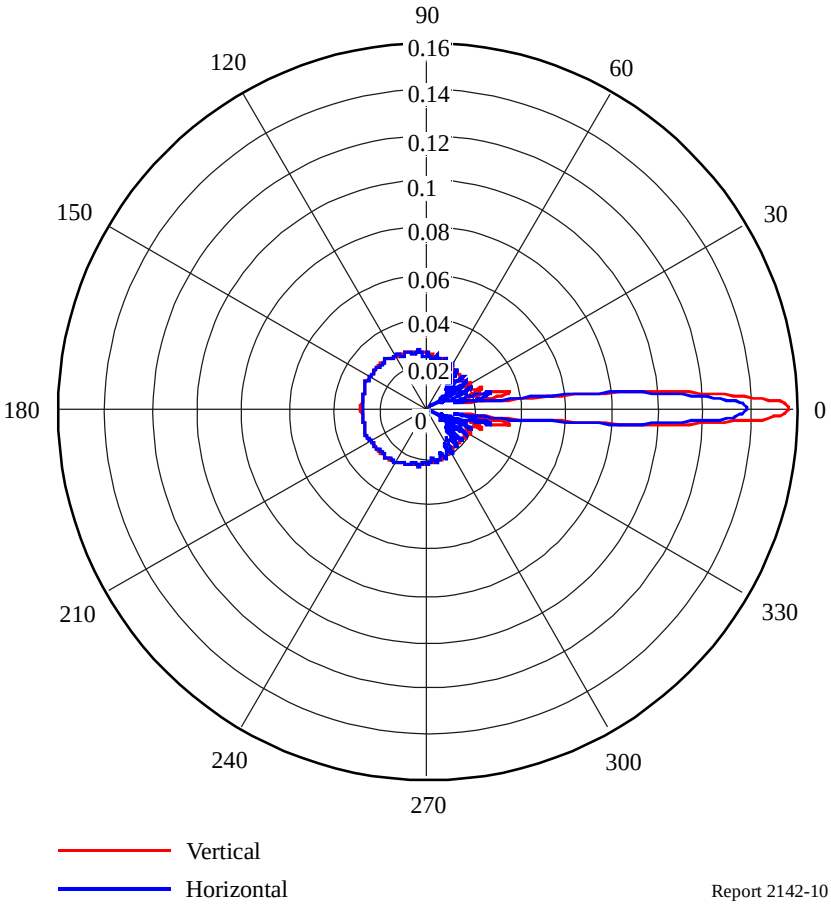

The behaviour of the reflection coefficient as a function of range is shown in Fig. A-11. As the radiation at a long range from an infinite cylinder approaches that of a pure cylindrical wave, the amplitude of the scattered signal varies as $1/\sqrt{r}$ at long range (or a 3 dB reduction for each doubling of range). In practice the scattered signal can be considered cylindrical only relatively close to the pylon, so the effect of the finite height must be considered for any practical predictions at long range. The following analysis estimates the correction factor to adjust the infinite cylinder solution to the finite length case, and provides an estimate of the vertical scattering beam pattern.

FIGURE A-11

Computed scattering coefficient from an infinite cylinder as a function of range

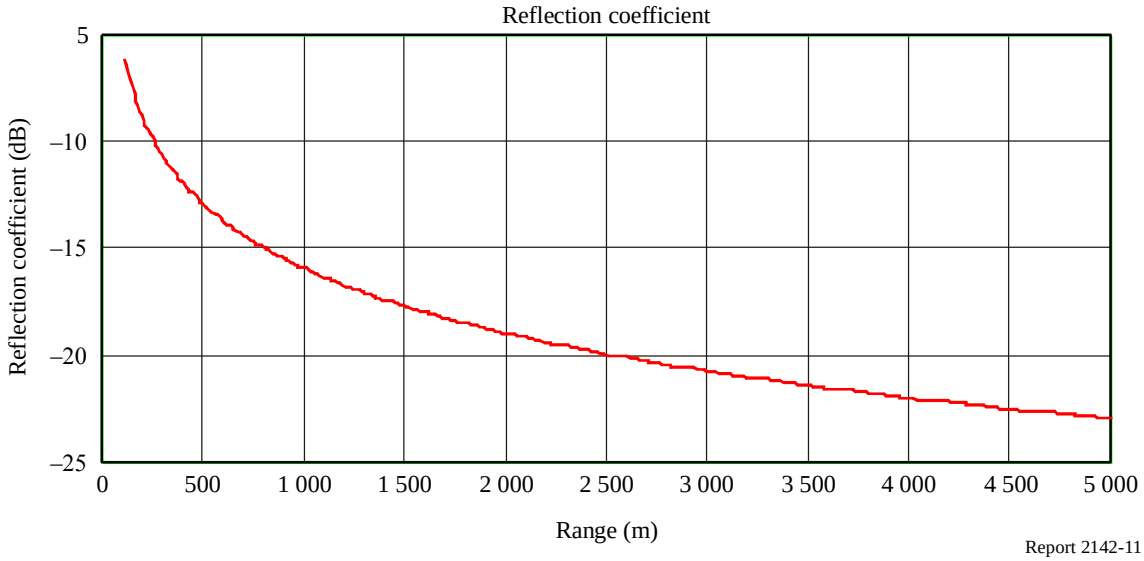

The correction factor for the finite case is estimated using a numerical physical optics solution. It is assumed that the incident signal is horizontal, and the vertical scattering angle relative to the horizon is θ, as shown in Fig. A-12.

FIGURE A-12

Geometry of the scattering from a finite height cylinder

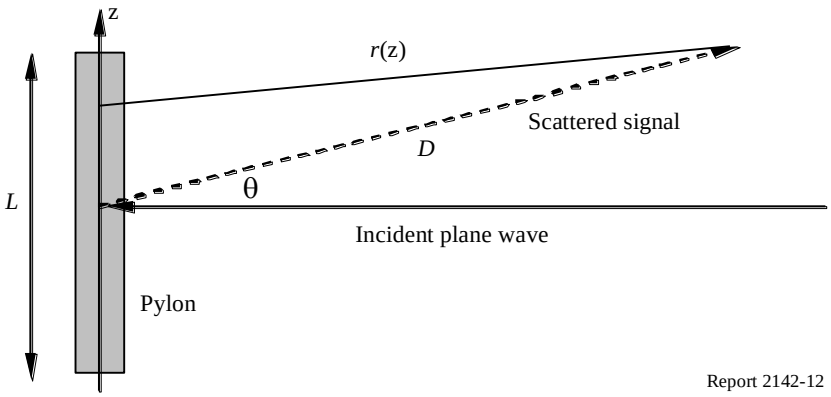

The effect of the pylon height and range is based on the vertical integral:

$$I_{vert} = \int_{-\frac{L}{2}}^{\frac{L}{2}} \mathrm{e}^{-jkr(z)}\ \mathrm{d}z \approx 2\mathrm{e}^{-jkD} \int_{0}^{\frac{L}{2}} \mathrm{e}^{-j\frac{kz^2}{2D}}\ \mathrm{d}z \tag{A-28}$$

where D is the horizontal range from the pylon, and L is the height of the pylon. The integral can be evaluated to give:

$$\begin{aligned} & I_{vert}(\theta, D, L) = \frac{\sqrt{\lambda D}}{\sqrt{2}\cos\theta}\, \mathrm{e}^{j(\alpha - kD)} \left[CS\left(\eta\left[\frac{L}{2}\right]\right) - CS\left(\eta\left[-\frac{L}{2}\right]\right)\right] \\ & \alpha = \pi \frac{r}{\lambda} \tan^2\theta \\ & \eta(z) = \sqrt{\frac{2D}{\lambda}}\left(\frac{z}{D}\cos\theta - \tan\theta\right) \\ & CS(x) = C(x) - jS(x) \end{aligned} \tag{A-29}$$

where $C(x)$ and $S(x)$ are the cosine and sine Fresnel integrals. The complex Fresnel integral $CS(x)$ can be expressed in terms of the error function by:

$$CS(x) = \frac{1-j}{2}\,\mathrm{erf}\left(\frac{\sqrt{\pi}}{2}[1+j]x\right) \tag{A-30}$$

As the height of the pylon becomes large the integral approaches the limiting solution:

$$I_{vert}(\theta, D, \infty) I = \left(\frac{\sqrt{\lambda D}}{\cos\theta}\right) \mathrm{e}^{j(\alpha - kD - \pi/4)} \tag{A-31}$$

which shows that the effective height of the pylon in terms of scattering is of the order of $\sqrt{\lambda D}$. For example, at a range of 1 km and a frequency of 600 MHz, the effective height is about 22 m. As the actual height is 68 m, in this case the infinite approximation is satisfactory.

For a scattering angle of $\theta = 0$ the normalization factor N is the ratio of the finite length cylinder solution to the infinite cylinder solution:

$$N(D) = \frac{I_{vert}(0, D, L)}{I_{vert}(0, D, \infty)} = \sqrt{2}\mathrm{e}^{j\pi/4} CS\left(\frac{L}{\sqrt{2\lambda D}}\right) \tag{A-32}$$

The scattered signal correction factor for a 68 m pylon is shown in Fig. A-13 for ranges up to 5 km. The correction factor is ±2 dB up to a range of 5 km for a frequency of 600 MHz, but at lower frequencies the correction factor is larger. Therefore at long range (particularly at lower frequencies) the scattered signal is somewhat smaller than that predicted by the infinite cylinder model, but the correction factor does not exceed ±2 dB for ranges up to 1.5 km. From equation (A-32) the correction

factor can be ignored provided the argument of the Fresnel integral functions is large. In practice, a suitable constraint is:

$$\frac{L}{\sqrt{2\lambda D}} > 1 \quad \text{or} \quad D < \frac{L^2}{2\lambda} \tag{A-33}$$

For a pylon height of 68 m the maximum ranges are 1 150 m, 2.3 km and 4.6 km at frequencies of 150 MHz, 300 MHz and 600 MHz respectively.

FIGURE A-13

Scattered signal correction factor for a 68 m high pylon (at three frequencies) as a function of range from the wind turbine. This value modifies the scattering coefficient from an infinite cylinder as given in Figs. A-10 and A-11

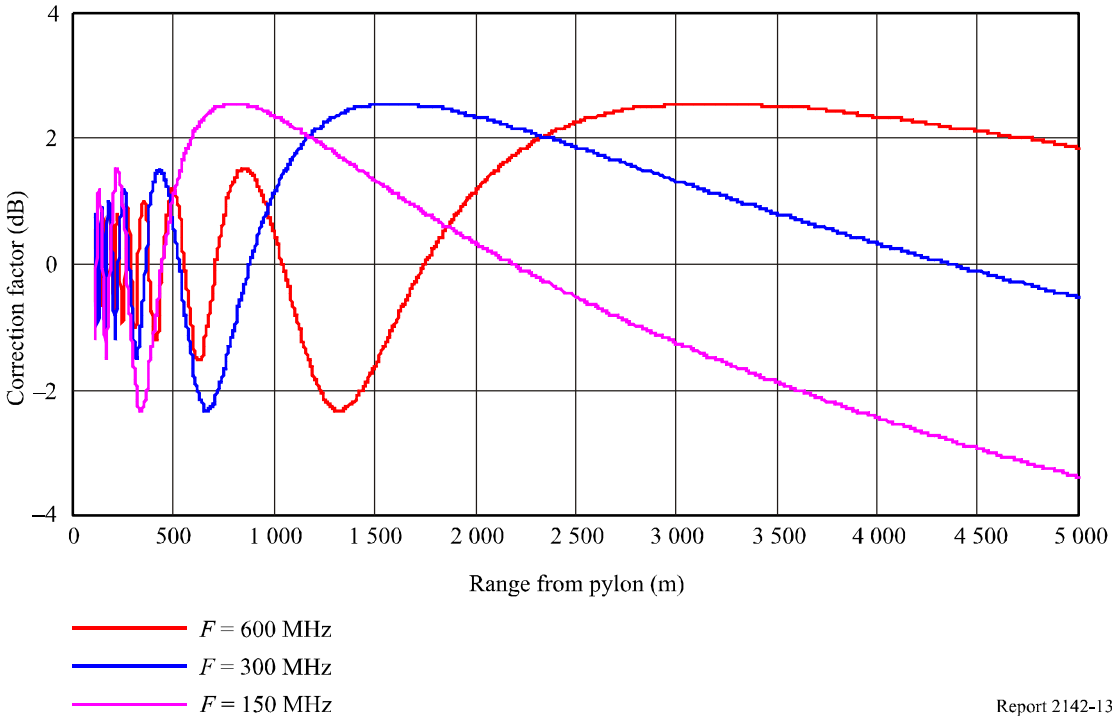

The vertical scattering pattern can also be computed from equation (A-29). Figure A-14 shows three examples at ranges of 250, 500 and 1 000 m. It is clear that the beamwidth decreases as the range increases. From equation (A-29) it can be shown that the beamwidth is of the order of:

$$BW \approx \pm \frac{L}{2D} \quad \text{rad} \tag{A-34}$$

For the above three ranges the corresponding beamwidths are ±8°, ±4° and ±2° which agrees generally with Fig. A-14.

At close range the scattering amplitude is approximately constant within a band of elevation angles, and the scattering in this band can be approximated by an infinite cylinder. As the range increases the beamwidth decreases, but an asymptotic limit is reached at a longer range.

FIGURE A-14

Computed scattering pattern in the vertical plane different ranges from a pylon of height 68 m and a frequency of 600 MHz

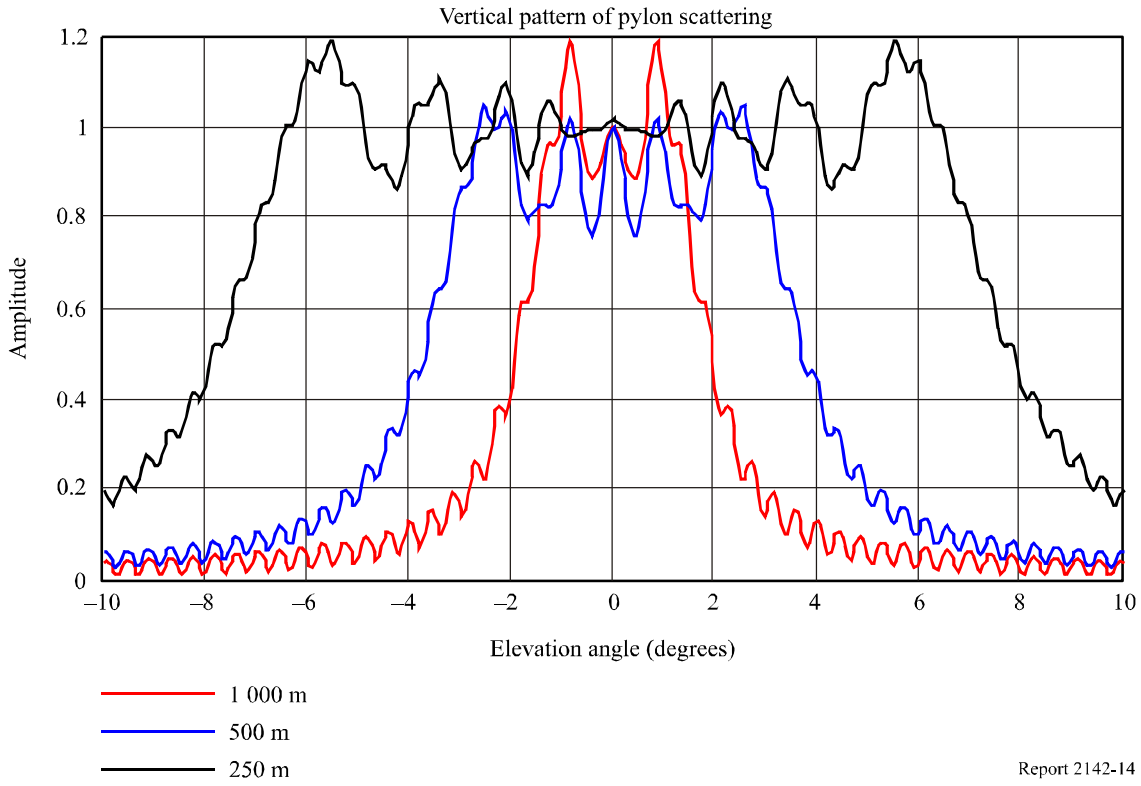

2.4.5 Effect of antenna directivity and reception geometry

It is assumed that in suburban and rural areas an antenna with reasonable directivity (12-20 dB) is used for television reception. The relative level of the direct and scattered signals will be influenced strongly by the antenna directivity in the direction of the direct and scattered signals. Three cases may be considered.

In the first case, shown in Fig. A-14, the signals are scattered from the turbine and arrive at the television antenna from the back. In this case the scattered signal is at its maximum, but will be significantly moderated by the antenna front-to-back ratio. Using (as an example only), a scattering coefficient of –15 dB, the signal-to-interference ratio will be at 27 to 35 dB, above the interference threshold of 20 dB used in digital TV planning.

In the second case, shown in Fig. A-15, the antenna directivity is similar for both the direct and scattered signals. However, the forward scattered signals are considerably smaller, even if the turbine is in direct line of sight. This geometry therefore combines lower scattered signal with no mitigating effect from the antenna directivity. In this case, the interference performance is approximately similar to the first case.

In the third case, which is more typical of rural Australian wind farms, the turbines are located on the top of a ridge, in the direct line of the television signals. The television receiver is in a valley without line-of-sight (LoS) to the television transmitter. In such circumstances the incident television signal at the wind turbines will be much greater than the wanted signal at the television receiving antenna. Because of the potentially wide range of conditions, no particular numerical case is given, but an incident signal difference of 20-30 dB is not unreasonable. A particularly difficult case is the geometry shown in Fig. A-16. The directivity of the television receiver antenna does not provide any protection from the interference scattered from the turbine.

FIGURE A-15

Geometry of minimal scattering and no protection from the antenna directivity

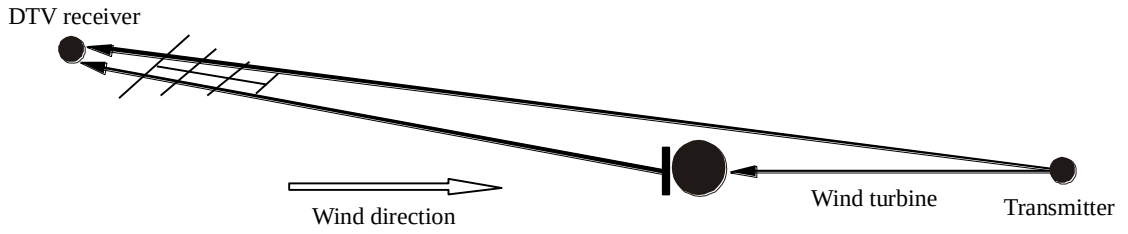

FIGURE A-16

Geometry which could result in a large interference signal relative to the "direct" signal

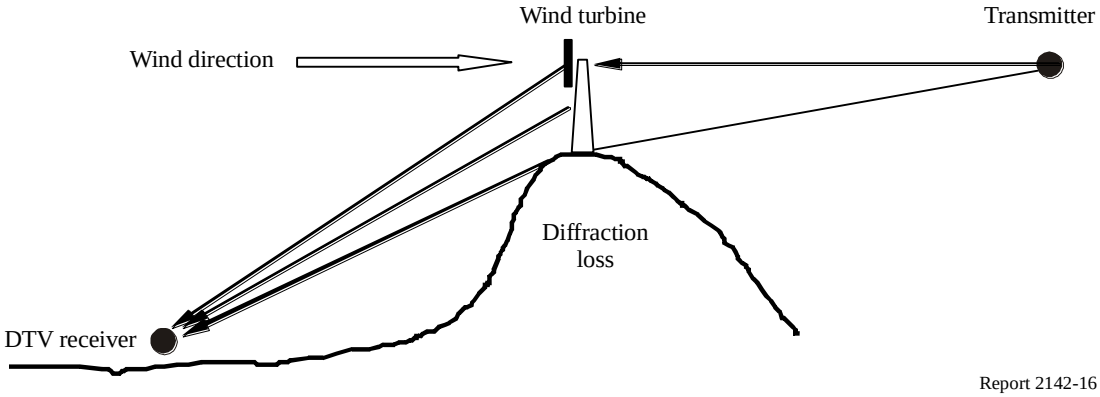

The overall conclusion is that the geometry and local terrain are critical in determining the interference effects from wind turbines.

Attachment 2 to Part A

The effect of the scattering of digital television signals from wind turbines

1 Introduction

The study in Attachment 1 is a study based on theoretical modelling that identified Recommendation ITU-R BT.805 is not adequate for predicting interference from wind farms for analogue and digital TV signals.

The study described in this Attachment indicates that the methods to assist in quality assessment of the coverage and service area for digital television broadcasting in System B in Recommendation ITU-R BT.1735 are not satisfactory for the type of dynamic signal variations from rotating wind turbine blades.

1.1 Overview of study

This text is part of a study to determine the effect on digital television reception due to interference arising from scattering from multiple wind turbines (referred to as a wind farm). Attachment 1 provided theoretical and computer simulation studies of the scattering of radio signals from the wind turbine structure, both from the static pylon and the dynamics from rotating blades. In this Report, the work is extended to measurements of the interference effects from multiple wind turbines, as well as computer simulations to predict performance of digital television receivers using information about the size and shape of wind turbines and the geographical layout of a wind farm.

Measurements reported in this text were made around the Challicum Hills wind farm, near Ararat in Victoria, Australia. Figure A-17 shows a surface map of the test area, with the wind farm at the lower left, and the transmitter on Lookout Hill at the upper right. The measurements, performed by the Commonwealth Scientific and Industrial Research Organisation (CSIRO), logged actual TV signals as files of digital data that can be analysed for multipath interference using a software receiver program. The logged signals also provide a reference signal with little multipath corruption, which can be used to generate simulated television signals with specific multipath interference. The multipath scattering impulse response can be estimated from the measurements. This provides the scattering coefficient, a single statistical parameter which represents the scattered signal relative to the incident signal and therefore summarizes the overall level of multipath interference at a point.

The measured or simulated television signal is processed by a software receiver, which performs the same signal processing as in an actual receiver, although limited to decoding the pilot signals to calculate the propagation impulse response. The software also estimates the channel bit error rate[1] (CBER) and the modulation error ratio MER, which can be used to specify the "quality" of the received signal. Although the measurement data come from specific multipath interference cases, the relationship between the CBER or MER and the scattering coefficient provides a generally applicable result.

The wind farm is located on rolling hills 100-150 m above the surrounding largely flat grazing land. There is direct LoS from the transmitter to the wind turbine on the hills. The main interference area is expected in the shadow of the hills at the lower left.

In addition to the measurements, software has been developed to estimate the EM scattering as a function of the size and shape of the wind turbines, the geometry of the wind farm, the location of the transmitter, and the receiving location. This was initially reported in Document 6E/398 but has been extended to arbitrary wind farm geometries. Maps of the scattering coefficient, MER and CBER can be calculated as a function of receiving position, which are useful in identifying areas where significant interference can be expected. The multipath impulse response can also be calculated, which when combined with the measured reference signal produces an artificial television signal for the location of interest. This can then be fed into the software receiver to estimate the CBER and MER.

The calculation of scattered signals from wind turbines and wind farms, as well as more general charts of digital television receiver performance as a function of the scattering coefficient, could be useful in the ongoing development of Recommendation ITU-R BT.805.

---

[1] The channel BER is the raw bit error rate before the Viterbi error correcting.

FIGURE A-17

Surface map of the measurement area

Lookout Hill-Challicum Hill area

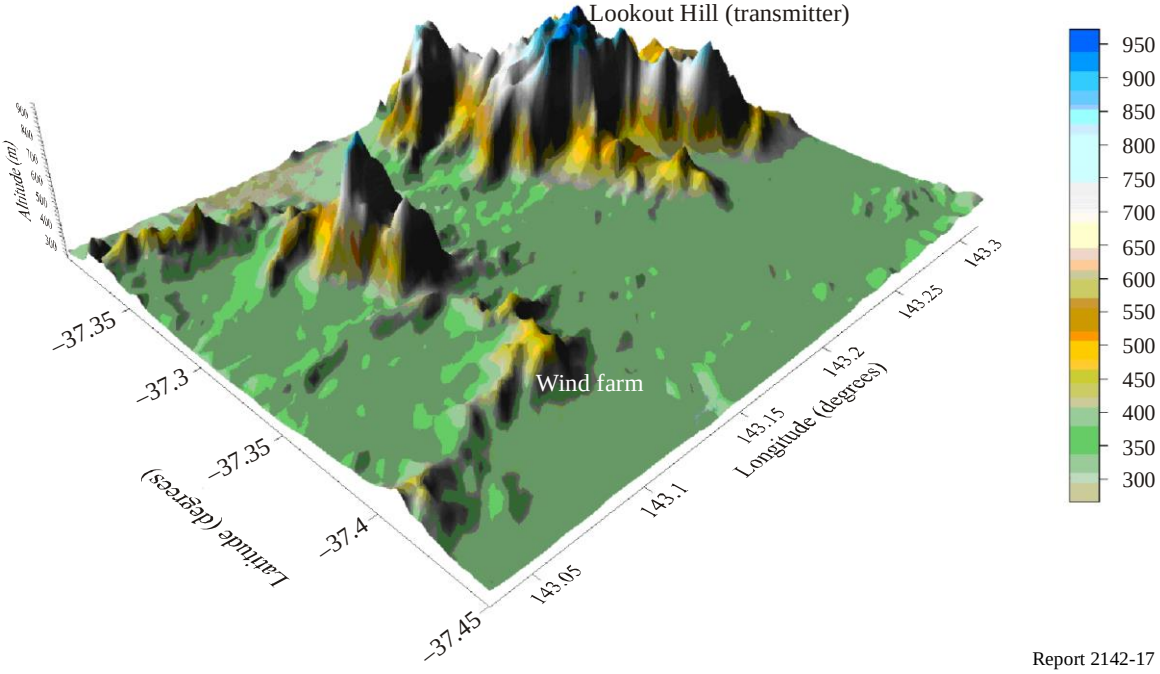

Report 2142-17

1.2 Measurement overview

The measurement programme was a joint effort between the CSIRO ICT Centre and Free TV Australia[2], over a period of three days (2-4 May 2006). The CSIRO measurements used a custom receiver and data logger to record the receiver IF analogue output in order to capture and analyse the fast-varying signals associated with the rotation of wind turbine blades. The Free TV Australia measurements were made using a 4T2 commercial test instrument, which logs a wide range of *average* signal parameters. This report concentrates on the analysis of the CSIRO data.

The measurements were made at eight locations surrounding the wind farm. The extent of scattering from wind turbine blades depends on the direction of the wind relative to the transmitter and receiver location(s). Unfortunately, the weather conditions on the first two days produced minimal blade scattering. On the third day the wind direction was more favourable, but still not optimum, for interference from the blades. Data from the third day shows the dynamic effects of interference from wind turbines on the reception of digital television signals.

2 Predicted performance with software models

2.1 Overview

Predictions for the scattering from a specific wind farm were based on the calculation of scattering from wind turbines as described in Attachment 1, and on software to implement the front-end signal processing of a digital television receiver. In the second case, the input signal was synthesized from received signals recorded at the CSIRO Radio Physics Laboratory at Marsfield in Sydney, Australia using a roof-mounted high-gain antenna to provide a good reference with minimal multipath.

[2] Free TV Australia is an industry body which represents all of Australia's commercial free-to-air television licensees.

This was then used as input to the simulation program to generate a synthesized multipath signal at specific locations near the wind farm. The synthesized signal is an input to the software receiver to estimate the channel bit error rate and the modulation error ratio.

2.2 Geographic summary

Figure A-18 shows the layout of the wind farm, with 35 turbines in an area of about 5 km^2, in three approximately linear groups along ridge lines. The altitude (at the base of the pylons) is between about 430 and 510 m. The surrounding land is approximately flat with a mean altitude of about 350 m. As the pylons are 68 m tall, the axis of the turbine rotors is about 150-200 m above the surrounding land where the interference effects were measured.

FIGURE A-18

Map of Challicum wind farm and transmitter location

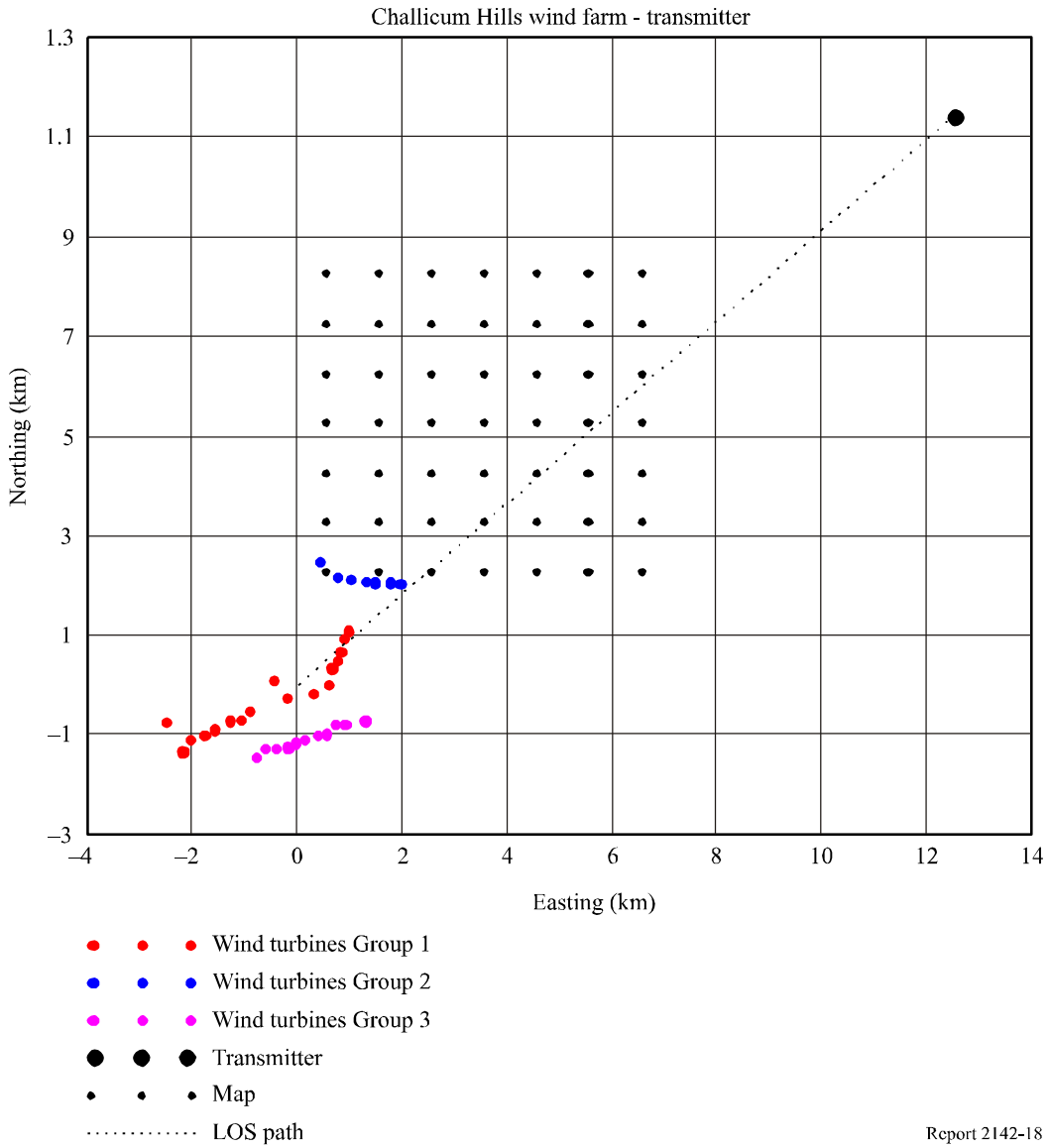

Figure A-18 also shows the geographic relationship between the wind farm and the nearby television transmitters. The distance to the transmitter is between 14 and 20 km. The altitude of the transmitting antenna is about 1 150 m, or about 700 m above the mean altitude of the wind turbine rotors. In Fig. A-18, the straight line joins the transmitter to the centre of the wind farm; backscattering from

the pylons is expected to be dominant near this line. The incident signal subtends an angle of about 2.4º above the horizon at the wind farm. As the pylons are tapered by about 1.2º, the corresponding reflections are at about 1.2º below the horizon, and intersect the surrounding land a few kilometres from the wind turbine.

The origin (0, 0) in the map is the mean of the grid coordinates of the 35 wind turbines. The black dots show where the interference map of § 2.3 was computed. The dotted line is from the transmitter to the centre of the wind farm.

2.3 Predicted interference map from pylon scattering

The scattering coefficient from the pylons was calculated (as described in Attachment 1) using geographic information for the wind farm and transmitter, and an interference map was produced covering the area between the wind farm and the transmitter, where the strongest scattering is expected.

Due to local terrain, the turbines further away from the transmitter (Groups 1 and 3 in Fig. A-18) are somewhat shielded by the closer ridge where Group 2 is located. A rigorous calculation of scattering would include diffraction losses over this ridge line. To simplify the calculations, the total interference was calculated assuming clear LoS propagation, which overestimates the scattering coefficient. The predicted scattering from the pylons is shown in Fig. A-19. The peak scattering coefficient is 0.17 (or –15.4 dB) in a "hot spot" 6 km east and 6 km north of the centre of the wind farm. A similar calculation was done with only the closest seven wind turbines (Group 2). The scattering coefficient using all turbines and LoS propagation was only moderately larger than that using only the nearest group and it can be concluded that the scattering coefficient in the area between the transmitter and the wind farm is due almost entirely to the closest turbines.

It is also clear from Fig. A-19 that forward scattering is small compared with the backscattering.

The maximum scattering coefficient is about 0.17 at about 6.3 km east and 5.1 km north of the wind farm central reference point. The grid is 2 km^2, based on the Australian Map Grid.

The impulse response of the multipath scattering environment can be estimated from the interference signal of each turbine. Figure A-20 shows the results for 35 pylons, at the hot spot location defined above and assuming an omnidirectional receiving antenna. For actual television reception, a directional antenna with significant front-to-back ratio would be used, resulting in much lower interference. However, to measure the interference signals, an antenna with a front-to-back ratio of about 25 dB was pointed **towards** the interference. Therefore the amplitude of the strongest interference signal should be comparable with the direct signal received through the back of the antenna. This procedure thus "amplifies" the scattered signal, making more accurate measurements possible.

Figure A-20 also demonstrates the large time delays of the scattered signals, up to about 60 μs, due to the round-trip distance of about 18 km between the measurement point and the most distant wind turbine. The common guard time parameter of 1/16 corresponds to 64 μs. The measurement technique using the scattered pilot signals has a maximum measurable delay of 42.7 μs[3], and could not determine the large scattered signal delays for this case.

[3] This value is related to the pilot separation frequency of about 12 kHz. As the maximum Nyquist "frequency" is half of 1/12 kHz, the maximum time delay is about 1/24 ms.

FIGURE A-19

Map of the scattering from all the pylons (red dots)

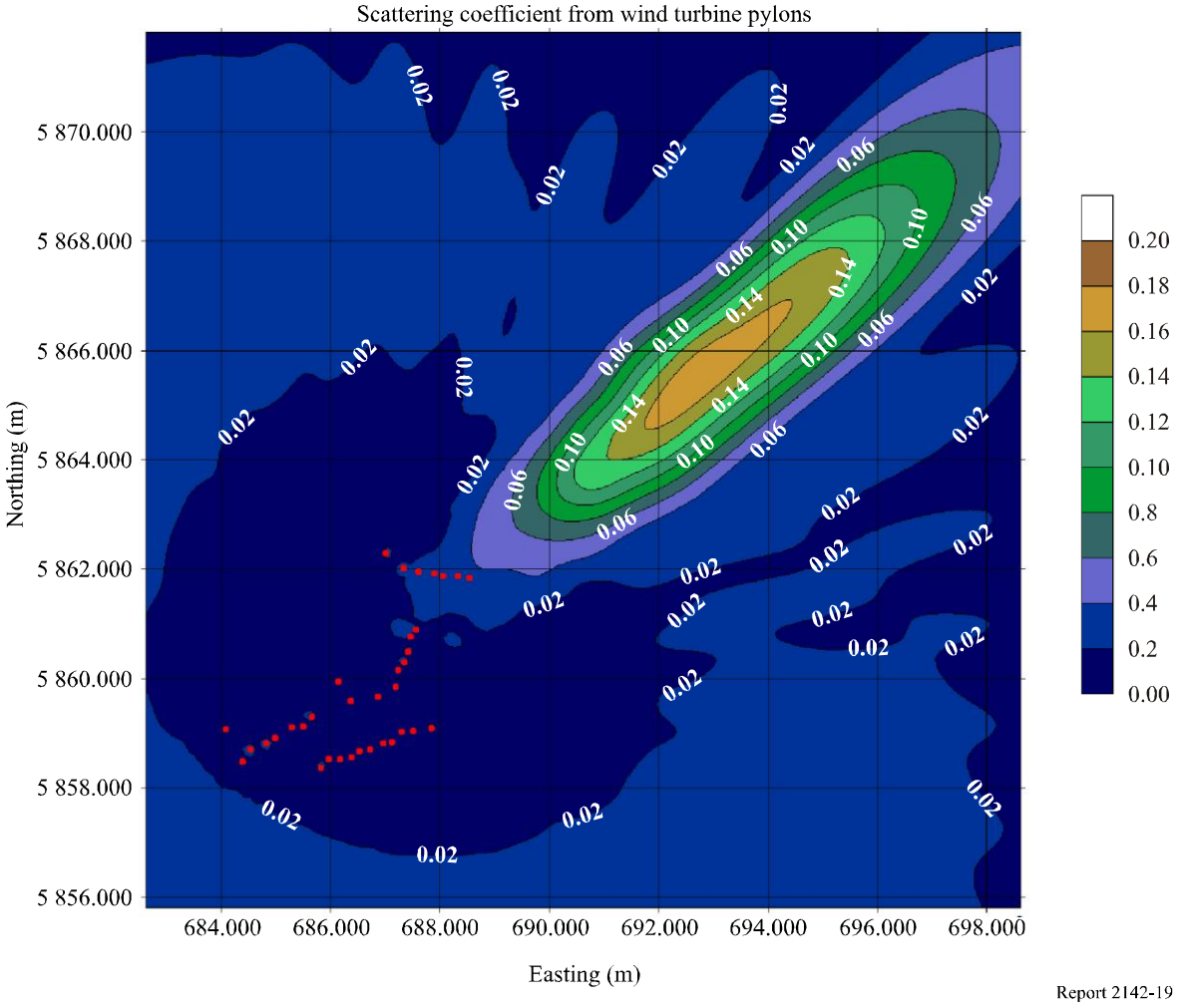

FIGURE A-20

Computed multipath impulse response for the scattering from all 35 wind turbine pylons at the interference hot spot location

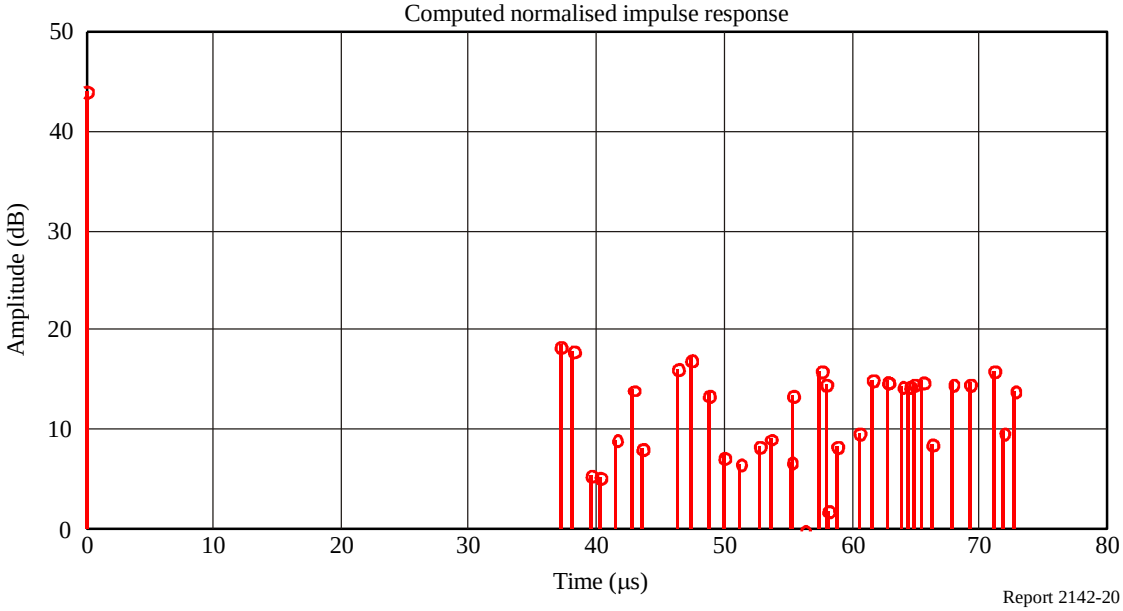

The direct signal is also shown at 0 μs. An omnidirectional antenna was assumed. The data are normalized so that the weakest signal from a wind turbine is 0 dB.

2.4 Predicted interference map from blade scattering

The calculation of the scattering from the turbine blades is similar to that from the pylons, but with two complicating factors. First, the rotation of the blades produces a scattering pattern which varies cyclically about every two seconds. Secondly, the axis of the rotor in the horizontal plane changes with the wind direction. Maximum scattering occurs when the wind direction is aligned with the line from the transmitter to the wind farm (see Fig. A-18), that is, when the wind direction is in the NE-SW direction[4]. The problem is further complicated by the fact that there are many independently operating wind turbines in a wind farm, so a deterministic solution for one particular orientation of the blades on each turbine is not useful for planning purposes.

To calculate the scattering from the blades, therefore, a wind direction is assumed, and it is assumed that the plane of the blades are all orientated normal to this direction. As the rotation angles of the turbines are unsynchronized, it is assumed that the angles are distributed with a uniform random distribution in the range 0º to 360º. Because all the turbines rotate at the same rate, these angle distributions remain constant. The scattering coefficient at each point in the map was calculated as the average scattering coefficient with this random offset angle for each wind turbine. The maps therefore represent a statistical average of the scattering, with the dynamic variations ignored. Because the blades rotate only a very small angle[5] during the OFDM symbol period of about 1 ms, the scattering can be considered as quasi-stationary. The scattering coefficient itself is a statistical parameter describing (approximately) a Rayleigh distributed signal amplitude, or a Ricean distributed signal amplitude is the direct signal is included.

As the blades rotate, the scattered signal received at a point will vary in a cyclical fashion. An example is shown in Fig. A-21, illustrating the variation at "hot spot" from Fig. 19. Scattering from all 35 turbines was calculated with the simplifying assumption of LoS propagation and all rotors oriented normal to the wind direction. Despite the complexity, a fundamental component at one-third the rotation period is clear. The scattered signal varies by a factor of about 2.25.

The relative angular positions of the rotors on each turbine were selected randomly. The scattering coefficient was computed at the position of maximum scattering shown in Fig. A-19.

In predicting scattering over a geographic area, the statistical approach described above will be used, ignoring the time-varying nature of the scattering. The resulting map with the wind direction NE-SW (worst case), based on all 35 turbines and with no diffraction loss, is shown in Fig. A-22. An omnidirectional antenna is assumed, and the material reflection coefficient is assumed to be unity. As the blades are not metallic, a more realistic material reflection coefficient would be about 0.5. With these assumptions, the maps are will overestimate the scattering coefficient.

Figure A-22 shows that, for the blades as for the pylons described earlier, the backscattering is largely confined to a narrow beam along the line from the transmitter to the wind farm. The position of maximum interference is 5.5 km NE of the centre of the wind farm. The interference in the forward scatter direction is much less than in the backscatter direction. The scattering coefficient map has a complex spatial distribution. Although not visible in this version of the plot, the interference "hot spot" has a value of 0.11 and is confined to a narrow region a few hundred metres long.

---

[4] If the small blocking effect of the pylon is ignored, then the scattering geometry is symmetrical about two directions 180º apart. The small axial rotation of the blade is ignored in this analysis.

[5] With a rotation period of 2 s, the angular rotation during an OFDM symbol period is 0.18º.

FIGURE A-21

Calculated scattering coefficient variation from 35 turbines for the period of one rotation of the rotor

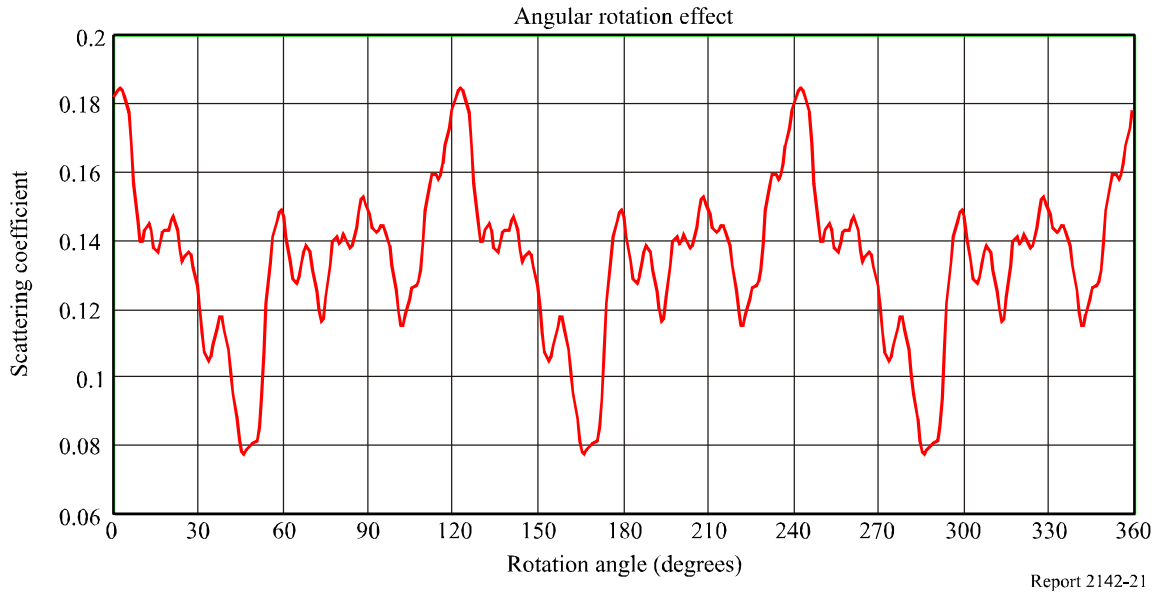

FIGURE A-22

Calculated scattering coefficient from the blades of 35 wind turbines (red dots)

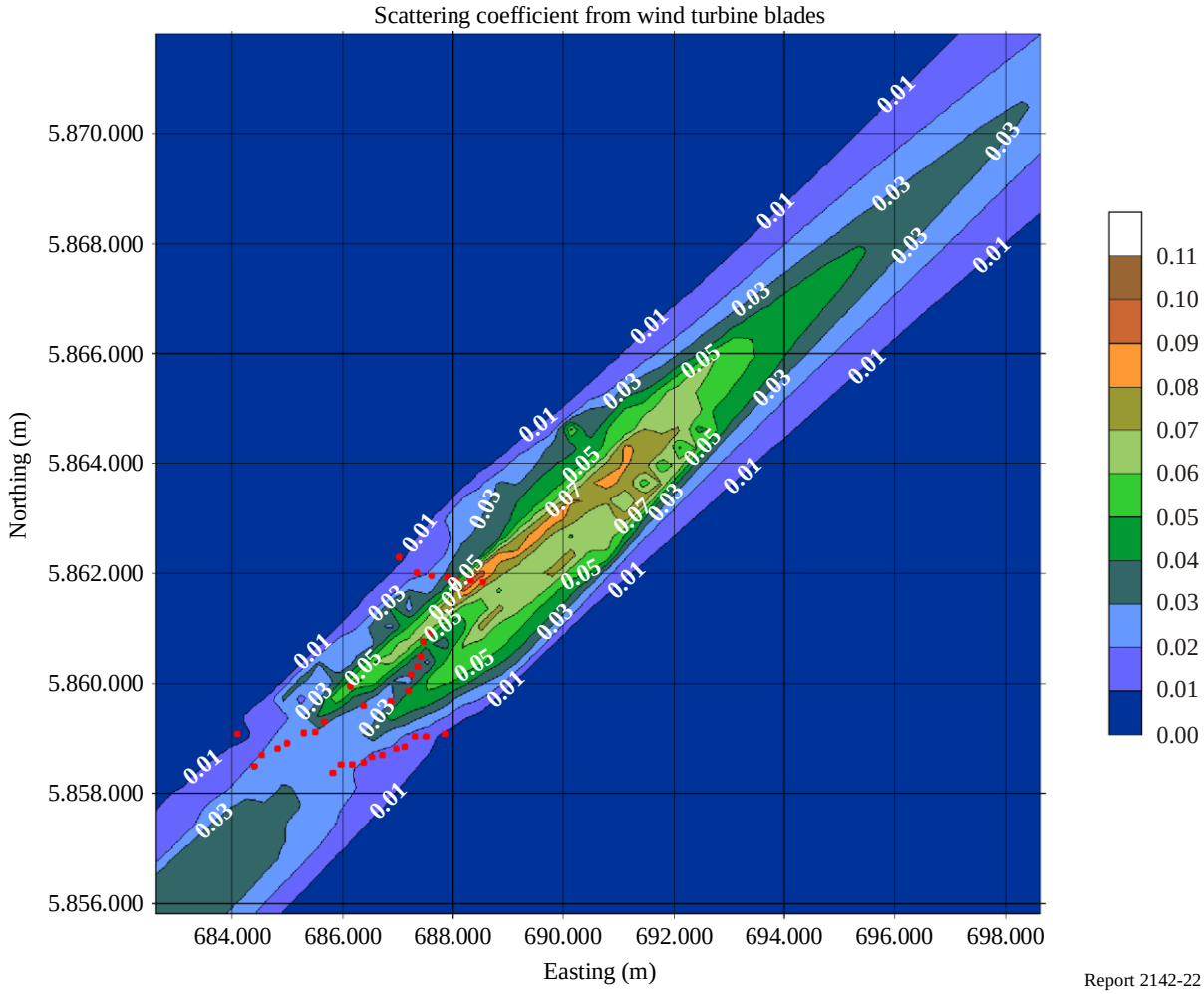

The wind direction is SW-NE, approximately along the line from the transmitter to the wind farm, which results in worst-case interference. The rotor rotation angle is assumed to be a random variable with uniform distribution. The peak scattering coefficient is about 0.11. The grid size is 2 000 m.

The calculated scattering coefficients for other wind directions are shown in Figs. A-23 and A-24. In Fig. A-23 the wind direction is N-S, and the backscattered and forward-scattered signals are approximately at right angles. As the incident signal is not normal to the blades, the peak value of the interference signal is somewhat less (0.08 compared with 0.11) than in Fig. 22, but the backscattered signal is still much greater than the forward-scattered signal.

Figure A-24 represents scattering when the wind direction is SE-NW and blades are edge-on to the incident signal. The scattering is quite small, confined to a region close to the wind farm, and approximately omnidirectional. However, the effect of the motion of the blades should be considered. The speed at the tip of the blades is of the order of 100 m/s, and the associated Doppler frequency for an RF frequency of 600 MHz is ±200 Hz. As the OFDM signal tone spacing is about 1 000 Hz, the scattered signal could result in appreciable spectral widening, with consequential effects on the digital television receiver decoding performance. However, as the magnitude of the scattered signal is low, this effect should be relatively small.

FIGURE A-23

Calculated scattering coefficient from the blades of 35 wind turbines (red dots)

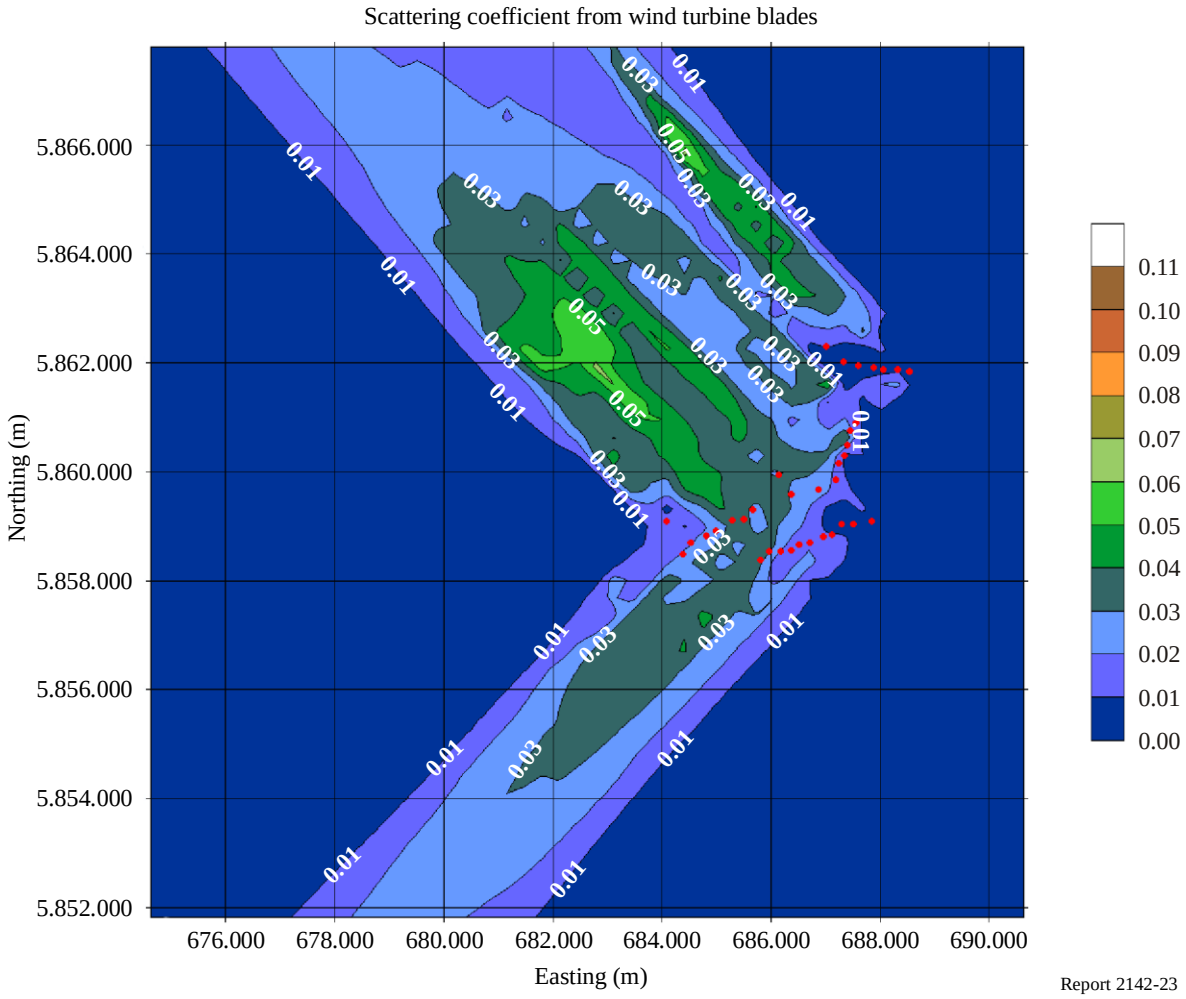

The wind direction is S-N. The rotor rotation angle is assumed to be random with uniform distribution. The peak scattering coefficient is about 0.08. The grid size is 2 000 m.

FIGURE A-24

Calculated scattering coefficient from the blades of 35 wind turbines (red dots)

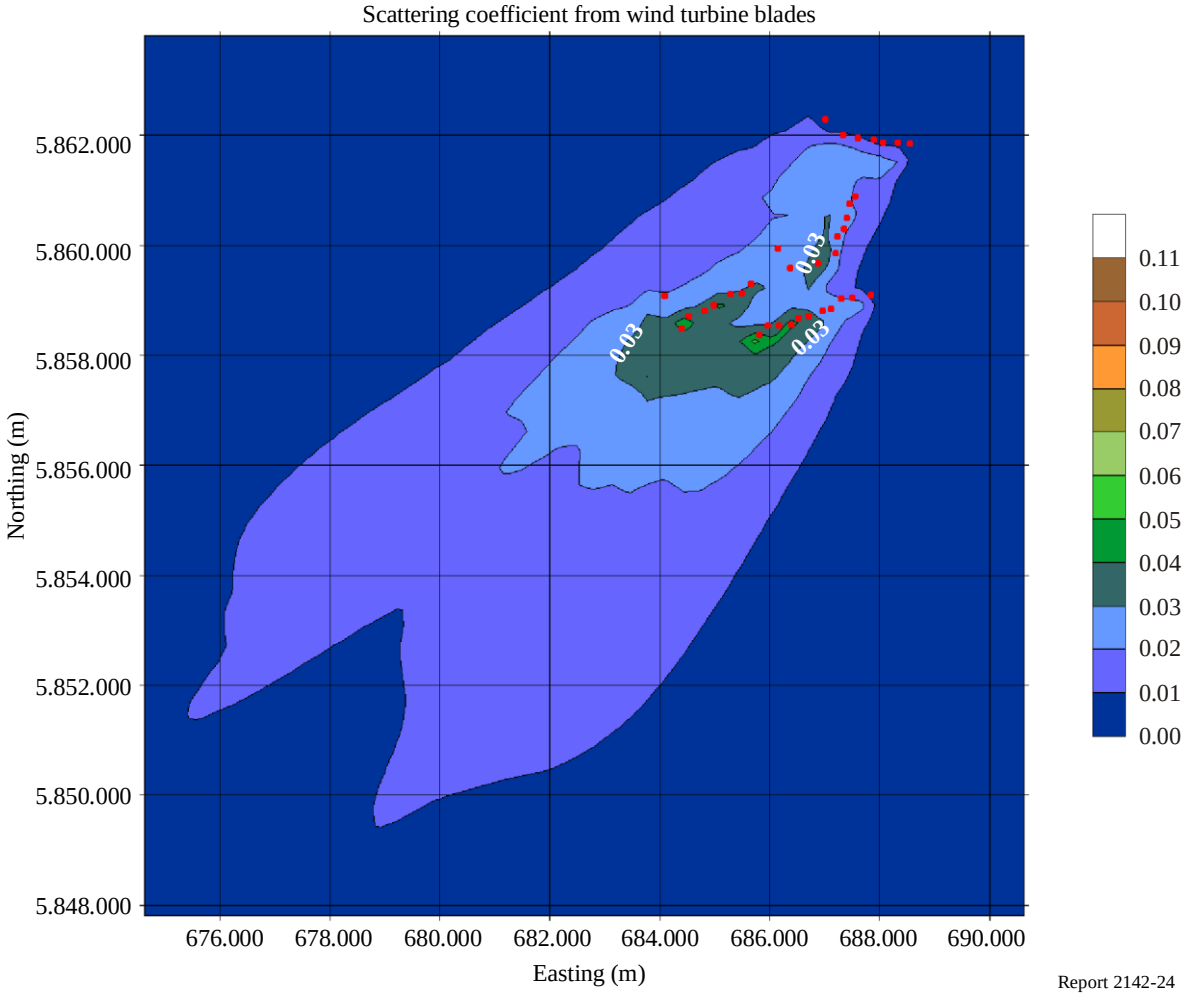

The wind direction is SE-NW, approximately normal to the line from the transmitter to the wind farm, resulting in minimum scattering of the signal, both in magnitude and geographic area. The rotor rotation angle is assumed to be random with uniform distribution. The peak scattering coefficient is about 0.06. The grid size is 2 000 m.

2.5 Predicted receiver performance

The performance of digital television receivers was assessed using methods described in Recommendation ITU-R BT.1735 – Methods for objective quality coverage assessment of digital terrestrial television broadcasting signals of System B specified in Recommendation ITU-R BT.1306. This Recommendation defines the "quality" of the receiver output in terms of the bit error rate (BER) and the signal strength. In the context of the scattering from wind turbines, the most important parameter is the BER out of the receiver demodulator, before error correction.

The BER for locations near the wind farm was estimated from the predicted impulse response. Using a good antenna, about 100 ms of signal was recorded in suburban Sydney, Australia. This received signal had low multipath corruption, with a measured modulation error ratio (MER) of about 27 dB, and a channel BER (termed CBER in Recommendation ITU-R BT.1735) of about 0.002. This reference signal was used to generate simulated signals based on the propagation impulse responses computed by the scattering simulation program.

The reference signal is shown in Figs. A-25 and A-26. The impulse response in Fig. A-25 is largely free from multipath corruption. The computed channel BER for about 100 symbols is shown in Fig. 26 with a mean value of BER of 0.0019. As defined in Recommendation ITU-R BT.1735, satisfactory operation for a rate 2/3 Viterbi decoder requires a BER less than 0.04.

FIGURE A-25

Computed impulse response of the reference signal, largely free from multipath interference

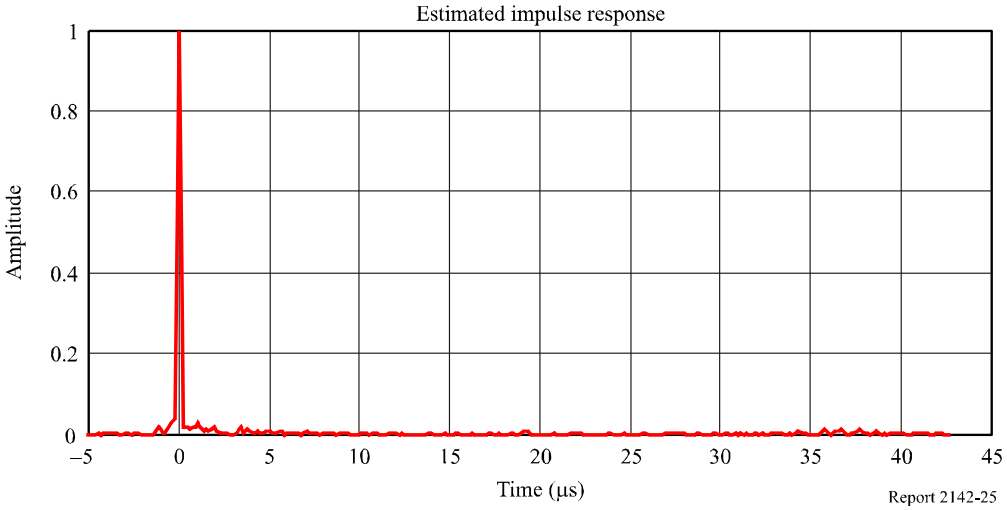

FIGURE A-26

Computed channel BER for the reference signal for 96 symbols

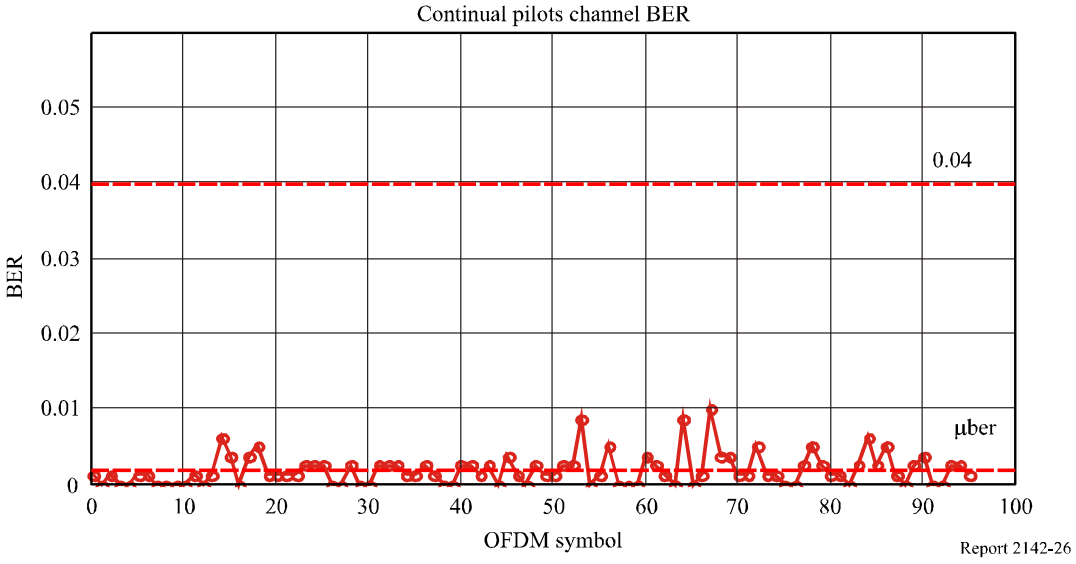

The mean BER is 0.0019, but with some symbols peaking at about 0.01. The limit for satisfactory operation is 0.04.

The same parameters were then calculated for the wind farm “hot spot” location, assuming an omnidirectional antenna. The results are shown in Figs. A-27 and A-28. Compared to the ideal response in Fig. A-25, the impulse response of Fig. A-27 has components at delays greater than about 35 µs. Figure A-28 demonstrates that the BER is significantly degraded relative to the reference signal, and the BER is well above the acceptance limit of 0.04, so digital television reception would not be possible. However, the calculations assumed an omnidirectional antenna, and considerable improvement would result from an antenna with a good front-to-back ratio.

FIGURE A-27

Computed impulse response at the Challicum Hills "hot spot" with scattering from 35 wind turbines (pylons and blades)

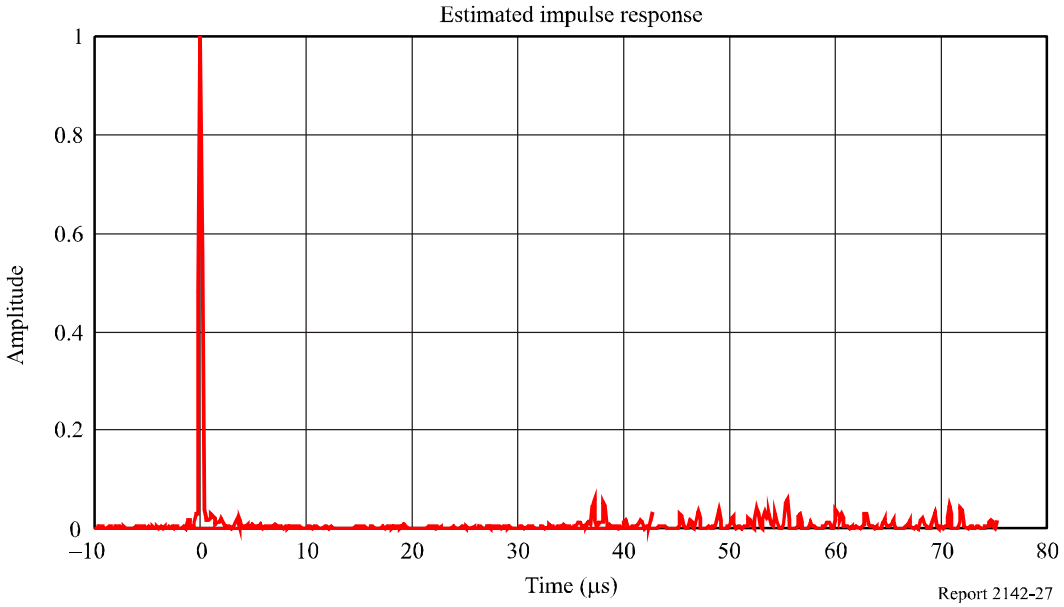

The receiving antenna is omnidirectional. The peak multipath interference occurs at about 35 µs delay, and has a value of about –23 dB.

The mean BER is about 0.123, far above the acceptable limit of 0.04.

Figures A-25 to A-28 were calculated with an omnidirectional antenna, but by changing the assumed antenna gain, the performance of the receiver over a range of operating conditions can be estimated. The results are summarized in Figs. A-29 and A-30.

Figure A-29 shows the effect of the scattering coefficient on the channel BER. At the BER of 0.04 (satisfactory performance), the allowable scattering coefficient is about –21.5 dB.

The effect of the scattering coefficient on the signal modulation error ratio (MER) at the "hot spot" is shown in Fig. A-30. Based on the scattering coefficient of –21.5 dB, the limiting MER for satisfactory operation is 21 dB.

While the results summarized in Figs. 29 and 30 are for a specific receiver performance, due to the random processes[6] involved, it is expected that these results can be applied to the general case. If the scattering coefficient (at the output of the antenna) can be measured or calculated, the performance of the receiver can be determined from these figures. The importance of the antenna gain and the scattering geometry is clearly evident, as the scattering coefficient can be affected by 10 dB or more by the antenna directivity.

[6] The multipath signal is the sum of a large number of random scattering processes. The statistics are approximately Gaussian with the single defining parameter being the scattering coefficient.

FIGURE A-28

Computed channel BER at the Challicum Hills "hot spot" with scattering from the 35 wind turbines (pylons and blades)

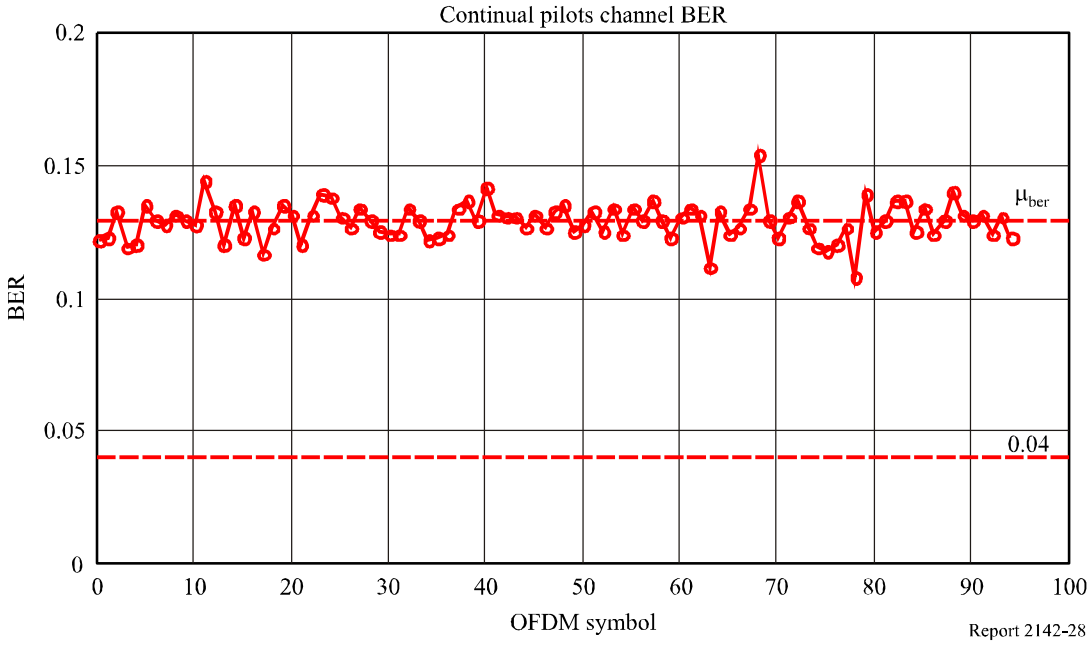

FIGURE A-29

Computed channel BER at the Challicum Hills "hot spot" with scattering from the 35 wind turbines (pylons and blades) as a function of the scattering coefficient

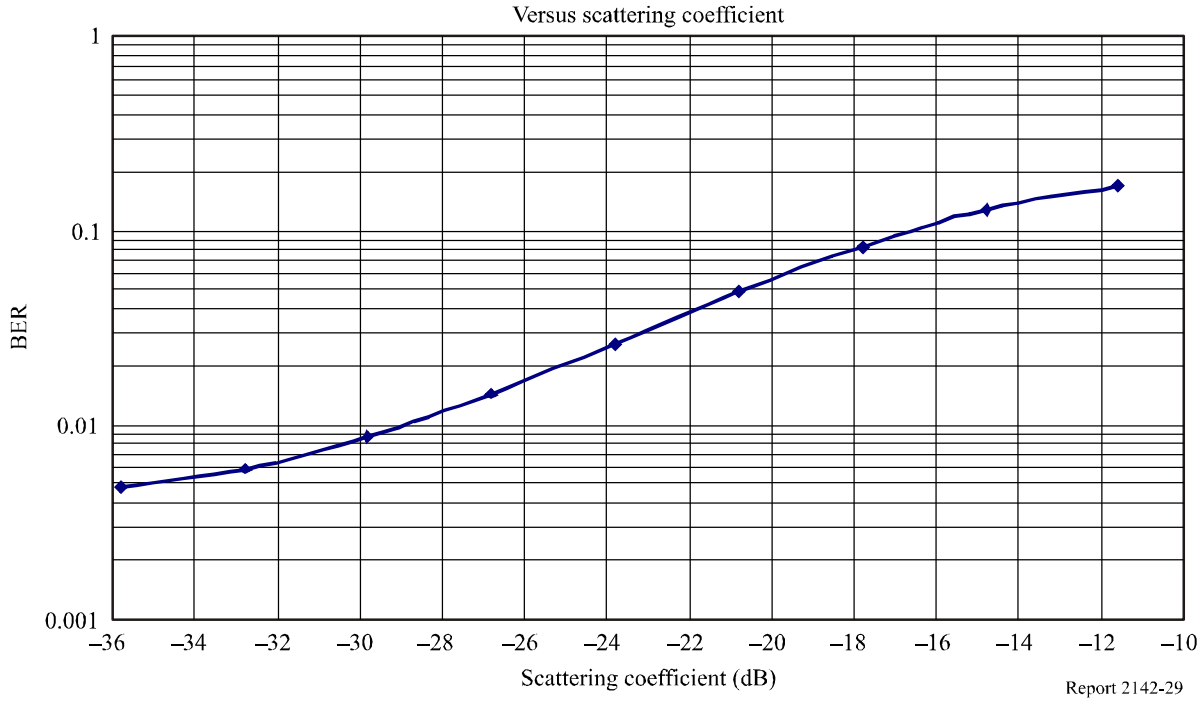

The limiting BER for satisfactory operation of the receiver is 0.04, so the limiting scattering coefficient is about 21.5 dB.

FIGURE A-30

Computed channel MER at the Challicum Hills "hot spot" with scattering from the wind turbine pylons as a function of the scattering coefficient

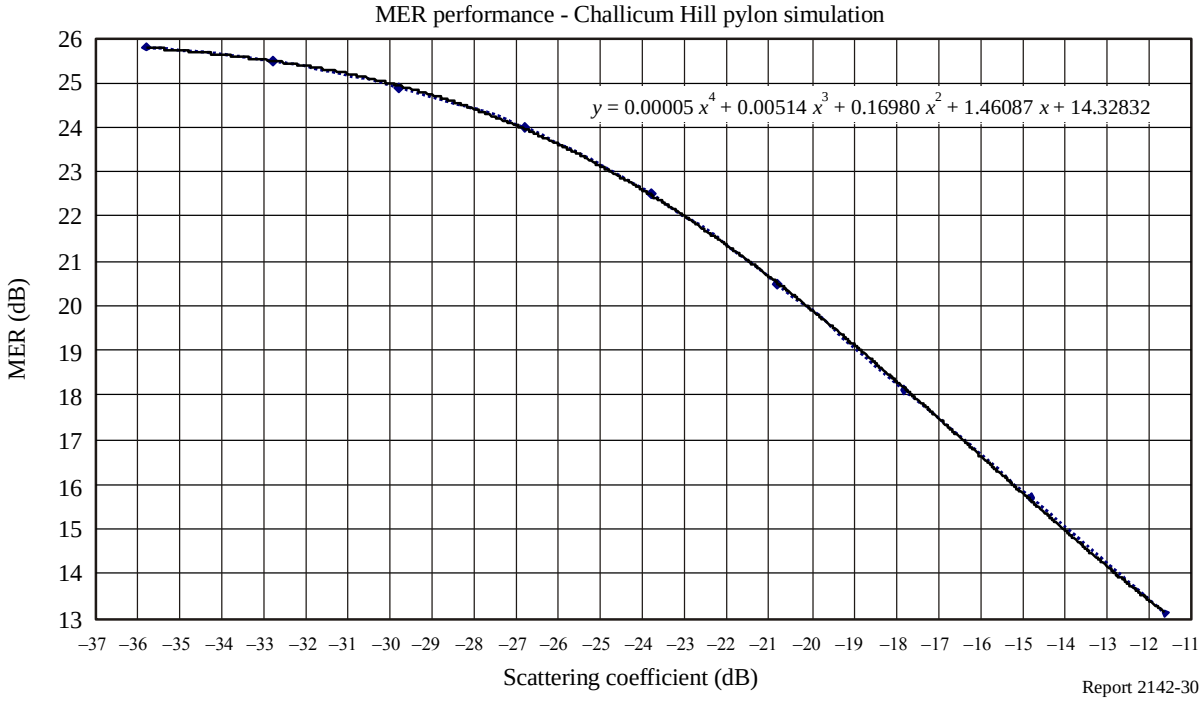

The MER curve is fitted with a fourth-order polynomial, which can be used to estimate the MER from the scattering coefficient (or vice versa).

In Fig. A-31 the scattering coefficient from the pylons and the blades together was converted to prediction of MER using the relationship in Fig. A-30. Similarly, Fig. A-29 could be used to convert the scattering coefficient map to a CBER map. Assuming an omnidirectional receiving antenna, the minimum MER in Fig. A-31 is 18.2 dB. As the minimum acceptable MER is 21.5 dB, the areas of blue and dark green, in the backscatter direction, would have unsatisfactory reception with an omnidirectional antenna. Locations for measurements, as described in § 3, were chosen by overlaying Fig. A-30 on a map of the local terrain.

Scattering from the blades assumes a material reflection coefficient of 0.5. The wind direction is SW-NE (worst case).

3 Measurement results

3.1 Overview

Measurements were made in the area surrounding the wind farm, both in the forward scattering and the backscattering regions, at locations where interference was expected. As described in § 2, at any given point, scattering from the pylons is constant, but scattering from the blades depends on the wind direction. The wind directions during the measurements were such that the blade scattering region was generally in a different direction from that from the pylons, so the worst-case scenario could not be measured. For all but one location, the interference was mainly from the pylons. However, one location did include scattering from the blades, where the scattered signal varied quite rapidly in time which could significantly affect the performance of digital television receivers.

Section 3.2 provides results from a measurement with a single interference source. Section 3.3 gives the results of the dynamic interference from the rotating blades, including the time variation of the signal. Section 3.4 provides details of the measured impulse response compared with predictions. Finally, § 3.5 provides results relating to the effects of ground reflections on the reception of the digital television signals.

FIGURE A-31

Computed MER map for the wind farm (blue dots) for scattering from the wind turbine pylons and blades

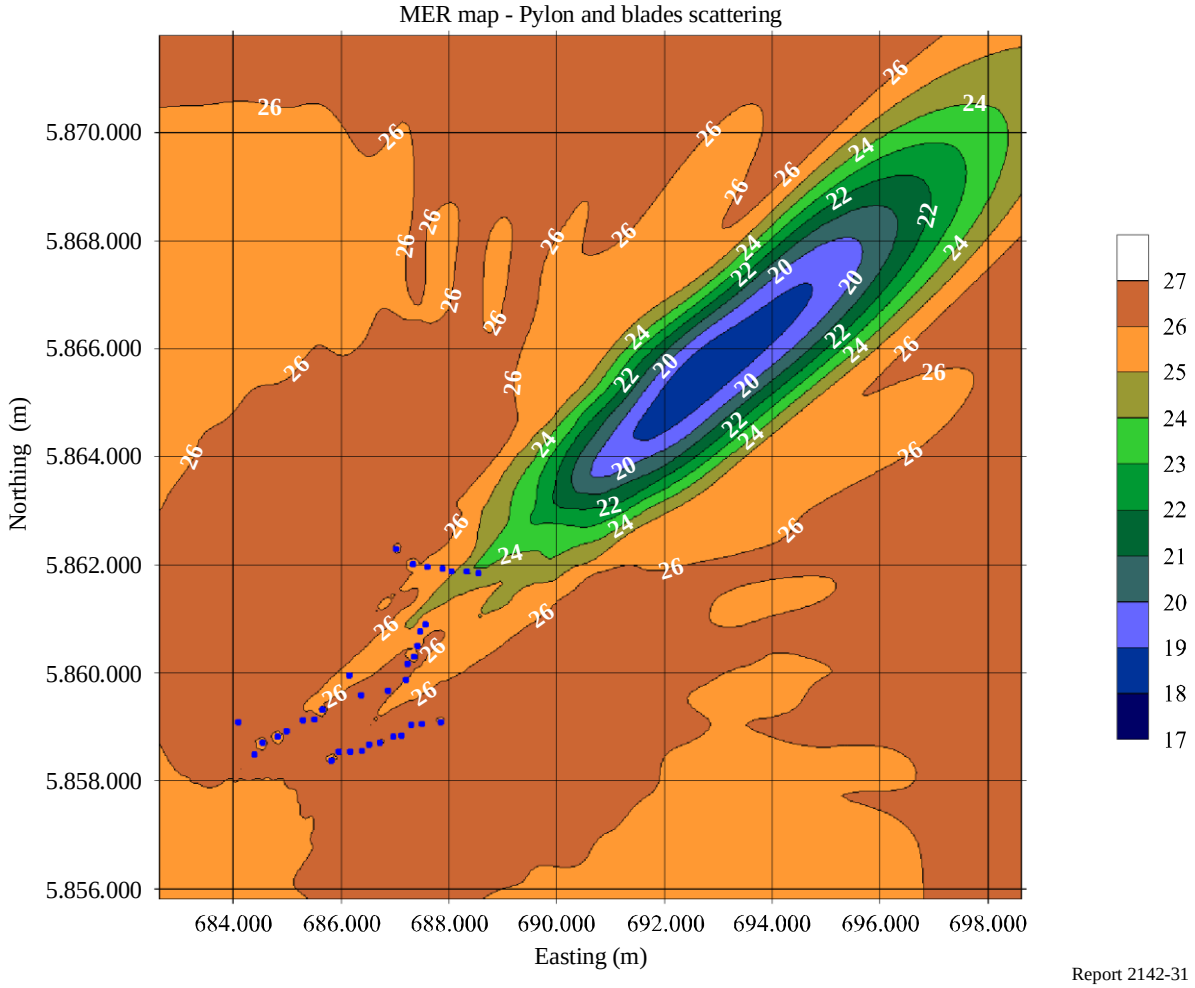

3.2 Measurement with single multipath component scattering

The first measurement location was originally chosen to obtain a reference signal, but the measured data show evidence of a single interference source. The measurement point was some distance from the wind farm, although visually LoS to almost all the wind turbines, and had a clear LoS to the transmitter. It was in an open area away from other interference objects such as trees and hills. However, the measurements show the presence of a significant multipath signal which potentially could degrade the reception performance.

The averaged spectrum of the channel is shown in Fig. A-32. The data are measured at the receiver IF output which has a nominal frequency of 32/7 MHz. The maximum frequency is half the sampling rate of 20 Msample/s. The two spikes below 1.2 MHz are associated with an adjacent (analogue) TV channel. The slow slope across the channel is believed to be an artefact of the transmitted signal.

The averaged spectrum clearly shows the 64-QAM data and the larger pilot signals. The nominal shape of the spectrum should be a constant amplitude across the channel, but this measurement shows an approximately sinusoidal component with a period of about 550 kHz. This spectral shape indicates a single interference source, with the sinusoidal amplitude being the relative amplitude of the multipath signal, and the reciprocal of the spectral period being the multipath delay. In this case the relative amplitude of the multipath signal is about 0.1, and the delay is 1/0.55 = 1.8 μs. The average signal-to-noise ratio is 28 dB, which is typical of the maximum SNR from the receiver.

FIGURE A-32

Measured spectrum of channel averaged over 500 symbols

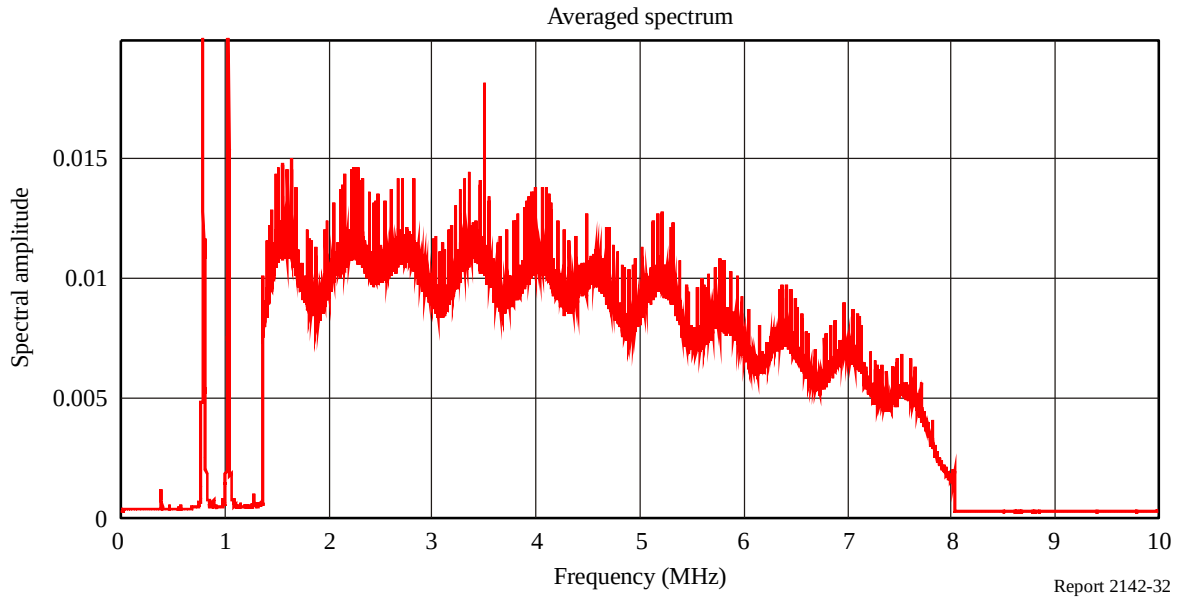

The amplitude scale is arbitrary, as the equipment does not measure absolute signal strength.

Figure A-33 shows the calculated impulse response from the measured spectrum. The multipath signal is essentially confined to a single interference source with a delay of 1.65 μs and a relative amplitude of 0.1. These results agree with those derived from the spectrum, but are more accurate as the spectral data has more “noise” due to the 64-QAM data modulation. While the two methods result in similar conclusions, the impulse response method is preferred.

Calculated impulse response for the spectrum shown in Fig. A-32. The relative amplitude is 0.1 (–20 dB), and the multipath delay is 1.65 μs. The measurement time resolution is 0.3 μs.

As the receiver is located in an open area, the multipath interference is most likely located at the transmitter end. The most probable location for the interference source is a ridge about 2 km from the transmitter along the propagation path.

FIGURE A-33

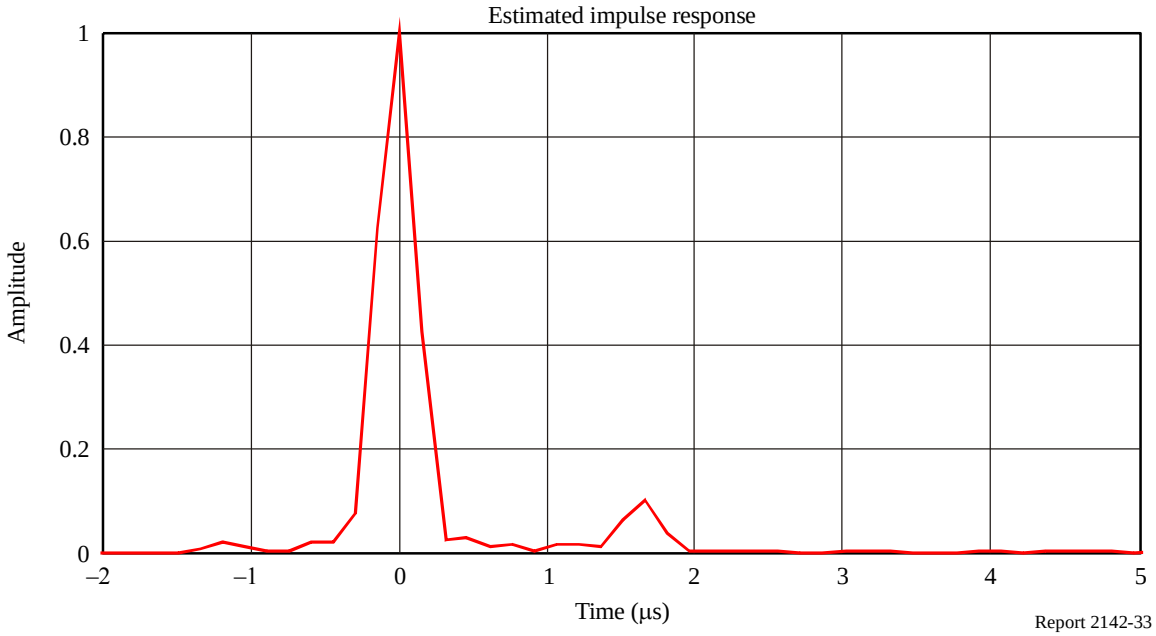

The signal spectrum variation due to multipath signals can be corrected in the receiver by using the scattered pilot signals as a reference. Residual errors after this correction are random due to receiver noise and are not due to the multipath interference. The measure of this noise can be expressed as the Ricean factor (ratio of the signal power to the noise power). The Ricean factor is closely related to the MER typically used for digital television quality specification. In this case it is calculated as 26 dB, and the associated 64-QAM MER is 24.6 dB. This relatively poor MER performance is due to the phase noise in the receiver rather than the signal itself.

3.3 Dynamic interference signal performance

A second example is taken from a site which was close to four wind turbines, where the direct signal was blocked by nearby hills and therefore reduced by about 30 dB. Consequently, the signal-to-interference ratio was considerably reduced, making the variation in the signal large relative to the direct signal. Further, the wind direction was such that the reflections from the blades (from one wind turbine in particular) were directed towards the receiver.

The measurements at this point are shown in Figs. A-34 to A-38. The parameters were calculated every fourth symbol (approximately every 4 ms). The dynamic effects due to the rotating blades result in time variations on the time scale of the order of 10-50 ms. All the data are based on a transmission with a 1/8 guard period, which is sufficient to ensure there is no inter-symbol interference.

The variation in the signal SNR (based on the guard period and the corresponding section of the useful part of the symbol) and the Ricean factor (derived from the impulse response) is shown in Fig. A-34. The pattern is complex due to the scattering from more than one wind turbine. The main feature is the sharp drop in the SNR/Ricean factor, which occurs at about a 1 s period, which is the period of repetition for the rotating blade. Simulations suggest and these measurements confirm that when a blade is appropriately orientated, a narrow scattered beam is created. The signal magnitude can drop to a minimum then increase to a maximum in a period of about 30 ms. While this period is relatively long compared with the symbol period of about 1 ms, the performance is critically dependent on how the receiver tracks these changes.

FIGURE A-34

Computed SNR and Ricean factor as a function of time at location site 8

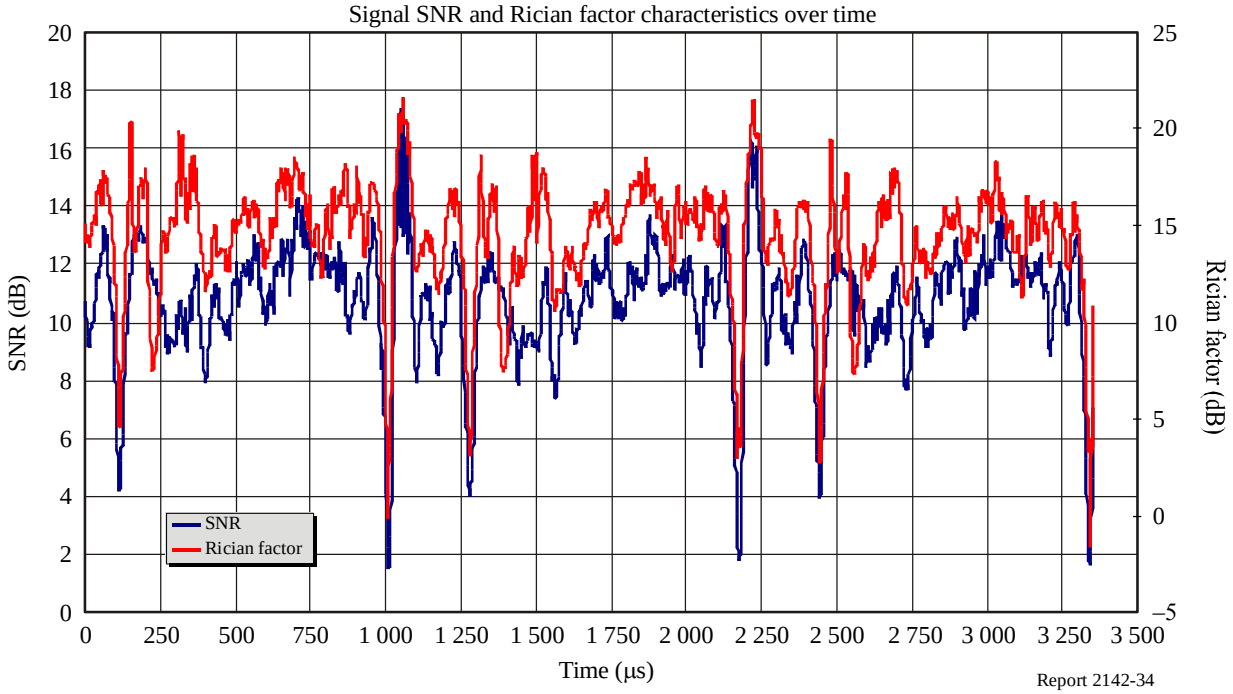

The effect on the computed frequency error is shown in Fig. A-35. The frequency error is incorrectly computed when the scattered signal is large, and some form of averaging is required to avoid mistuning the receiver. In addition, the receiver tuning "noise" is increased to 21.6 Hz from the reference signal value of 15 Hz.

FIGURE A-35

Computed fine tuning frequency correction as a function of the symbol number

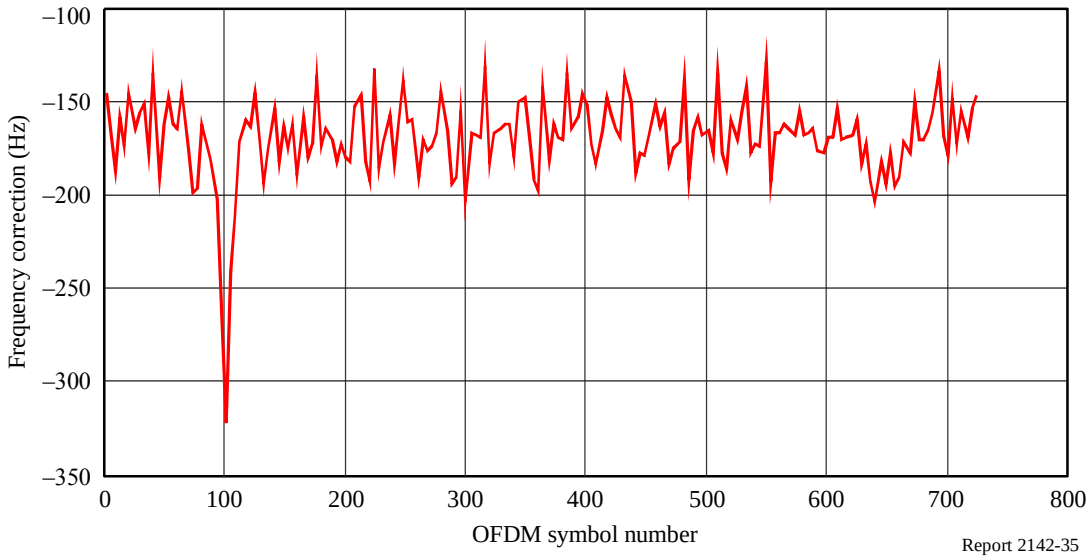

There is a large incorrect frequency error estimate at about symbol 100 due to the scattering. The frequency error noise in other symbols is a combination phase noise in the local oscillator and the effects of signal scattering. The standard deviation in the frequency estimate is 21.6°.

The effect on the measured pilot phase error is shown in Fig. A-36. The interference signal causes large phase errors when the interference is maximum, but the general phase error increased from the reference level of about 2.5° (due to oscillator phase noise) to about 4° due to the interference environment.

FIGURE A-36

Computed standard deviation in the continual pilots phase (using the scattered pilots as a reference) as a function of symbol number

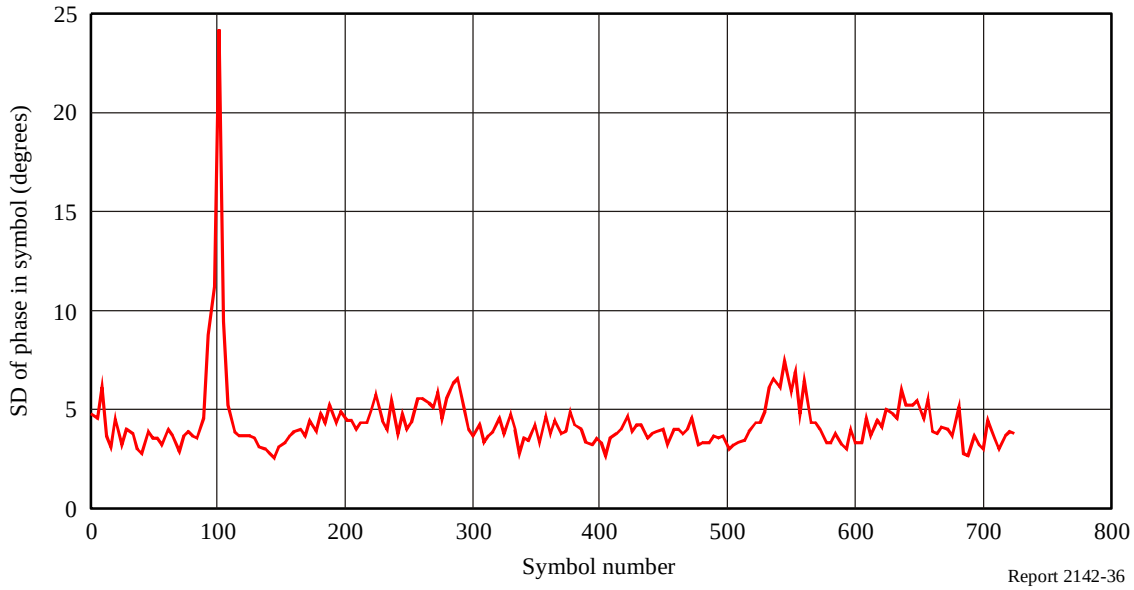

The large error at about symbol 100 and the smaller error at about symbol 550 are due to scattering.

The phase noise will limit the MER, as shown in Fig. A-37. The MER decreases sharply when the interference effect is greatest, and the mean MER is also decreased to about 22 dB, a value close to the operational limit. The MER also shows slower, smaller variations which are due to scattering from rotating blades. The observed effect of the lower mean MER on the receivers was that the picture quality was variable but generally satisfactory, with occasional loss of picture and sound.

The BER as a function of time is shown in Fig. A-38. This essentially mirrors the characteristics of the MER with both slow and fast variations. While the mean BER of 0.027 is satisfactory compared to the limit of 0.04, the BER frequently exceeds this value, so the characteristics of the error correcting schemes will determine the overall performance.

Overall, the received signal was considered unsatisfactory at this location. The relationship between the mean MER, the slow MER variations, the short-term MER notches and the receiver performance is not clear, but normally a MER of 22 dB should be satisfactory according to Recommendation ITU-R BT.1735. Clearly this Recommendation does not account for dynamic signal variations such as those from rotating wind turbine blades. An additional margin in the required MER should be specified when operating near wind turbines, although the magnitude of this increase has not yet been determined.

FIGURE A-37

Computed MER of the scattered pilot signals as a function of time

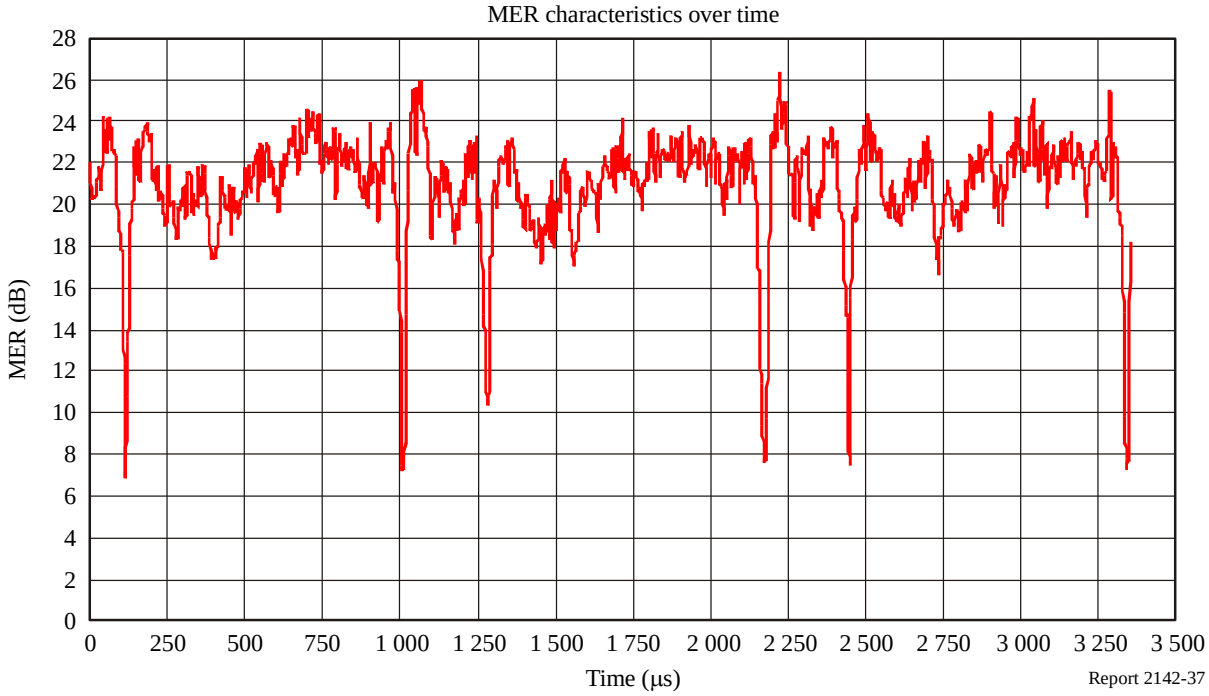

FIGURE A-38

Estimate BER of 64-QAM symbols based on the scatter diagram of the continual pilots after equalization using the scattered pilots

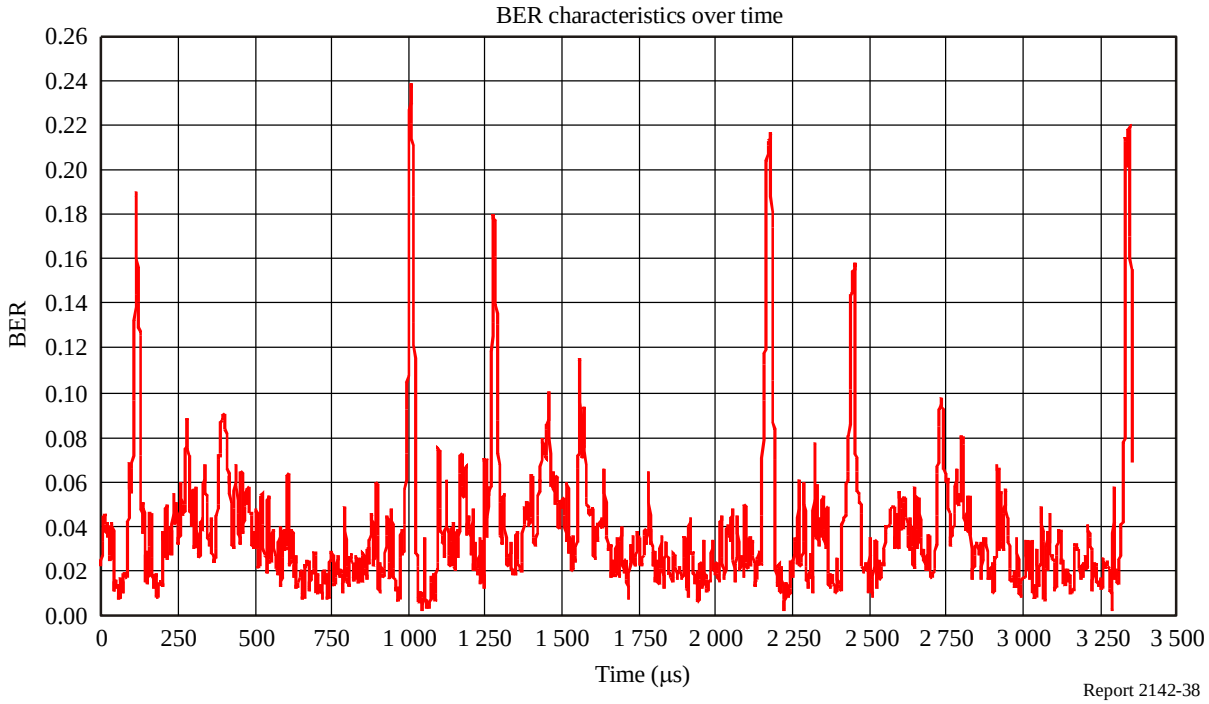

The main sections of poor performance occur at around symbols 100, 550 and 650, although there are other areas where the BER exceeds the required BER threshold for satisfactory operation. The performance was unsatisfactory as confirmed by subjective observations of the picture and sound quality.

3.4 Measured impulse response

3.4.1 Overview

As described in § 3.2, the impulse response can be calculated from the measured spectrum of the scattered pilots. With typical receiver noise, it is possible to detect interference sources 45 dB below the direct signal, with a signal-to-noise ratio of typically 10 dB.

While the impulse response method is perfectly general, the actual implementation is different for the backscattering case and the forward scattering case. The simplified geometry of these two cases is illustrated in Fig. A-39. From the geometry it is easily shown that the multipath excess delay (range) for the two cases is given approximately by:

$$\Delta R \approx (1 - \cos\alpha) R \approx 0 \qquad \text{Forward}$$

$$\Delta R \approx (1 + \cos\alpha) R \approx 2R \qquad \text{Back}$$

where R is shown in Fig. A-39. For the backscattering case, the main scattered component occurs at a small reflection angle α, so the delay excess is nearly twice the delay from the wind turbine to the receiver. As this distance is typically a kilometre or more, the resulting delay excess is typically greater than 10 μs in the measurements. Therefore the backscattered signals are easy to detect in the measured impulse response.

FIGURE A-39

Geometry of forward scattering and back scattering from a wind turbine in relationship to the transmitter and the receiver in each case

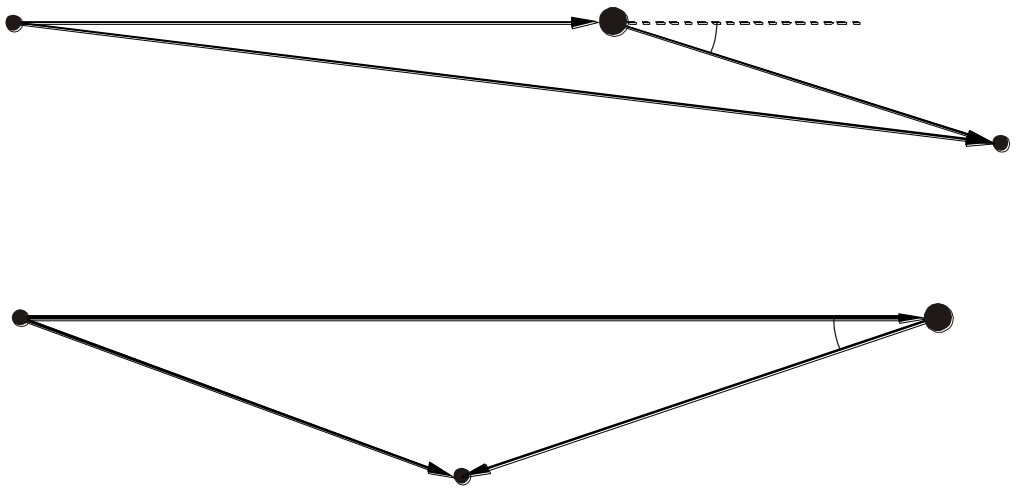

Report 2142-39

In contrast, the forward scattering occurs over a wide angle, but measurements were taken at points for which the scattering angle was relatively small. As a consequence, the delay excess is typically quite small, less than a few microseconds. The resolution of the impulse response is about 0.3 μs, due to the signal bandwidth of about 7 MHz, and therefore the multipath signals are difficult to distinguish from the direct signal.

3.4.2 Backscattering case

The measurement points for backscattering were all located near the straight line joining the wind farm to the transmitter. Figures A-40 to A-42 show the impulse response from three sites. The wind direction was such that minimal interference from the blades would be expected.

FIGURE A-40

Impulse response at Test Point 4

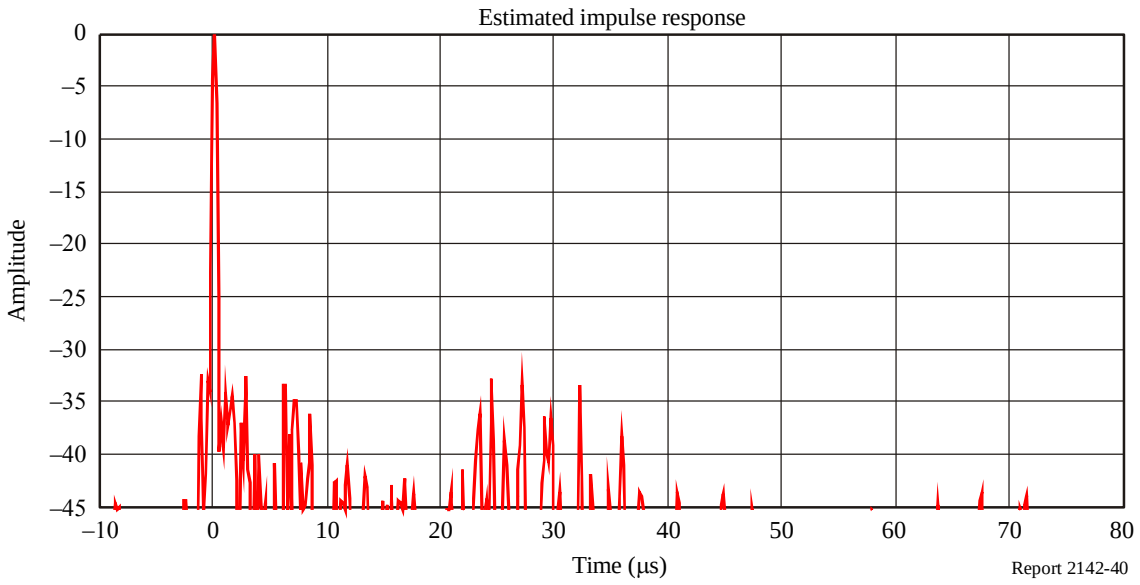

FIGURE A-41

Impulse response at Test Point 5

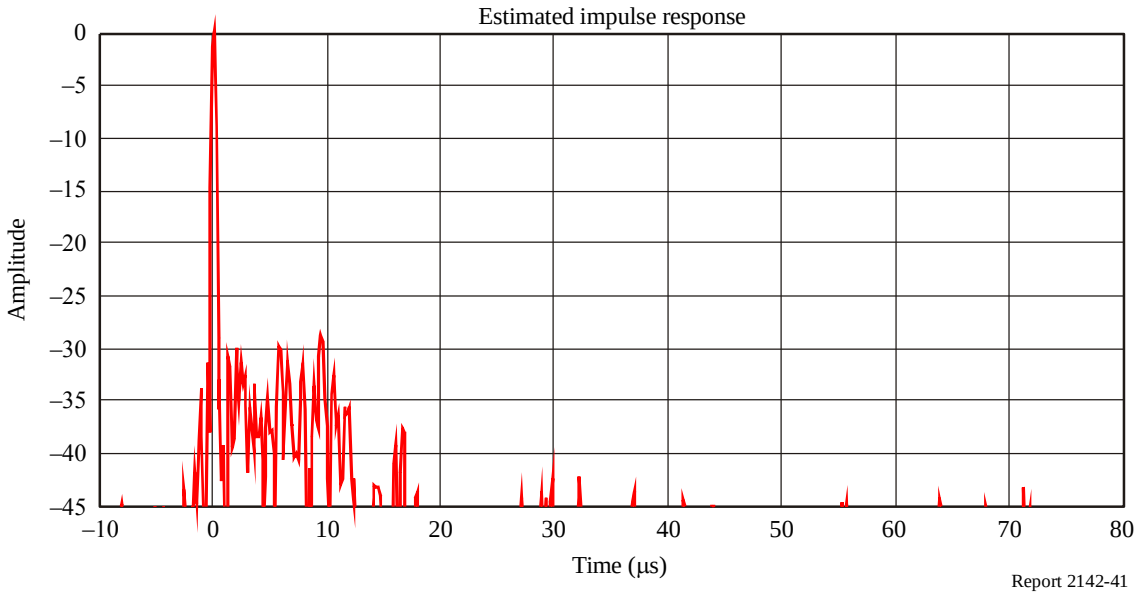

FIGURE A-42

Impulse response at Test Point 7

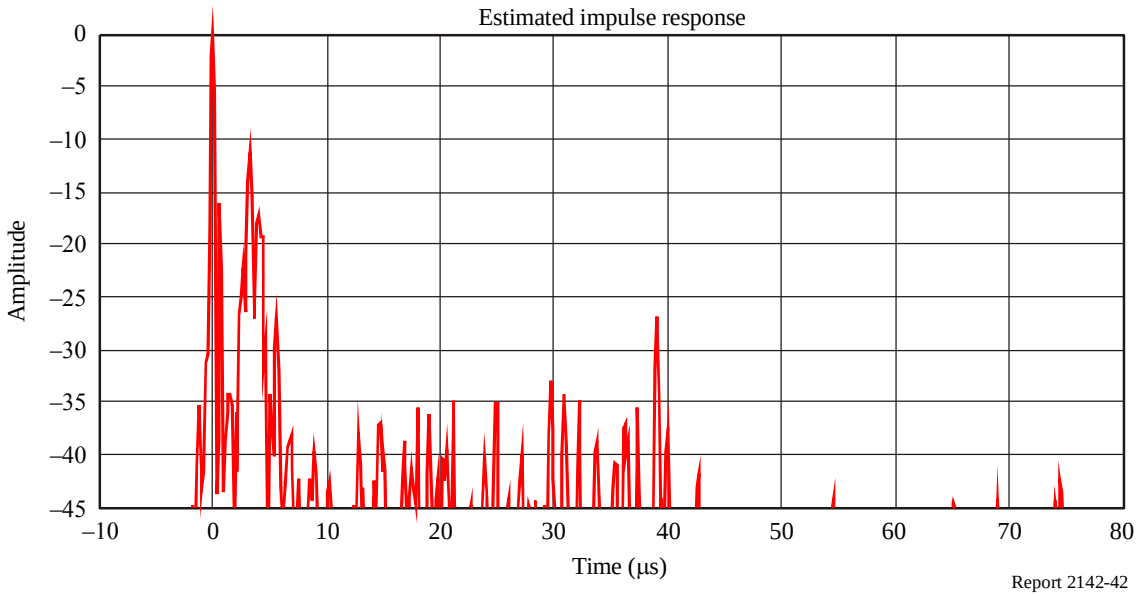

Measurements were made with the antenna pointing towards the wind farm and away from the transmitter, which enhanced the scattered signals relative to the direct signal by a factor equal to the antenna front-to-back ratio, about 25 dB. Even with the antenna pointing away from the transmitter, the dominant signal remains the direct signal from the transmitter. Multipath signals from terrain in the direction of the transmitter were also measured; these had an excess delay of up to 10 μs, while scattering from the wind farm had excess delays greater than 10 μs. As the measurement technique allows multipath signals to be reliably detected down to at least –45 dB, the impulse components in the following graphs indicate multipath signals rather than noise.

The closest wind turbine is 1.8 km, or a 10.5 μs delay. The wind turbine furthest from the measuring point (not LoS) is 7.2 km, or a 47 μs delay. The maximum scattering coefficient is –33 dB (–58 dB with an omnidirectional antenna). The wind turbines closest to the measurement point do not cause the maximum interference. Multipath signals up to 9 μs are due to terrain scattering near the transmitter. Mean BER = 0.022, and mean MER = 23 dB.

The closest wind turbine is 1.5 km (9.5 μs delay). The wind turbine furthest from the measuring point (LoS along the ridge) is 2.4 km (16 μs delay). The maximum scattering coefficient is –28 dB (–53 dB with an omnidirectional antenna). Multipath signals up to 9 μs are due to terrain scattering near the transmitter. Mean BER = 0.023, and mean MER = 23 dB.

The closest wind turbine is 2.0 km (13 μs delay). The wind turbine in this group furthest from the measuring point (LoS along the ridge) is 3.8 km (24 μs delay). Reflections also occur from a second group of wind turbines. The closest wind turbine in this group is 4.1 km (27 μs delay). The maximum scattering coefficient is –28 dB (–53 dB with an omnidirectional antenna). The multipath signals up to 10 μs are due to terrain scattering near the transmitter, including a very strong multipath signal at 3 μs delay. Mean BER = 0.023, and mean MER = 23 dB.

The following conclusions can be drawn for backscattering:

1 Scattering from individual wind turbines is clearly observed.

2 The excess delay for some turbines (nearest and furthest) was calculated and the results agree well with expectations.

3 The magnitude of the scattered signals varied considerably, but the strongest signal measured was a relatively modest –28 dB (or –53 dB after correcting for the antenna front-to-back ratio). There was not a strong relationship between the signal amplitude and the delay. One explanation is that the wind turbines closest to the measurement point have reflected signals that are well above the height of the measurement antenna.

4 The backscattering from the wind turbines was due almost entirely to the pylons alone, as the wind direction during the measurements resulted in the scattering in different direction from the blades. Thus the measured levels of scattering were largely constant over time. This is in contrast to the forward scattering results below.

3.4.3 Forward scattering case

The measurement of the impulse response in the forward scattering case is difficult, as the multipath excess delays from nearby wind turbines is quite small, often less than the measurement resolution. At the two measurement locations, the scattering angle was small with the wind turbines approximately lying along the path from the transmitter. The direct path from the transmitter was also obscured by a nearby hill, resulting in significant diffraction losses. Measurements and diffraction theory give diffraction losses in the range of 25-30 dB. In the forward scatter measurements, the antenna was pointed at the transmitter, which was also the general direction of scattering from the nearest wind turbines. As the wind turbines were located at the top of the hills, there was a considerable enhancement of the scattered signals relative to the direct signal, and therefore the ratio of the scattered signal to the direct signal was greater than in the backscattering case, despite the actual scattering coefficient being smaller for forward scattering.

The measurements are shown in Figs. A-43 and A-44. Only the first 10 μs of the impulse response, where the expected scattering occurs, is shown. As the signals are weaker, the cut-off amplitude is –40 dB. Despite the difficulty in resolving the scattered signals, it is clear that there are interference signals for delays less than about 1 μs. The amplitude of this interference from Fig. A-44 is plotted as a function of symbol number in Fig. A-45, where the variation in the scattered signal as a function of the blade rotation can be observed; the amplitude varies by a factor of 5:1 over a period of about 20 ms. Figures A-44 and A-45 are from the site detailed in § 3.3.

FIGURE A-43

Impulse response at Test Point 2

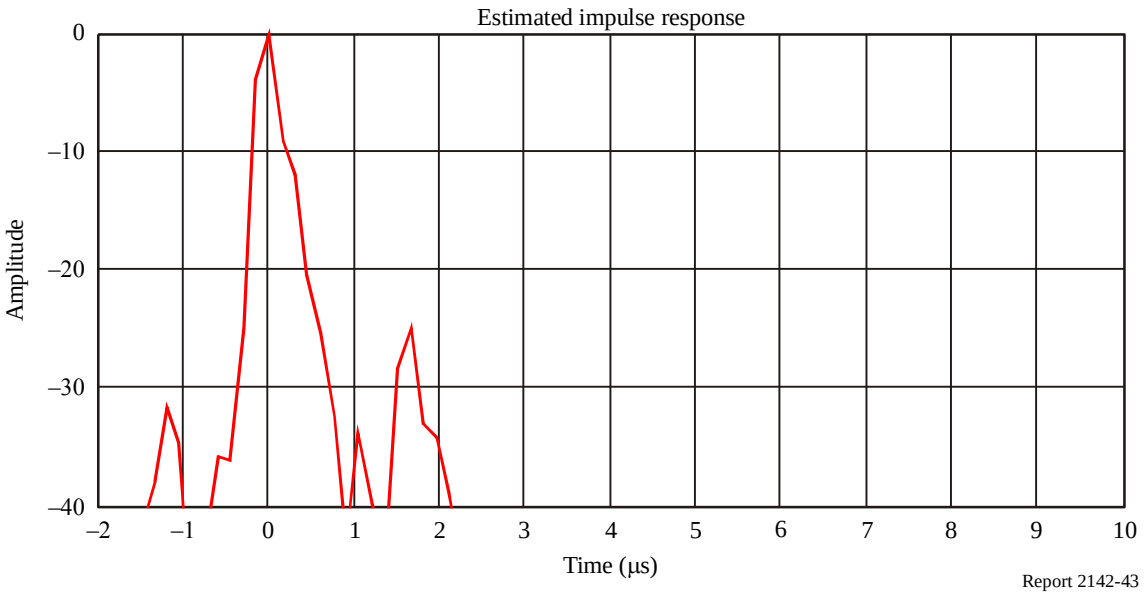

Report 2142-43

FIGURE A-44

Impulse response at Test Point 8

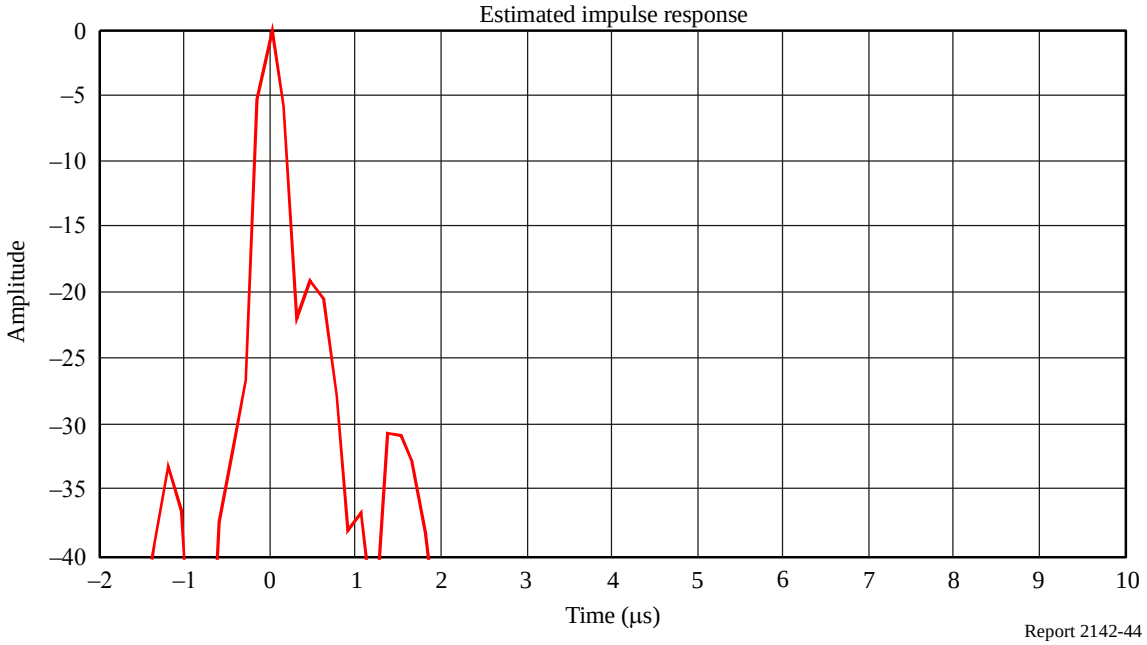

FIGURE A-45

Scattering at Test Point 8 as a function of symbol number

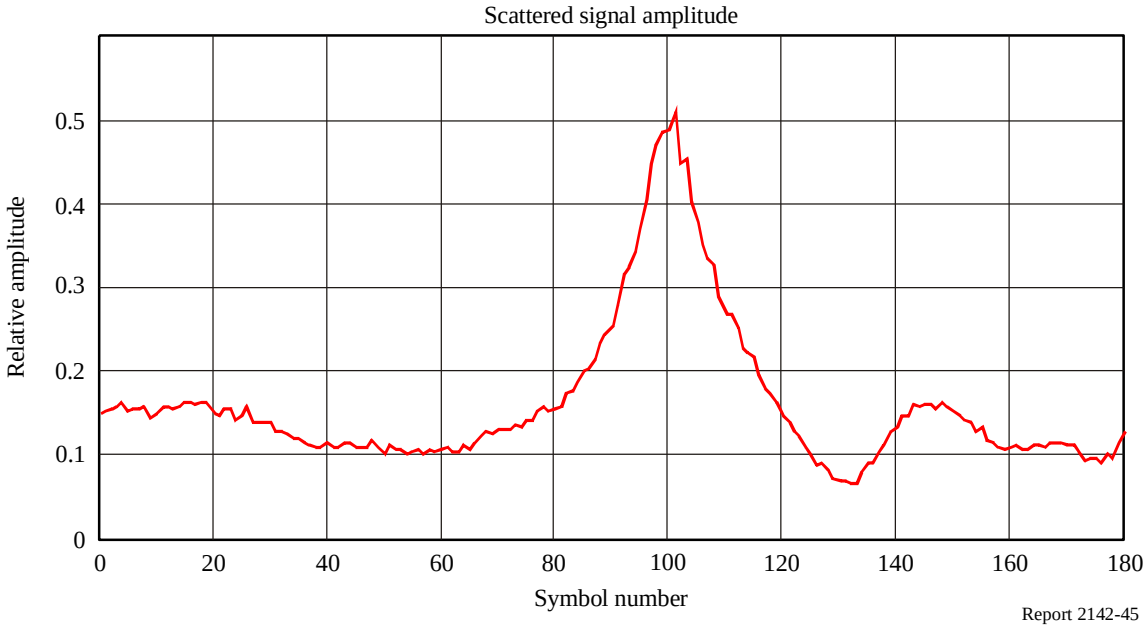

The delays to the nearest turbines are between 0 and 0.9 µs, with another wind turbine having a delay of 1.6 µs. The scattering from the first group can barely be resolved, but the more distant wind turbine can be observed. The mean MER is 24 dB, and the mean BER is 0.015.

As all but one of the wind turbines are nearly on the same line as the direct path to the transmitter, the excess delays are close to zero. The one exception is the wind turbine 1 100 m away (0.5 µs delay). The smaller peak at about 1.5 µs is believed to be the reflections from a row of large trees on the hill with clear LoS to the transmitter. The median MER is 22 dB, and the median BER is 0.028.

The amplitude variation is due to the rotation of the wind turbine blades.

3.5 Effect of receiving antenna height and ground reflections

Two characteristics of the receiving antenna, directivity and height, are particularly important in determining the quality of the television reception. The effect of directivity was not investigated except as an incidental consequence of the procedure of pointing the antenna at the transmitter (normal situation) or pointing the antenna at the wind farm and away from the transmitter (to enhance the relative strength of the scattered signals). For all measurements in the backscatter region, when the antenna was pointed at the transmitter, there were no observable effects due to the scattering from the wind turbines. This was expected, as the small reflections from the wind turbines were further reduced by the front-to-back ratio of about 25 dB.

However, the effect of height and ground reflections on the received signal strength should be considered. As the ground near the measurement sites was relatively flat and free of obstacles such as trees, it causes reflections which enhance or decrease the received signal relative to the free path signal strength. The effects of ground reflections are shown in Fig. A-46 using a two-ray model path gain for a 10-metre receiving antenna. The path gain oscillates as a function of range from the transmitter, so the received signal strength relative to the free path can be as great as +4 dB or as small as –9 dB. Therefore ground reflections can have a significant effect on the received signal.

The parameters used are transmitter height 800 m, receiver height 10 m, surface roughness 10 cm, ground conductivity 0.012 Ω/m, dielectric constant 15.

The reference Test Site 1 is an example where the two-ray model would be expected to be valid. The range is about 20 km, and the effective transmitter height is about 800 m. Figure A-47 shows that the antenna height has a significant effect on the received signal strength. The signal strength does not increase monotonically with height, but has a null at around 6 m. Measurements at the site showed that the signal maximum was at an antenna height of about 10 m. At test site 1, the propagation conditions were such that the signal variation with height did not affect reception quality, but if there is no LoS to the transmitter, it can be significant.

FIGURE A-46

Predicted two-ray loss characteristics for path to receiving site

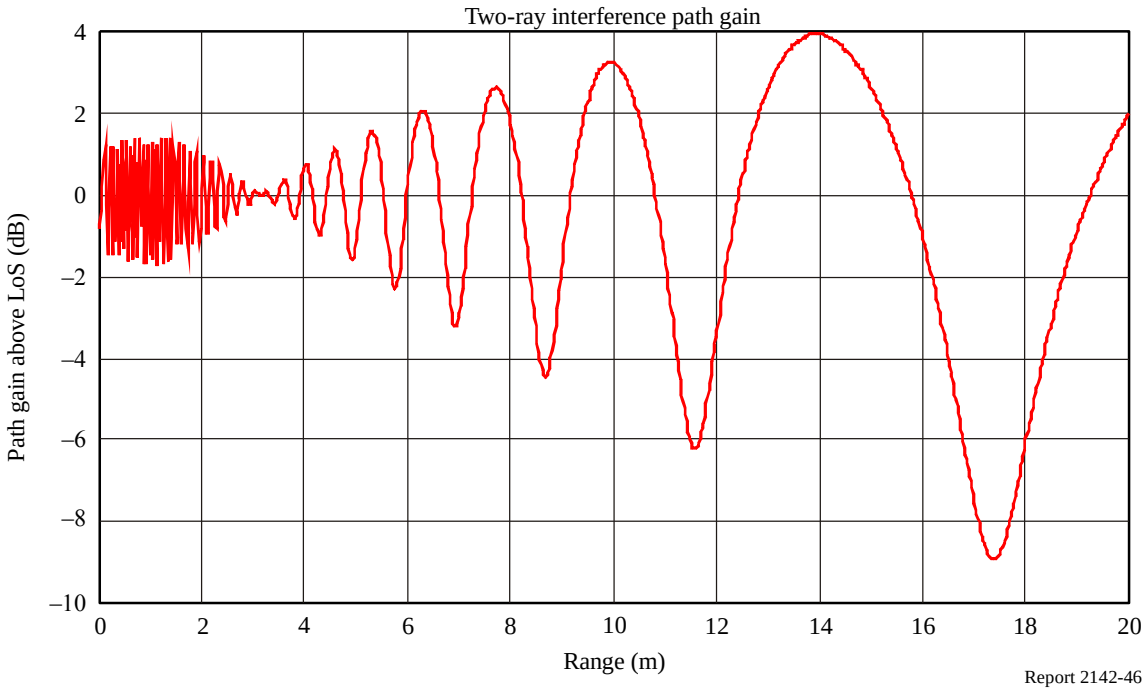

FIGURE A-47

Two-ray model predicted path gain as a function of height for Site 1

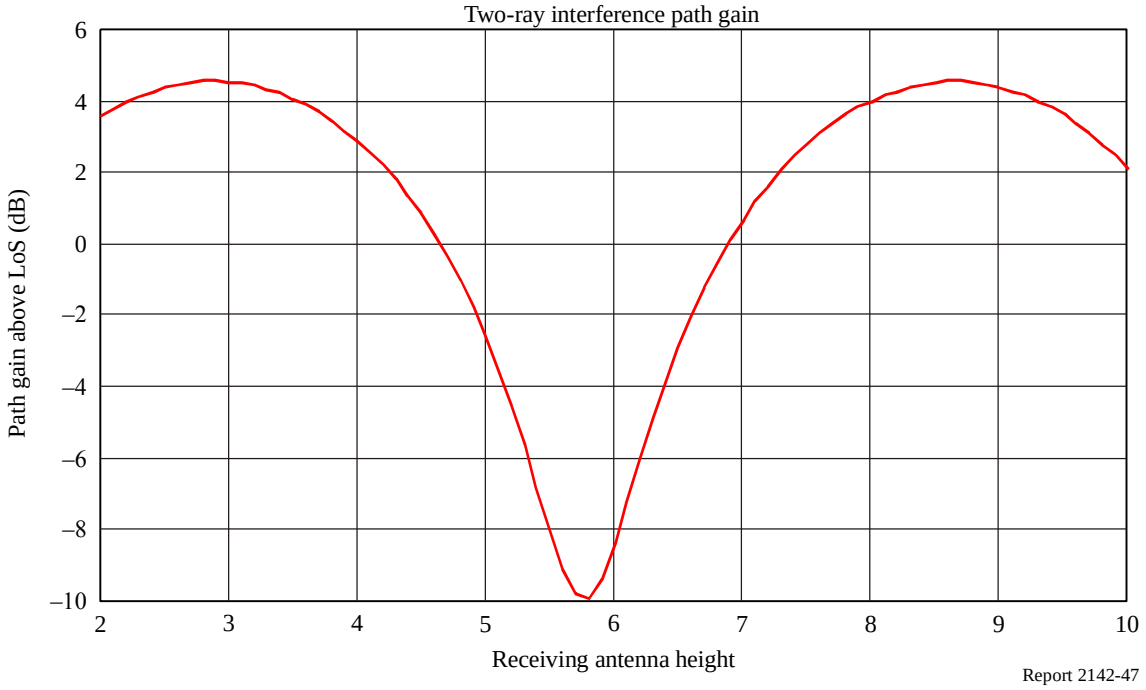

As described in § 3.3, the direct signal at Site 8 is blocked by a nearby hill. The computed effect of ground reflections on both the (diffracted around an adjacent hill) direct signal and the signal scattered from a wind turbine (on top of the hill) is shown in Fig. A-48. The ground effect on the scattering from the wind turbine is relatively small, but the effect on the diffracted direct signal is considerable. The initial measurement at Site 8 used an antenna at 10 m height, but none of the digital television receivers could receive the signal. When the antenna height was lowered to 4.5 m (approximately the maximum), the signal was received, though with marginal quality on some receivers. This illustrates the significance of the correct adjustment of antenna height for optimum performance in difficult reception areas. As this was a forward scattering case, antenna gain is of little benefit, in contrast to the backscattering case.

In conclusion, the effect of antenna directivity and ground reflections can have an important effect on the reception of digital television signals. It should not be assumed that increasing the antenna height will improve reception performance. Given the variability of propagation and terrain, installations at difficult reception areas should investigate several positions and heights to find the optimum position.

FIGURE A-48

Two-ray model predicted path gain as a function of height for Site 8, showing the effect of ground reflections on the direct signal (diffracted over the hill) and the wind turbine on top of the hill

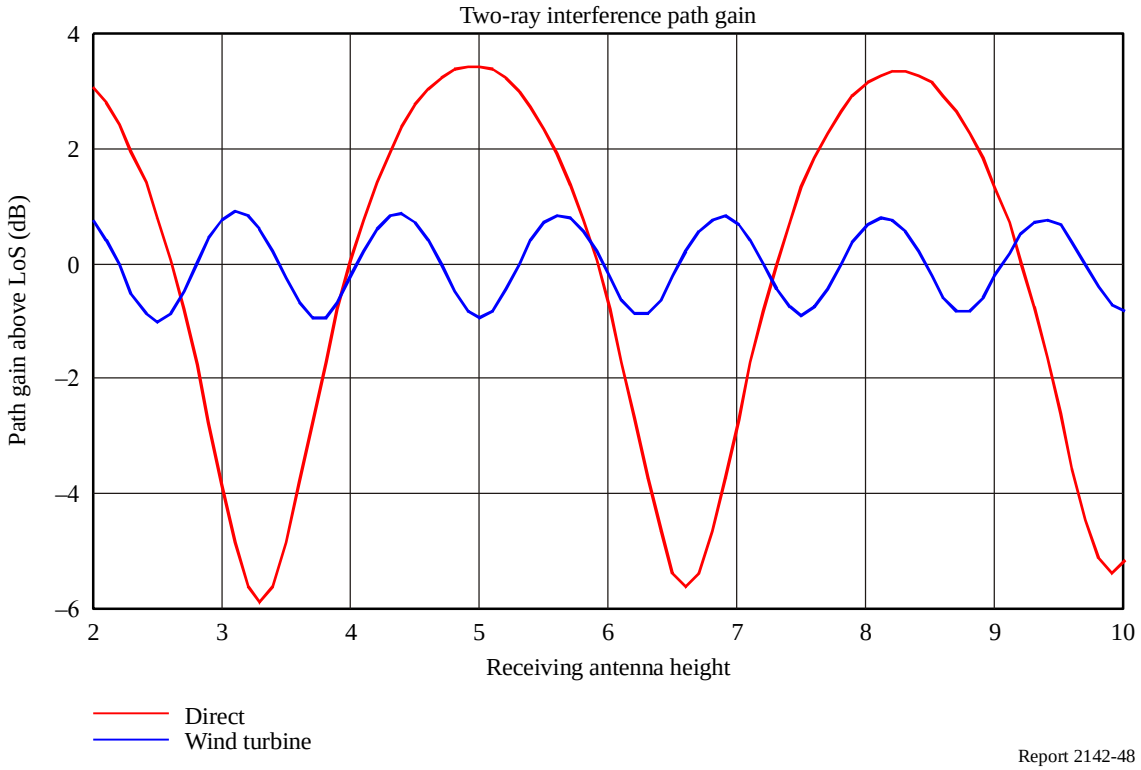

4 Conclusions

Theory and measurements have investigated the potential for interference to digital television from scattering by wind turbines. Modelling identified the region around a real wind farm where scattering was likely to be greatest, and measurements were then taken in those areas.

For scattering from wind turbines to cause disruption to the reception of digital television, the scattering ratio must exceed a certain threshold determined by the receiver signal processing characteristics. This perceived scattering ratio depends on the scattered signal and the directivity of the receiving antenna. If the interference signals are small a simple antenna will suffice, while with more severe interference a more directive antenna can typically mitigate the interference.

Measurements in the backscatter region, which is largely confined to a narrow region along the line joining the transmitter to the wind farm, using a test antenna of 13 dB gain, resulted in imperceptible interference from the wind turbines. The worst case for backscattering would occur when a hill blocks the direct signal, while clear LoS conditions exist to the wind turbines. In this case, the effective scattering ratio can be severely reduced by 30 dB or more. However, the measurements indicate that even under these extreme conditions it is unlikely that interference will be severe enough to cause disruption to the reception. Therefore for the backscatter case with an appropriate antenna it is unlikely that scattering from wind farms will cause interference.

Measurements in the forward scattering region were prompted by reports that analogue television reception was severely compromised by the presence of the wind turbines; this was confirmed by measurements. The multipath signals from rotating wind turbine blades is very dynamic and was a key interest in this analysis.

The following conclusions can be drawn concerning the dynamic scattering from the blades:

1 Scattering from the blades consists of a slow low amplitude variation at the geometric rotation repetition frequency (one-third the rotation rate) of the blades, as well as a large amplitude but short duration (about 30 ms) interference.

2 The MER measured as a function of time reflects the scattered signal amplitude. As a consequence, the mean value of the MER (as typically measured by instruments) does not reflect the time variations in the MER. The required MER for a receiver operating with interference from a wind turbine was not identified, but observations indicate that the required average MER must be increased above the required minimum of about 20 dB to at least 22 dB to cope with the slowly varying interference. The effect of the rapid, high-amplitude interference was not clear from the limited testing at the wind farm, and further investigations are required to determine the effects on typical receivers.

3 The signal quality as measured on two channels varied considerably. For example, the measured MER on channel 43 (631-638 MHz) was 26 dB, but on channel 37 (589-596 MHz) the MER was 20 dB. The reason for this variability is not clear, but is probably due to the time variation in the signal.

4 The characteristics of the BER before and after the Viterbi decoder are different from the nominal performance specified in Recommendation ITU-R BT.1735. For example, the recommended before-Viterbi BER is 0.04 for an after-Viterbi BER of 2×10^{-4}. However, for the example on channel 43 with a MER of 26 dB, the before-Viterbi BER was 0.021 (well below the recommended threshold), but the after-Viterbi BER was 0.001, well above the suggested level. This characteristic of the error correcting performance is clearly a consequence of the time-variable nature of the interference signal.

In the forward scatter region the antenna pointing towards the transmitter also points towards the wind farm, and the antenna directivity is of little benefit in reducing interference effects. The height of the antenna can be critical, as ground reflections can result in significant signal reduction.

In conclusion, in the backscatter region there is little effect from scattering from wind turbines on the performance of digital television, but in the forward scattering region, if there is significant blockage of the direct signal, significant interference to the reception of the digital television signal is possible. Further study is required to assess the performance of DVB-T receivers operating in the environment of time-varying interference from wind turbines.

PART B

Results of studies in Spain

TABLE OF CONTENTS

Page

1 Introduction

The following Attachments analyse the effect of the scattering of digital television signals from multiple wind turbines and describes a propagation channel model due to the potential effect of the presence of a wind farm. An example of use and the results of an actual study of the effect of scattering from wind farms on the quality of television signal case of the analysis are also described.

Attachment 1
to
Part B

Field trials

This Attachment describes the transmission and reception systems as well as the planning of an extensive terrestrial DTV measurement campaign carried out in Spain. It is focused on analysing the scattering process of the broadcasting signal by the wind turbines of a wind farm and evaluating the potential impact of the scattered signals to the terrestrial DTV reception quality.

1 Objectives of the field trials

The field trials described in this section have two main objectives: the empirical characterization of the scattered signals from the wind turbines, and the assessment of the potential impact of these scattered signals to the reception quality of the terrestrial DTV systems.

The first objective is the determination of the most influential factors related to the wind turbine in the amplitude of the scattered signal. The analysis, which is intended to define an accurate model for predicting the area of influence of a wind turbine, is described in Attachment 2. The conclusions obtained in this analysis led to the proposal of a new scattering model, included in Attachment 3.

The second objective is to verify whether scattered signals from wind turbines could affect the threshold *C*/*N* ratio required for quasi-error-free reception in the DVB-T system. The analysis of the impact of scattering signal on DVB-T reception thresholds is reported in Attachment 4.

2 Geographical overview

The measurements were carried out in the surrounding area of a wind farm in Spain. The wind farm is located at the top of a mountain, close to two television transmitter sites providing digital services in the UHF Band. The wind turbines are aligned in two groups along the crest of the mountain, at both sides of the transmitters. Wind Farm I is located at the east of the transmitters, and Wind Farm II at the west. Figure B-1 shows the location of the transmitter sites and the wind farm. There are three additional telecommunication towers close to the transmitters, which also cause static scattering of the DTV signals.

The surrounding area at the south of the wind farm is quite flat, with a mean altitude of about 200 m. The area at the north of the wind farm is hilly, with altitudes between 200 and 450 m.

The study focused on the turbines closest to the transmitter sites. Figure B-2 shows the location of the first eight wind turbines of Wind Farm I and several broadcasting towers on the top of the mountain. The television transmitter antennas are located on the right and the left. The three additional towers located between them correspond to other telecommunication services.

FIGURE B-1

Surface map of the measurement area around the wind farm and the transmitter site location

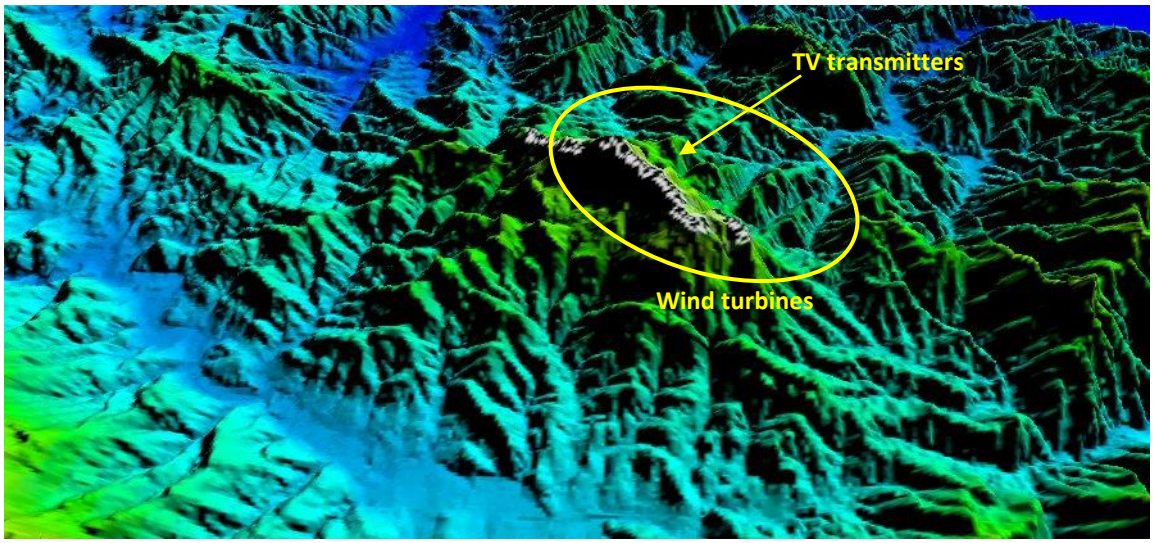

FIGURE B-2

Television transmitter sites and the closest wind turbines to the east of the transmitter sites

The distance between the television transmitter antennas and the nearest wind turbines is in the range of 250 to 950 m. The radiating systems are located at an altitude just a few metres above the wind turbines (1 055 m and 1 034 m for the transmitting antennas, and 950 m to 1 010 m for the wind turbine rotors). Therefore, considering the tilt of the transmitting antennas, the television signal reaches the turbines with the maximum gain value of the antenna radiation pattern.

The masts of the wind turbines are 55 m tall, and the diameter of the rotor is 52 m for the turbines located at the east of the transmitters (Wind Farm I), and 58 m for the turbines at the west (Wind Farm II).

3 Planning

Figure B-3 shows the measurement area around the wind farm and the transmitter antenna sites. More than 40 reception locations have been planned for the field trials. These reception locations are distributed over a wide range of azimuth and elevation angles around the wind farm, being all of them in line-of-sight to the wind turbines. The distance from the transmitter to the planned reception locations range from 2.4 km to 13.5 km.

In most of the reception locations, measurements have been carried out in different days in order to evaluate the influence of several wind farm operation conditions on the scattering signals.

FIGURE B-3

Selected reception locations around the television transmitters and the wind farm

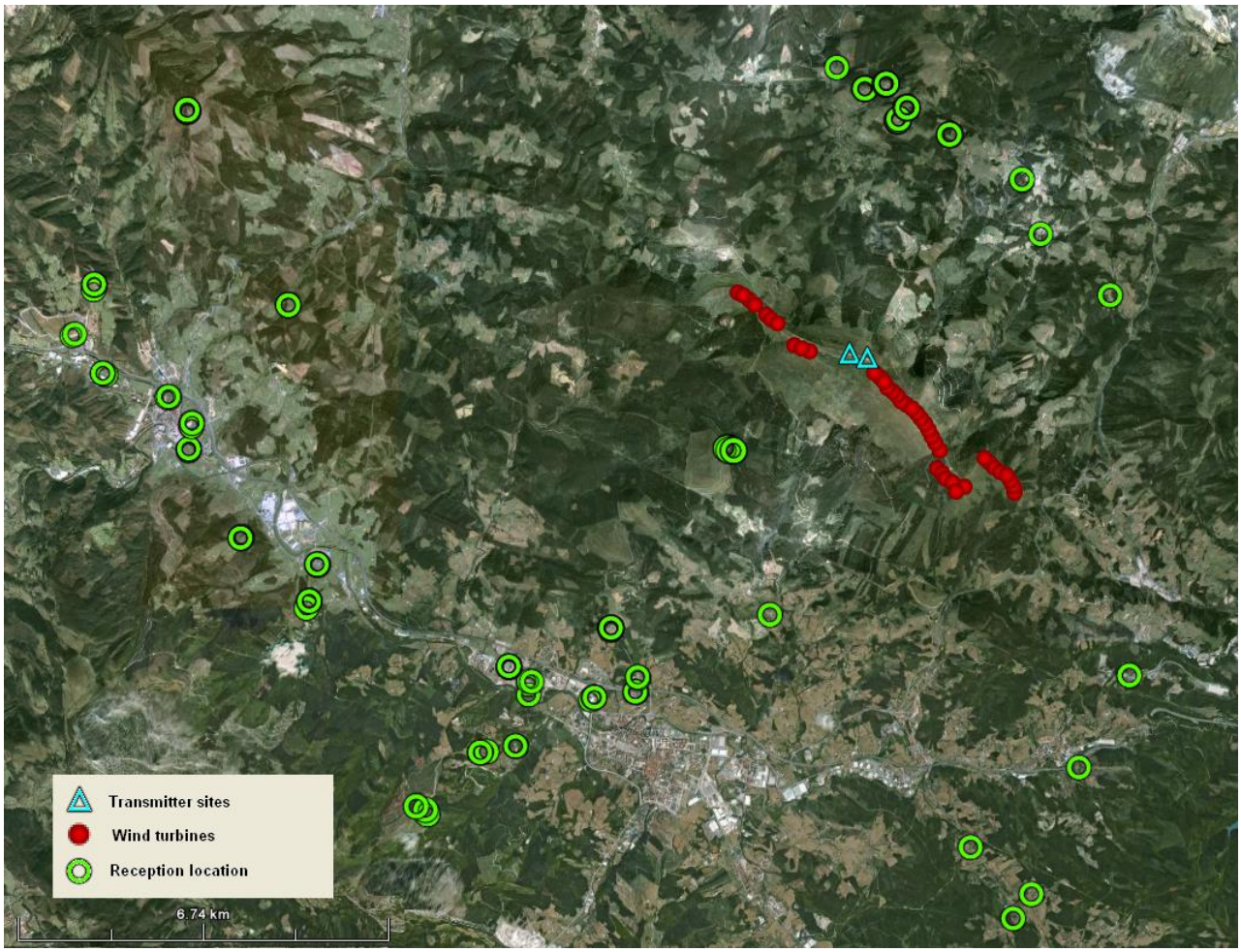

4 Measurement equipment

A mobile unit equipped with a mast for positioning the receiving antenna at a height of 6 m was used for the measurement campaign.

The measurement system was based on the RF recorder ADIVIC TCX 3 000 [8], for real-time capture and record of the DTTB signal (DVB-T in Spain). The sample rate is 12.5 Msamples/s for a span of 10 MHz, with 16 bit resolution. These features allow a detailed characterization of the received signal, and the possibility of recording several minutes in real-time enables the analysis of the effect of the blades rotation.

The signals were analysed by using the DBA (Digital Broadcast Analysis) software receiver [9]. This tool was developed by the University of the Basque Country to provide the channel frequency response, the channel impulse response, the IQ constellation and the main quality parameters of the DVB-T signal. The DBA receiver analyses the DVB-T signal symbol by symbol.

Additionally, a professional DVB-T test receiver was used to evaluate the effect of the scattered signals on the DVB-T reception quality.

Attachment 2
to
Part B

Empirical analysis of the scattering signals from wind turbines

1 Preliminary results from field trials

1.1 Signal scattering from a wind turbine

The first results obtained after analysing the measurements from the field trials point to some important conclusions related to the scattered signals from wind turbines:

– In the measurement locations planned for the field trials, the relative amplitude of the scattered signals from the wind turbines range from –10 dB to –50 dB below the direct signal from the transmitter. Most of the reception locations showed scattered signals around –30 dB below the direct ray. This multipath level may cause DTTB reception problems due to the dynamic nature of the interference, especially in cases of non LoS to the transmitter but LoS to the wind farm.

– Signal scattering due to the wind turbines was observed for reception locations up to 13.5 km away from the wind farm.

– The relative amplitude of the scattered signal from wind turbines with static blades is noticeable. The high levels of the scattered signal registered with static blades suggest that the mast contributes significantly in the scattered signal level.

– The scattering signal due to the mast may be at least as high in amplitude as the dynamic scattering from the blades.

– The time variability of the scattered signal for static blades shows low variations in amplitude (probably caused by scintillation in signal propagation), while the variability of the scattered signal increases considerably when the blades start rotating.

– The analysis of the signal variability should consider the three types of possible movement of the blades (rotation, pitch and yaw).
  – The wind turbines with rotating blades present higher variations in the scattered signal level with respect to the situation of static blades.
  – The results show that the pitch variation (the variation of the effective area of the blade with respect to the incident signal) does not imply a significant change in the amplitude of the scattered signal. In fact, the fluctuation of the scattered signal when varying the blades pitch is much lower than the case of rotating blades.
  – The fluctuations in the amplitude of the scattered signal due to blade rotation vary in amplitude as wind turbines change their orientation against the wind (and thus change their orientation with respect to the receiver location). The variations showed in the scattered signals when controlling the yaw movement with static blades may be influenced by the position of the blades while rotating the rotor.
– The amplitude of the scattered signals seems to significantly vary with the azimuth and elevation angles of the receive antenna location with respect to the transmit antenna and the wind turbine. In fact, this relative geometry transmitter-wind turbine-receive antenna could probably affect both the static scattering from the mast and the dynamic scattering from the blades.

2 Preliminary conclusions of the analysis

The results from the field trials suggest that the following aspects should be considered in the Recommendation ITU-R BT.1893-0 – Assessment of impairment caused to digital television reception by wind turbines:

– Recommendation ITU-R BT.1893-0 in force is based only on the blade area of the wind turbine. The results of the measurements with pitch control show that changes in the section of the blades do not imply a significant variation of the scattered signal level. Consequently, the conclusions lead to reconsider this issue and suggest that a method including additional aspects should be developed.
– The area that may be influenced by the signal scattering of the wind turbines could extend more than 5 km from the wind farm, especially in cases of non-line-of-site to the transmit antenna but LoS to the wind farm.
– The effect of the wind turbines is not negligible during periods when the wind turbines are not rotating. The reflected signals can be of significant amplitude even when the blades are static.
– The effect of the mast should be included in the model. An accurate quantification of the signal level reflected by the mast is necessary to properly estimate the overall scattered signal.
– The effect of the rotating blades, which may cause important variations in the scattered signal, should be characterized and included in the model.
– The scattering pattern from wind turbines in both the horizontal plane (azimuth angles) and vertical plane (elevation angles) should be considered in the estimation method, as they seem to be a decisive factor in the scattered signal level. The elevation angle accounts for the difference in height of the transmitter, the wind turbine and the receiver location. The size of the affected reception area can be notably modified by the incorporation of the elevation angle in the estimation method. Only the azimuth angle is considered both in Recommendation ITU-R BT.805 in force and in Recommendation ITU-R BT.1893-0. The data from these trials suggest that considering also the elevation angle would provide more accurate estimations.

In summary, instead of a model based on the physical area of the blades as the predominant factor in the estimation of the scattering coefficient, the empirical results suggest that the model should be composed of the combination of the scattered signals from both the metallic mast and the non-metallic rotating blades. The effect of the rotating blades should be properly characterized and incorporated. Last, the vertical scattering pattern (elevation angle) should also be included in the model.

Additional empirical results would be valuable to define and validate the model. Further analysis is also needed to assess the influence of the time-varying multipath interference from the wind turbines on the DTTB reception quality, considering not only the multipath level but also the relative delays and the dynamics of the scattered signals.

Attachment 2.1
to
Part B

Summary of measurements and analysis of the results

1 Introduction

Several authors have theoretically studied the effect of the wind turbines on the propagation of the electromagnetic waves [3]-[9]. Unfortunately, these authors do not agree on the predominant effect of the wind turbines. It should also be mentioned that some of the conclusions from different studies are contradictory.

Also, and due to the difficulties of evaluating the scattered signals from wind turbines in the field, very few empirical studies have been carried out in order to determine the validity of the above-mentioned studies. Therefore, it is necessary to carry out empirical experiments based on field measurements, in order to properly characterize the phenomenon and determine the most influential parameters.

The following analysis aims to improve the prediction of the scattering signals, and as such would apply equally to both analogue and digital television and may also apply in general to any communication service in the UHF band.

1.1 Wind turbines structure and nature of the scattered signals

Some basic aspects related to the wind turbines must be considered in the development of a method for estimating the scattered signals from these elements:

– The material of the mast (or pylon) is metallic. Blades are typically made of composite materials which have much lower reflection coefficients. However, blades have an inner metallic element for lightning protection which may increase their overall reflection coefficient.

– The mast of the wind turbine is static.

– The blades have three type of movements: rotation, yaw (orientation of the nacelle relative to the wind direction) and pitch (the angle of the blades relative to the wind can be actively adjusted by the pitch control system in order to control the power output). Figure B-4 shows the three types of movement of the blades.

Consequently, the study of the scattered signals from a wind turbine must take into account the different nature and dynamics of the mast and the blades. Hence, the overall scattered signal is composed of:

– The scattering signal from the mast, which is expected to be static and of significant amplitude, due to the great dimensions of this metallic part of the turbine.

– The scattering signal from the blades, which is expected to be variable, as a function of the bearing against the wind, the speed and the pitch of the rotating blades. The amplitude of this component of the scattering signal also depends on the blade materials.

FIGURE B-4

Types of movement of the blades in the wind turbines

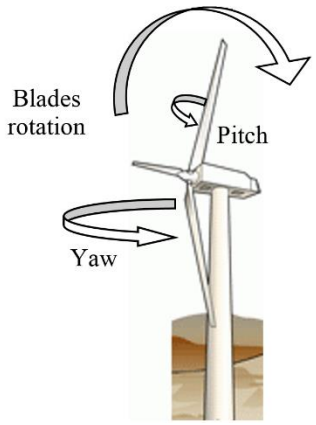

1.2 Scattering pattern

The scattering pattern refers to the variation of the scattering signal as a function of the location of the receiver relative to the transmitter and the wind farm.

Radiocommunication system transmitters and wind farms are usually located on the top of the mountains, while the reception areas surrounding the transmitters have usually lower altitudes. Thus, the size of the reception area influenced by a wind farm can be notably modified by the incorporation of the vertical plane in the estimation method.

Therefore, the scattering pattern from wind turbines in both the horizontal plane (azimuth angles) and vertical plane (elevation angles) should be considered.

2 Modification to Recommendation ITU-R BT.1893-0

The analysis of the above-mentioned aspects would constitute an improvement of both Recommendation ITU-R BT.805 and Recommendation ITU-R BT.1893-0, where the scattering is based on a static metallic rectangular blade situated in a vertical orientation (rectangular shaped in Recommendation ITU-R BT.805 and triangular shaped in Recommendation ITU-R BT.1893-0). The scattering from the mast is not considered, and the dynamics of the scattered signals with blades rotation are not included in the method. Moreover, only the horizontal plane of the scattering pattern (azimuth angle) is included in the method proposed in the mentioned Recommendation.

The following subsections aim to describe the scattering process of the DTV signal by the wind turbine using particular examples from field measurements. The next phase of the study will focus on quantifying the effect of all the factors involved in the signal scattering by the turbine and combining them to obtain an empirical model for evaluating the potential interference from wind farms in general.

3 Methodology

3.1 Use of the channel impulse response for the evaluation of the scattered signals

Due to the signal reflection on the turbines, attenuated, time-delayed, and phase shifted replicas of the transmitted signal coexist with the direct transmitted signal at the receiver input. The amplitude and variation of these scattered signals from the turbines of the wind farm can be measured using the channel impulse response, as described in [10]. The impulse response is estimated from the pilot carriers of the DVB-T signal by applying an Inverse Fast Fourier Transform every four symbols, and thus contains amplitude and phase values of all the pilot carriers [11].

Figure B-5 shows an instantaneous channel impulse response recorded in the measurement campaign. As illustrated in the figure, the impulse response of the DTV signal at the measurement system will be composed of the direct path (at measurement locations where LoS exists) and a series of signal replicas caused by signal scattering on the turbines. Other telecommunication towers located near the transmitter site cause reflections too.

Vertical lines on the figure represent the theoretical delays calculated from the relative location of the transmitter, the receiver and each wind turbine (the numbers in the figure reference the wind turbines). As it can be clearly observed, the measured reflected signals fit the theoretical delay positions. Therefore, accurate values of the signal strength of the scattered signals can be obtained for every wind turbine in the channel impulse responses.

The high sample rate of the measurement equipment and the analysis capability of the DBA software receiver allow the estimation of the channel impulse responses for every group of 4 symbols, which in time equals to 4 ms for the DVB-T configuration used in Spain [10]. As a result, the recorded signals show the time variation of the scattered signals in great detail. Considering that the period of the rotating blades is about several seconds (depending on the wind speed), the resolution of 4 ms between consecutive measurements allows the proper analysis of the dynamic variations of the scattering signals with the blade's movement.

FIGURE B-5

Channel impulse response of the DVB-T signal, where the direct ray and the reflected signals are shown. The reflected signals fit the theoretical delays, symbolized as vertical lines

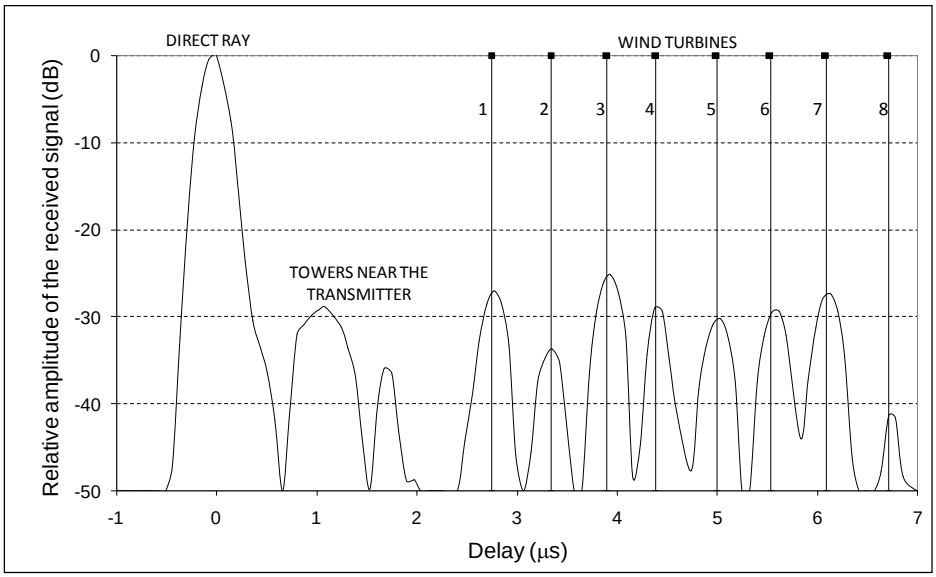

3.2 Types of measurements

In order to properly differentiate the effect of the static metallic pylon and the moving non-metallic blades and to evaluate the scattering variation due to different working regimes of the wind turbines, four different types of measurements were carried out in the field trials:

– Measurements of scattering signals from wind turbines under normal operation (rotating blades).

– Measurements of scattering signals from wind turbines with static blades (the wind speed is not enough for the blades start moving or the blades are forced to stop).

– Measurements of scattering signals from wind turbines with static blades controlling the rotor orientation. That is, the rotor is forced to turn around, controlled by the yaw engines.

– Measurements of scattering signals from wind turbines with static blades varying the pitch (the angle of the blades can be actively adjusted by the pitch control system in order to control the power output).

The last two types of measurements were carried out in cooperation with the wind farm promoter and they are very useful for the characterization of the scattered signals, as they allow the evaluation of the scattered signal variation for a specific factor (pitch variation or rotor orientation), while the rest of the aspects remain constant.

Therefore, the measurements controlling the wind turbines operation are valid for determining the relevance of each of the three possible movements of the blades (pitch, yaw, rotation) on the scattering signal variation.

4 Results and discussion

In this section, first, some representative values of the scattered signals from wind turbines are presented. Then the following subsections present some particular examples from field measurements to illustrate the scattered signal variation due to the different parameters involved in the phenomenon.

4.1 Relative amplitude of the scattered signals from wind turbines

In the measurement locations planned for the field trials, the relative amplitude of the scattered signals from the wind turbines range from –10 dB to –50 dB below the direct signal from the transmitter. Most of the reception locations showed scattered signals around –30 dB below the direct ray.

The scattered signals from wind turbines can be clearly differentiated for reception locations up to 13.5 km away from the transmitter site.

4.2 Variability of the scattered signals due to the blade rotation

First, the effect of the rotating blades on the variability of the scattered signal was analysed. For this purpose, situations with static blades and rotating blades were compared. In both situations, DVB-T signals during several seconds were recorded.

Figure B-6 shows the channel impulse response at a reception location of the measurement campaign. Only the instantaneous impulse response is depicted (impulse response corresponding to a group of four consecutive DVB-T symbols). Therefore, the figure does not represent the time variation.

The calculation of the theoretical delays of the scattered signals allows the proper identification of each wind turbine in the channel impulse response. The wind turbines under study in this measurement are WT 1 to WT 4, the four turbines from Wind Farm I located closest to the DTTB transmitters. The “Wind Farm II” indicated in the figure corresponds to a group of wind turbines located at west of the transmitter site. The delays of the scattered signals from Wind Farm II are, in this case, lower than 0.5 μs. As illustrated in Fig. B-6, the scattered signals from WT 1 to WT 4 can be clearly identified in the channel impulse response.

FIGURE B-6

Instantaneous DVB-T channel impulse response for static wind turbines

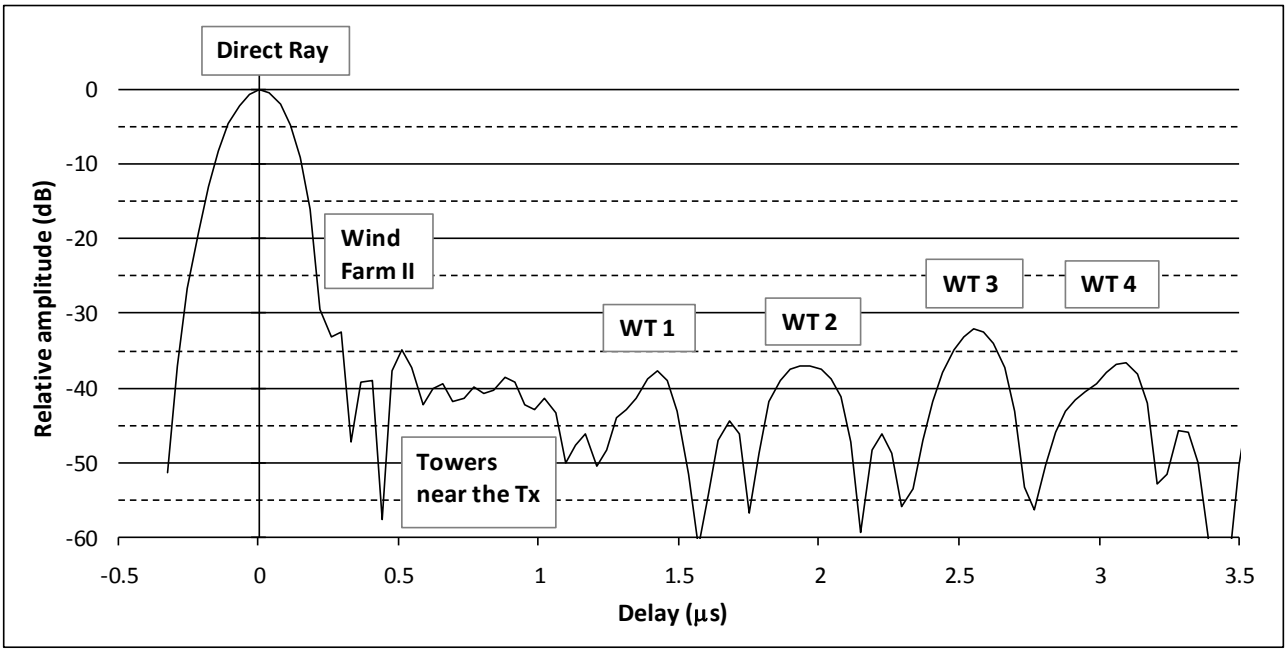

In order to evaluate the time variation of the reflected signals from static blades, 50 consecutive impulse responses were assessed and superimposed in Fig. B-7. Each line in the Figure represents the impulse response obtained from a group of 4 consecutive DVB-T symbols. Consequently, the Figure shows the evolution of the channel impulse response for 200 DVB-T symbols (a measurement interval of about 200 ms). As illustrated in Fig. B-7, although the wind turbines were static, fluctuations of 2 dB in the reflected signals from wind turbines are observed. These fluctuations are probably caused by signal scintillation in propagation (in the UHF band, scintillation can be around 1-2 dB) or vibration in the surface of wind turbines.

The high levels of the scattered signal registered for static blades suggest that the metallic mast contributes significantly in the scattered signal level.

Figure B-8 shows 50 superimposed consecutive impulse responses (about 200 ms of measurement time) corresponding to the same reception location when some of the wind turbines start rotating. The situation is the following:

– The blades of all wind turbines, except for the wind turbine 2 (WT 2 in the Figure) were rotating.

– The blades of the WT 2 were forced to stop.

FIGURE B-7

DVB-T channel impulse responses for static wind turbines during 200 consecutive symbols

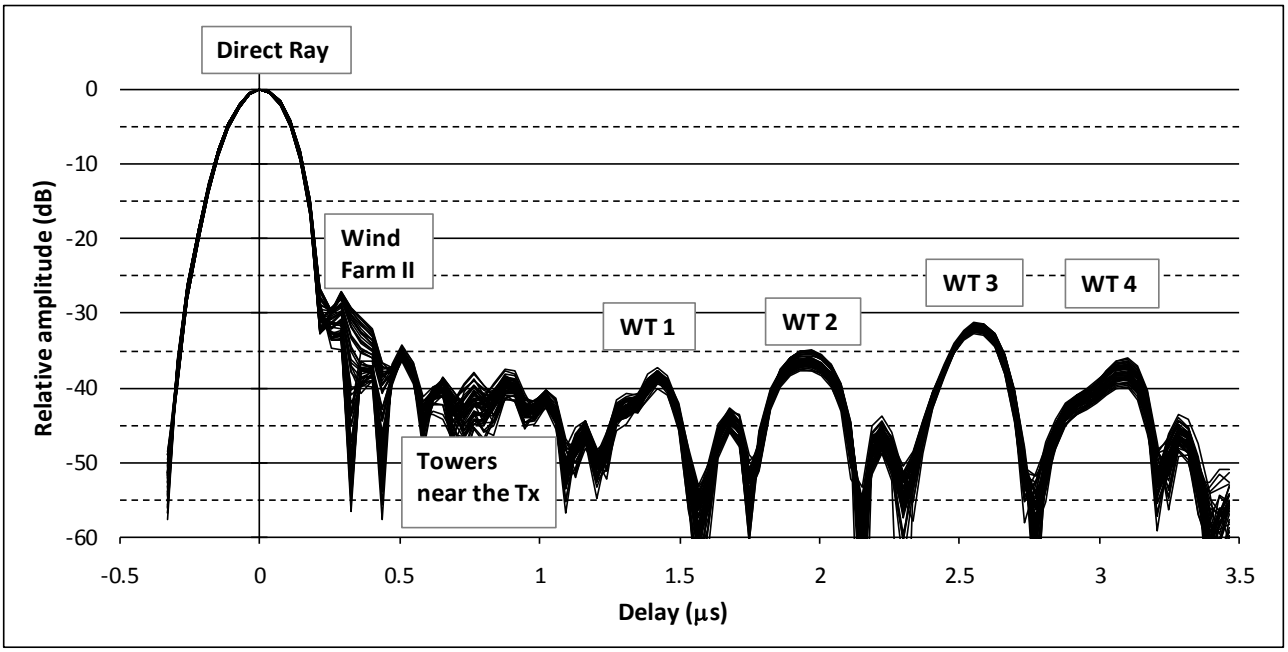

FIGURE B-8

DVB-T channel impulse responses recorded during 200 consecutive symbols. All the wind turbines were rotating, while WT 2 was forced to stop

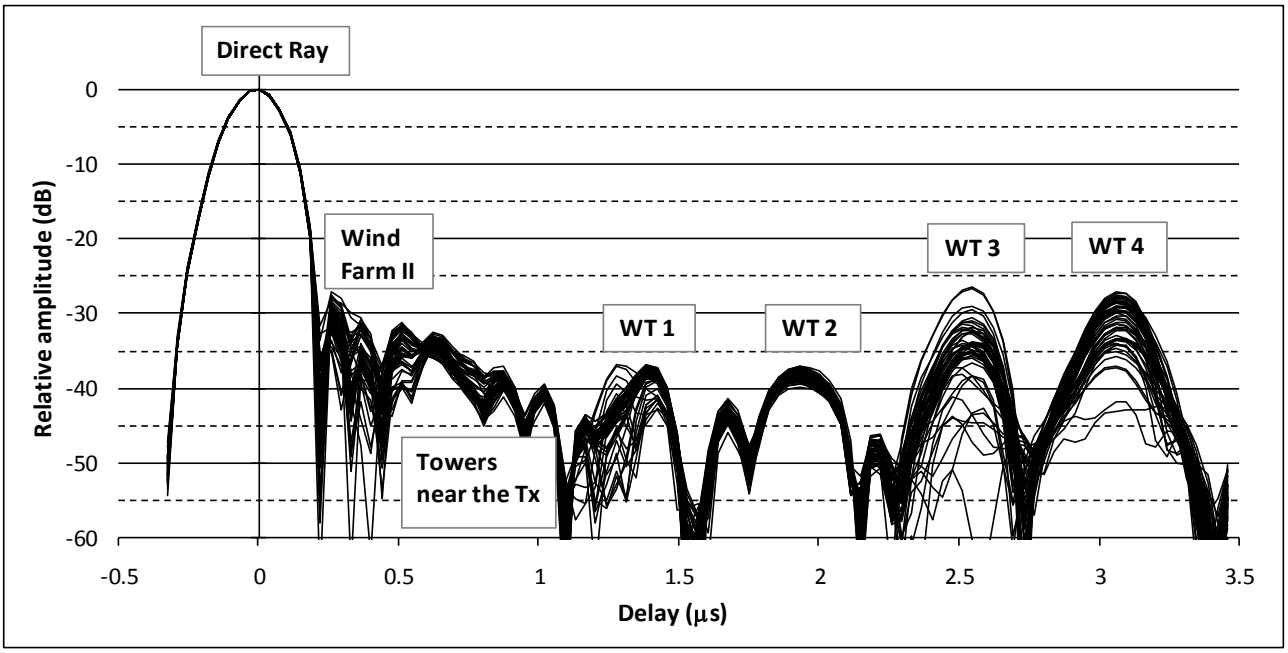

As it can be observed in Fig. B-8, the scattered signal from the WT 2 remained stable at a level 40 dB below the direct path, showing the same variability as in the previous case (B-7). On the contrary, the wind turbines with rotating blades (WT 1, WT 3 and WT 4) presented higher signal variations.

The amplitude of the variation of the scattered signal when blades are rotating depends on the relative geometry of the reception location with respect to the transmitter and the wind turbine location, as well as on the nacelle orientation with respect to the receiver location. A characterization of the Doppler characteristics of the scattering signals as blades rotate is included in the channel model described in Attachment 3.

4.3 Variability of the scattered signals due to blade pitch variation

Measurements of scattered signals from wind turbines with static blades, but varying the pitch of the blades were also carried out. The pitch represents the section of the blades that faces the wind, and in this experiment, the section of the blade that faces the electromagnetic wave from the DTV transmitter. The pitch variation implies that the section (the effective area of the blades) increases or decreases, depending on the direction of the pitch control.

Several different situations were measured, with differences in the rotor orientation and in the receive antenna location. Two representative cases are presented to illustrate the effect of the blade pitch on the variation of the scattered signals by the wind turbines.

Case 1

The transmit antenna, the wind turbine and the receive antenna were located as shown in Fig. B-9. In the first measurement, the wind farm was under normal operation, and the wind turbines were approximately facing towards the reception location.

FIGURE B-9

Measurement for pitch variation (Case 1)

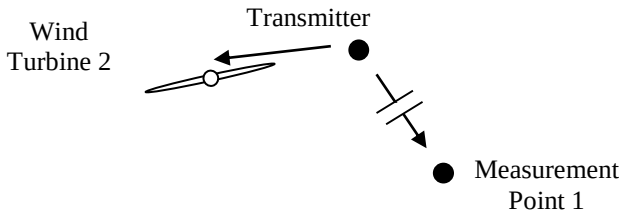

Figure B-10 shows 200 consecutive channel impulse responses for the situation depicted in Fig. B-9 when the wind farm was under normal operation.

FIGURE B-10

DVB-T channel impulse responses recorded during 800 consecutive symbols.
Case 1 (Wind farm under normal operation)

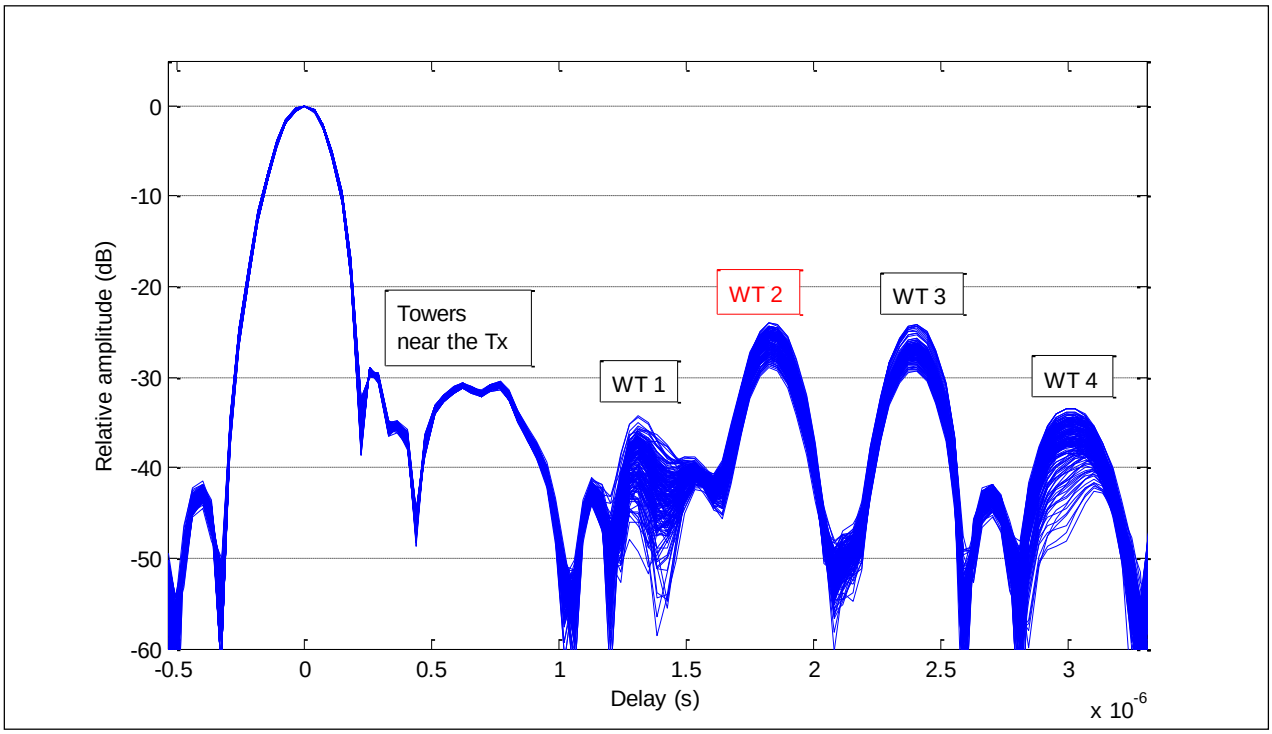

In the second measurement, the blades of WT 2 were forced to stop and the pitch of the blade was changed by the pitch control from the minimum to the maximum resistance to the wind. In order to compare the scattered signal variation under the different working regimes of the WT 2, the variation with time of the difference between the direct field strength signal and the field strength signal scattered by WT 2 are linearly represented in Fig. B-11.

It should be pointed out that this relative amplitude of the scattered signal with respect to the direct signal does not only depend on the scattering pattern of the wind turbine but also depends on the distance between the transmit antenna and the wind turbine, the distance between the transmit antenna and the receive antenna locations, and the difference in gain value of the radiation pattern of the transmit antenna towards the wind turbine and towards the receive antenna location. However, these factors are not relevant when comparing the variations due to the different working regimes of WT 2 in the same reception location.

FIGURE B-11

Pitch control measurement (Case 1). Comparison between the relative amplitude of the signal scattered by WT 2 under normal operation (above) and during pitch variation from minimum to maximum resistance to the wind (below). Note that different time scale is used

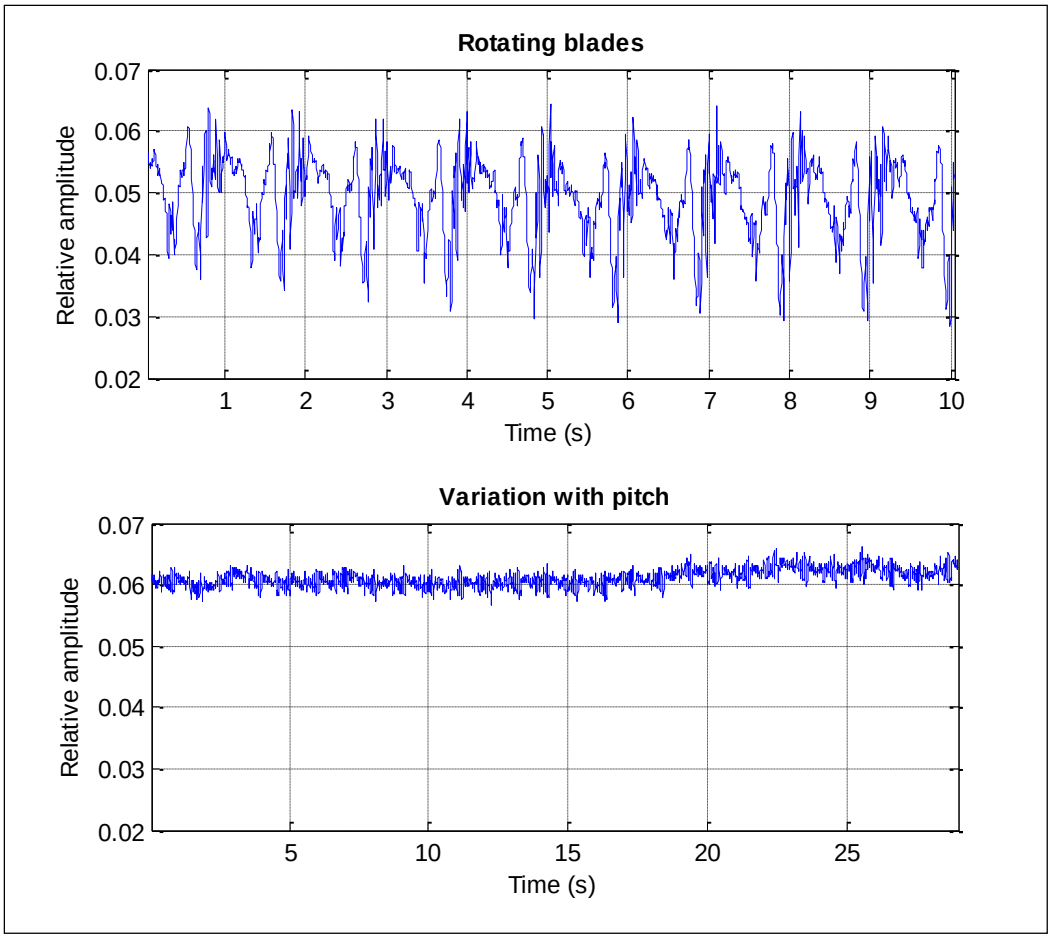

The upper graph of Fig. B-11 corresponds to the relative amplitude of the signal scattered by WT 2 under normal operation. A periodic variation is clearly observed. The period of this variation is approximately 1 s, corresponding to 1/3 of the rotation rate of the wind turbine, as expected for a three-blade rotor.

The relative amplitude of the signal scattered by WT 2 during pitch variation is depicted below. During pitch control the blades were not rotating and thus there is no periodic variation observed. It can be appreciated that the variation due to pitch control is limited to a narrow margin if compared with variation due to blades rotation.

A very similar result was obtained for the opposite pitch variation (from maximum to minimum resistance to the wind).

Case 2

The transmitter, the wind turbine and the receiver were in line, with the receiver located on the opposite direction, as shown in Fig. B-12. The wind turbine was forced to be oriented to the television transmitter. The mobile unit was located near the opposite direction (not exactly in the opposite direction because the irregular terrain did not allow the LoS to the wind turbine).

Figure B-13 shows 200 consecutive channel impulse responses for the situation depicted in Fig. B-12 when the wind farm was under normal operation. In this case, the blades of WT 2 were not rotating.

FIGURE B-12

Measurement for pitch variation (Case 2)

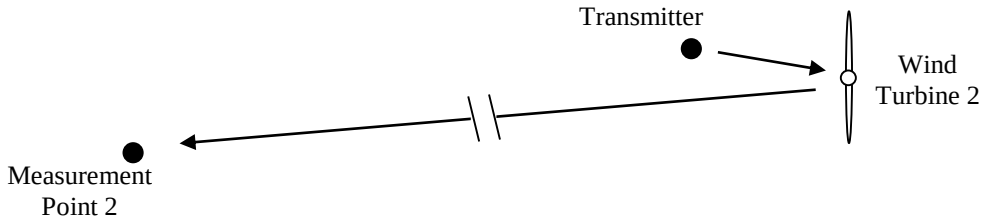

FIGURE B-13

**DVB-T channel impulse responses recorded during 800 consecutive symbols.
Case 2 (Wind farm under normal operation, WT 2 blades are not rotating)**

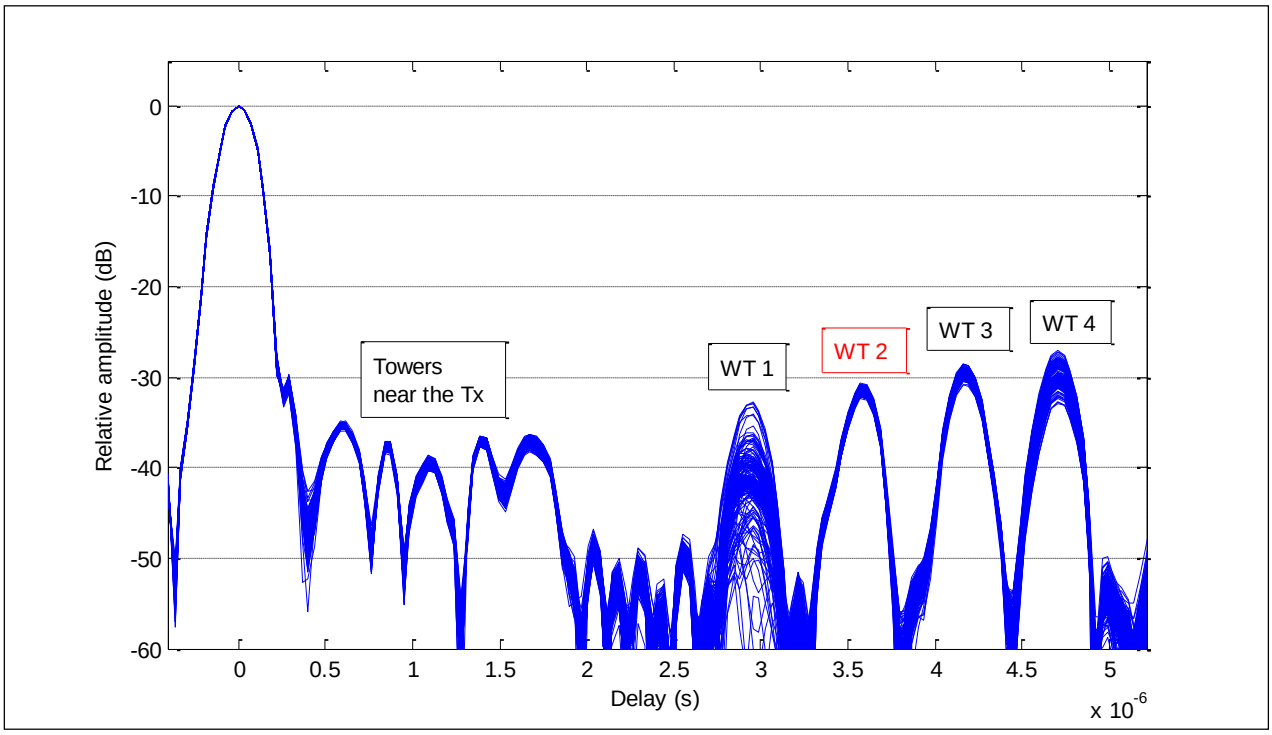

Figure B-14 shows the variation along the measurement time of the difference between the direct signal and the signal scattered by WT 2 when blades are static and during pitch control from maximum to minimum resistance to the wind.

As it can be observed in Fig. B-14, the fluctuation with time of the scattered signal associated to pitch variation is similar to the situation of static blades. There is no clear tendency in the scattered signal level between the pitch corresponding to the minimum resistance and the pitch corresponding to the maximum resistance.

Other cases

Measurements controlling the pitch of the blades were carried out in other receive antenna locations and different nacelle orientations with respect to the measurement point.

FIGURE B-14

Pitch control measurement (Case 2): Comparison between the relative amplitude of the signal scattered by WT 2 with static blades (above) and during pitch variation from maximum to minimum resistance to the wind (below). Note that different time scale is used

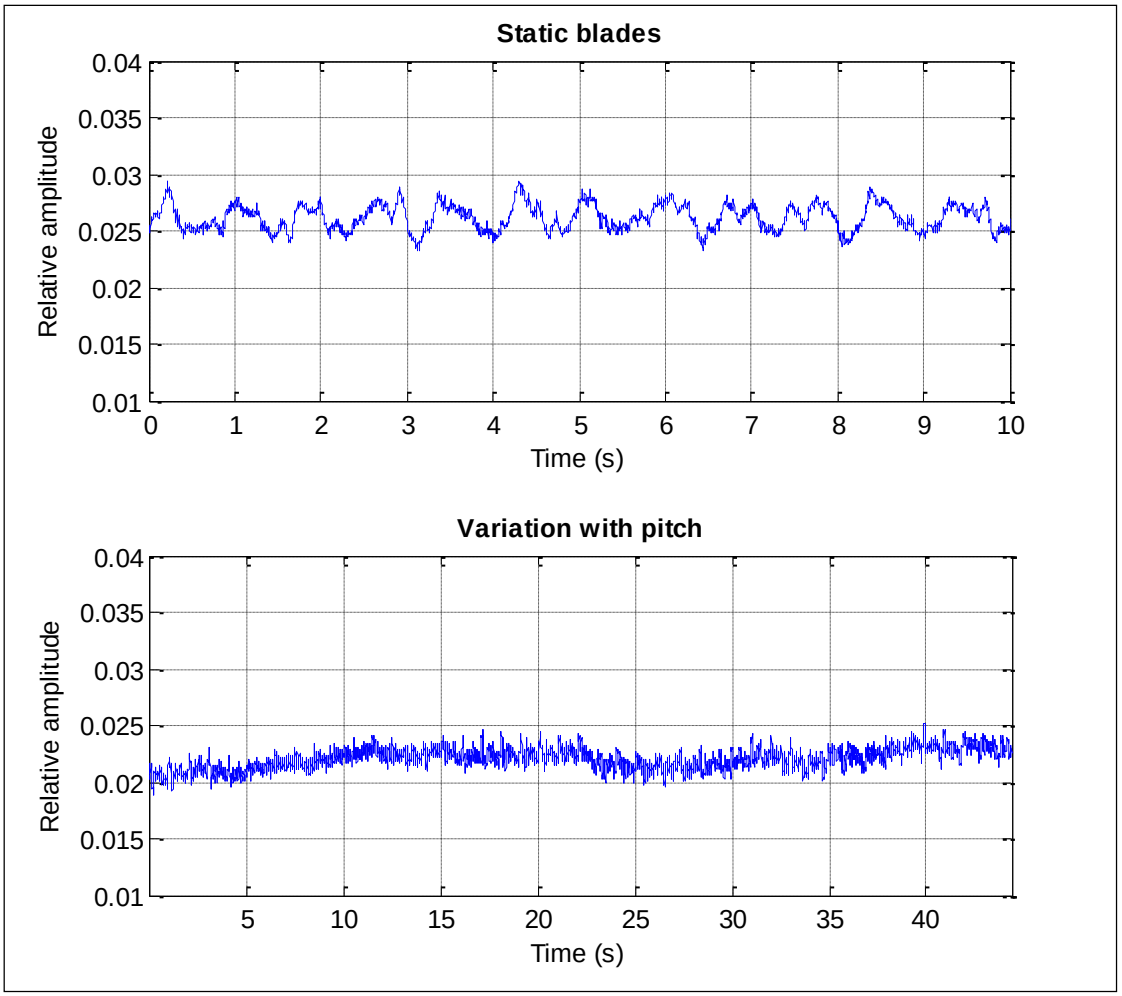

During pitch control the blades were not rotating and thus there is no periodic variation observed. The obtained results are similar to the results in Case 1 (Fig. B-11), so that they can be considered as representative. That is, the fluctuation of the scattered signal when varying the blades pitch is much lower than the fluctuation due to rotating blades.

4.4 Variability of the scattered signals due to the variation in the rotor orientation (yaw)

During the field trials, in some measurements the yaw control was used to turn the nacelle of the wind turbine and analyse the effect of this manoeuvre. Similarly to the previous subsection, two representative examples are presented to evaluate the influence of the rotor orientation on the scattered signal.

Case 1

This example corresponds to the same reception location presented in Case 1 for pitch variation in § 4.3. The channel impulse response corresponding to Measurement Point 1 is shown in Fig. B-9.

Once the blades were forced to stop, the yaw engines turned the nacelle of WT 2 clockwise approximately 90°, as shown in Fig. B-15.

FIGURE B-15

Measurement for yaw variation (Case 1): Start position (left) and final position (right)

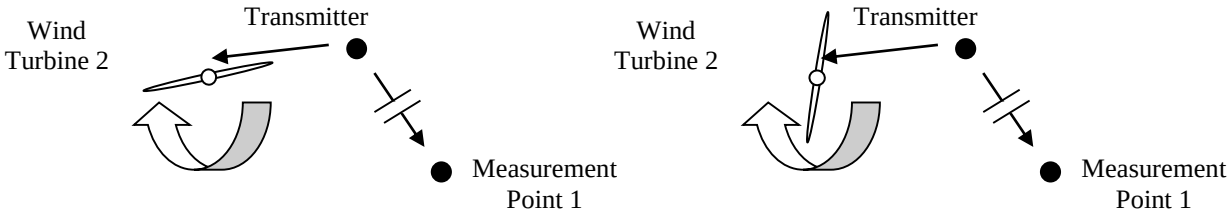

In order to analyse the scattered signal variation due to the yaw movement, the variation with time of the difference between the direct signal and the signal scattered by WT 2 is represented in Fig. B-16. In the graph above the relative amplitude of the signal when WT 2 was facing towards the reception point with rotating blades is depicted. The graph below shows this variation while the nacelle rotated 90º clockwise with static blades.

FIGURE B-16

Yaw control measurement (Case 1). Comparison between the relative amplitude of the signal scattered by WT 2 under normal operation (above) and during yaw variation (below). Note that different time scale is used

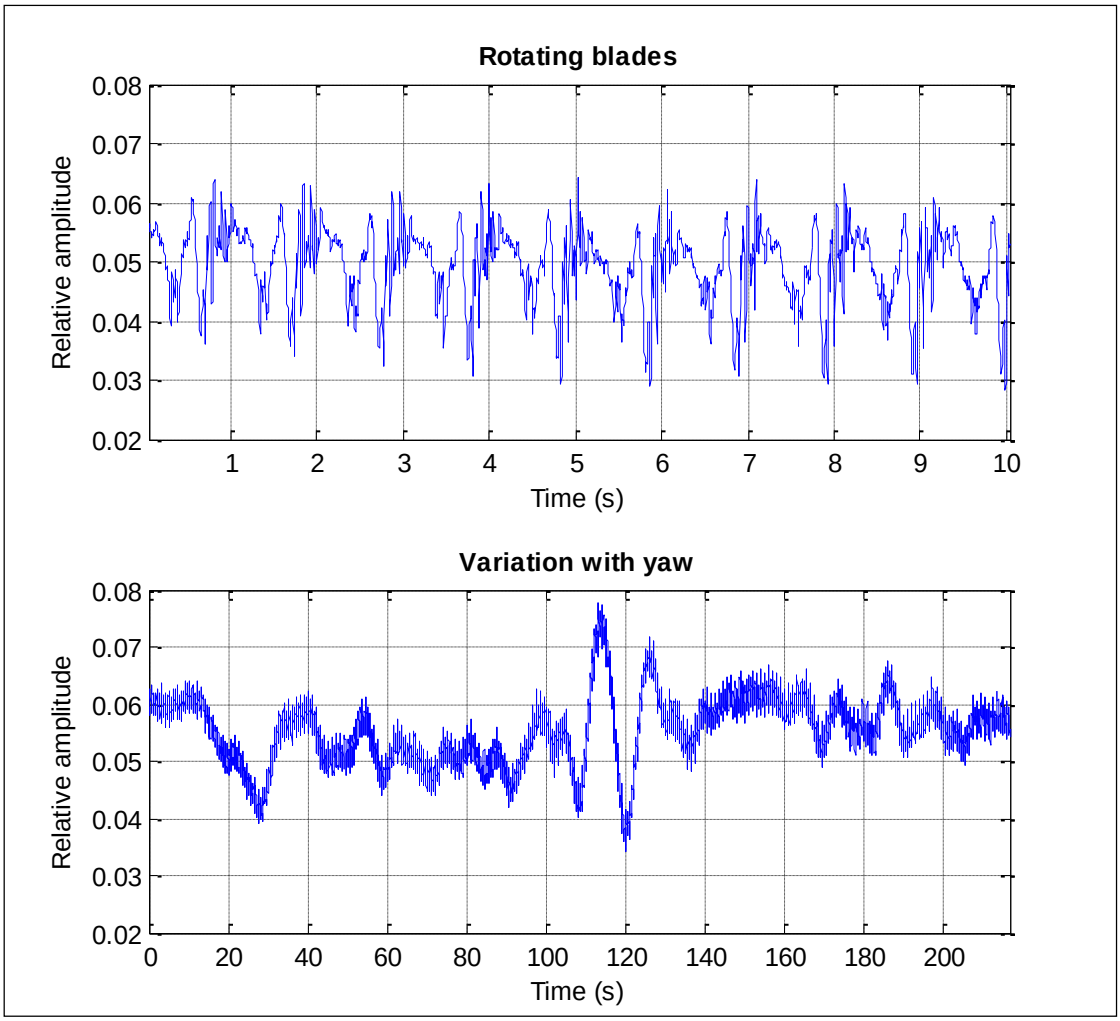

Fluctuation of the reflected signal due to the yaw variation can be observed. This fluctuation features a maximum variation between 110 s and 120 s when the yaw has rotated approximately 45°, but in general the variation does not show a clear tendency.

Other measurements controlling the yaw movement of the turbines with static blades were carried out, but there is not a clear tendency of the effect of this manoeuvre on the scattered signal.

Case 2

Case 2 gives an example of an uncontrolled yaw movement, with WT 1 and WT 3 varying their orientation to the wind while blades are rotating. The scattered signals by WT 1 and WT 3 can be clearly differentiated in the channel impulse response, as shown in Fig. B-13.

As shown in Fig. B-17, WT 1 rotates some degrees anti-clockwise and WT 3 rotates some degrees clockwise.

FIGURE B-17

Measurement for yaw variation (Case 2)

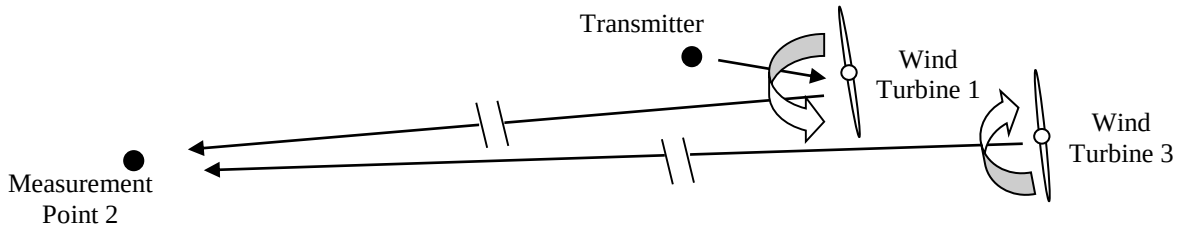

The relative amplitude of scattered signals by WT 1 and WT 3 while reorienting their rotors is depicted in Fig. B-18. It can be observed that the variations due to blade rotation affect the amplitude as wind turbines change their orientation with respect to the measurement point.

FIGURE B-18

Yaw effect analysis with rotating blades (Case 2). Relative amplitude of the scattered signals by WT 1 rotating anti-clockwise (above) and by WT 3 rotating clockwise (below)

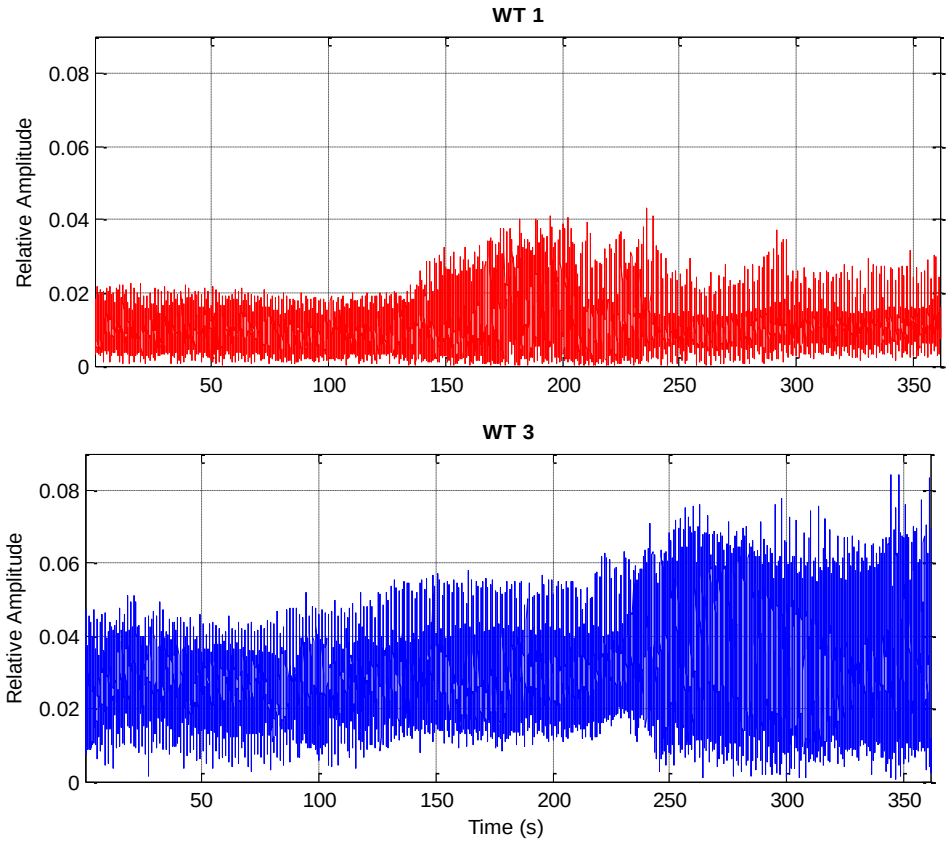

Therefore, the variations showed in scattered signals when controlling the yaw movement with static blades may be influenced by the position of the blades while rotating the rotor. Nevertheless, a more in-depth study is necessary in order to evaluate this aspect.

4.5 Geometry of wind turbines location with respect to transmitter and receiver locations

The relative location of the wind turbines with respect to the transmitter and receiver locations is identified as a decisive factor in the scattered signal level in the receiver. It is decisive as this geometry determines the direction of the incident and scattered signals in the wind turbine.

The preliminary results of the measurement campaign point in that direction. In fact, the relative position of the receive antenna with respect to the transmit antenna and the wind farm will affect the level of interference received from both the static scattering from the mast and the dynamic scattering from the blades. The influence of the different parts of the wind turbine on the scattered signal is difficult to assess and further analysis is being carried out, but it seems clear that the azimuth and elevation angles of the incident and scattered signals should be included in the method for estimating the effect of wind turbines.

Further study may be required to determine if the geometry of the transmit and receive antennas has any impact on the interference to the received television signal.

5 Analysis and discussion

Relative amplitude of the scattered signals from wind turbines

In the measurement locations planned for the field trials, the relative amplitude of the scattered signals from the wind turbines range from –10 dB to –50 dB below the direct signal from the transmitter. Most of the reception locations showed scattered signals around –30 dB below the direct ray. This multipath level may cause DTTB reception problems due to the dynamic nature of the interference, especially in cases of non line-of-sight to the transmitter but line-of-sight to the wind farm.

Variability of the scattered signal

The results obtained from the measurements with static blades (see Fig. B-7), when compared to the results from the measurements with rotating blades (see Fig. B-8), show that the variability of the scattered signal is due to the blades movement.

The time variability of the scattered signal for static blades shows low variations in amplitude. In this situation, the scattered signal is caused by both the mast and the static blades. It is clearly observed that the level of the scattered signal is noticeable even when the blades remain static.

Recommendation ITU-R BT.805 states that the effects of the wind turbines are reduced during periods when the wind turbines are not rotating. According to the results from the field trials, this statement should be reconsidered.

The variability of the scattered signal increases considerably when the blades start rotating. The analysis of this variability should consider the three types of movement of the blades (rotation, yaw and pitch), and the geometry of the wind turbine location with respect to the transmitter and receiver locations. It should be noted that the measurements were carried out by using horizontal polarization, while the rotating blades show a varying horizontal component to the incident electromagnetic wave.

Scattered signal from the mast

The high levels of the scattered signal registered for static blades (see Fig. B-8) lead to believe that the mast contributes significantly in the scattered signal level.

It was proposed that the effect of the mast should be included in the model for the assessment of the impairment caused by a wind turbine. Recommendation ITU-R BT.1893-0 would be improved if the effect of the mast would be also included.

Variation of the scattered signal with pitch

The pitch variation affects the section of the blades that face the electromagnetic wave, and thus represents the variation of the effective area of the blade with respect the incident signal.

The results show that the pitch variation does not imply a significant change in the amplitude of the scattered signal. In fact, the fluctuation of the scattered signal when varying the blades pitch is much lower than the case of rotating blades.

The reason may be that the blades are made of non-metallic materials (usually composite materials as fibreglass), and consequently the scattering of the signal may be mainly due to the metallic part for lightening protection inside the blade. The effective area of this lightening rod does not depend on the blade pitch.

This is a highly significant result, because Recommendation ITU-R BT.805 in force is based on the area of a rectangular metallic blade. Moreover, Recommendation ITU-R BT.1893-0 proposes a method also based on the area of a metallic blade, but now considering it to be triangular. However, Recommendation ITU-R BT.1893-0 also includes a note that states that considering that the blade is metallic could overestimate the scattering in 6 to 10 dB depending on the actual material of the blade.

Variation of the scattered signal with yaw

The variations in the amplitude of the scattered signal due to blade rotation vary in amplitude as wind turbines change their orientation against the wind (and thus change their orientation with respect to the receiver location). Thus, the variations showed in the scattered signals when controlling the yaw movement with static blades may be influenced by the position of the blades while rotating the rotor.

In conclusion, the orientation of the rotor against the wind seems to generate variations in the amplitude of the scattered signals.

Geometry of the location of wind turbines with respect to transmitter and receiver locations

The azimuth and elevation angles of the incident and reflected waves should be included in the method for estimating the effect of wind turbines, as they are a decisive factor in the scattered signal level. In fact, the relative location of the receive antenna with respect to the transmit antenna and the wind farm will affect the level of interference received from both the static scattering from the mast and the dynamic scattering from the blades.

Recommendation ITU-R BT.805 in force and Recommendation ITU-R BT.1893-0 only refer to the azimuth angle, although the latter includes the consideration that “the location of wind turbines and their scattering patterns have an impact on the level of impairment in the vertical and horizontal plane”. The elevation angle accounts for the difference in height of the transmitter, the wind turbine and the receiver locations. The size of the influenced reception area can be notably modified by the incorporation of the elevation angle in the estimation method.

Attachment 3
to
Part B

A multipath channel model to characterize signal propagation in presence of a wind farm in the UHF band

1 Introduction

New communication systems require the definition of wideband channel models that attempt to describe not only the field strength at some point away from the transmitter but also the variations in the field as a function of time, frequency, and location.

To date, there are no available channel models to characterize the propagation conditions encountered in the presence of a wind farm in the UHF band. Recommendation ITU-R BT.805 and Recommendation ITU-R BT.1893-0 provide simplified methods to estimate the potential degradation due to a wind turbine on analogue and digital television, respectively. However, these suggested methods have two main disadvantages: they only account for one wind turbine, without considering the contributions of all the turbines that compose a wind farm, and they do not model the time varying nature of the scattering signals. Therefore, the ITU keeps Question ITU-R 69-1/6 open, where further studies about these aspects are requested.

The main contribution of the research efforts that have been made by the University of the Basque Country (UPV/EHU) since the measurement campaign described in Report ITU-R BT.2142-1 is the adaptable channel model presented here. The two main issues of the channel model under consideration are the scattering model to account for the relative power of the scattered signals and the Doppler spectrum that characterizes signal variability due to blade rotation.

2 Summary of contributions to Recommendation ITU-R BT.1893

This Attachment proposes a Tapped-Delay Line channel model to characterize multipath propagation in the presence of a wind farm in the UHF band. The main advantage of this channel model is that it is adaptable to the particular features of any case under study, as the number of paths and their delays and amplitudes are calculated for the specific features of the wind farm, the transmitter and receiver sites under test. Moreover, the proposed Doppler spectra are also adjustable to the working frequency, wind turbines' size and relative positions of the transmitter, wind turbines and receivers. In addition to this, the channel model can be applied even when no accurate information about the wind direction or speed is available.

It should be remarked that although this study has been obtained from measured DVB-T signals, the proposed channel model is independent of the standard, and as such it is applicable to any television system provided in the UHF band.

Attachment 3.1
to
Part B

Wind farm channel model

The Wind farm channel model for propagation in the presence of wind turbines is a Tapped-Delay Line model with a number of paths, with:

– corresponding delays,

– mean amplitudes, and

– Doppler spectra associated to each path to account for the variability caused by the rotation of the blades.

In the channel model, all these components are adaptable to the particular features of any case under study. More precisely, these parameters are specified for each reception location in the coverage area of a potentially affected transmitter [13].

The adaptation of the channel model to the particular characteristics of a case under study requires some input data, which is gathered in Table B-1. Accordingly, the necessary parameters which are obtained from the input data of Table B-1 are included in Table B-2.

TABLE B-1

Input Data to Adapt the Channel Model to the Specific Features of a Case under Study

	Type	Description
For each wind turbine	Position	Geographical coordinates, including terrain height above sea level (m)
	Mast dimensions	Vertical dimension of the mast (m) Lower and upper diameters of the mast (m)
	Blades length l	Longitudinal dimension of the blades (m)
	Maximum rotation rate, ω_{max}	Maximum rotation rate of the blades (rpm)
Transmitter	Position	Geographical coordinates, including terrain height above sea level (m)
	Radiating pattern	Transmitting antenna pattern
	Antenna height	Transmit antenna height above ground level (m)
	Frequency, f	Working frequency within the UHF band (Hz)
	Power, P_t	Maximum transmitter power (W)
Receiver	Position	UTM (m) coordinates, including terrain height above sea level (m)
	Radiating pattern	Receive antenna pattern
	Antenna height	Receive antenna height above ground level (m)

TABLE B-2

Data Calculated from the Input Data of Table 1

Symbol	Description
$R_{Tx\text{-}WTi}$	For each wind turbine, transmit antenna to wind turbine distance (m)
$R_{WTi\text{-}Rx}$	For each wind turbine, wind turbine to receive antenna distance (m)
$R_{Tx\text{-}Rx}$	Transmit antenna to receive antenna Euclidean distance (m)
$G_{Tx\text{-}WTi}$	Transmit antenna gain toward *i*-th wind turbine (dimensionless)
$G_{Rx\text{-}WTi}$	Receive antenna gain toward *i*-th wind turbine (dimensionless)
$G_{Tx\text{-}Rx}$	Transmit antenna gain in the direction toward the receive antenna(it is not a ratio of the two antennas) (dimensionless)
$G_{Rx\text{-}Tx}$	Maximum gain of the receiver antenna (dimensionless)
r	Mean radius of the mast (m)
L	Length of the slanted surface of the mast, which is a truncated right circular cone (m)
ϕ_r	Bistatic angle in the horizontal plane (transmit antenna-wind turbine-receive antenna), for each wind turbine (radians)
θ_t	Angular position of the transmit antenna in the vertical plane, measured at the wind turbine under consideration from the vertical plane (radians)
θ_r	Angular position of the receive antenna in the vertical plane, measured at the wind turbine under consideration from the vertical plane (radians)

Figure B-19 shows a view of the general wind farm interference situation.

FIGURE B-19

View of the general wind farm interference situation

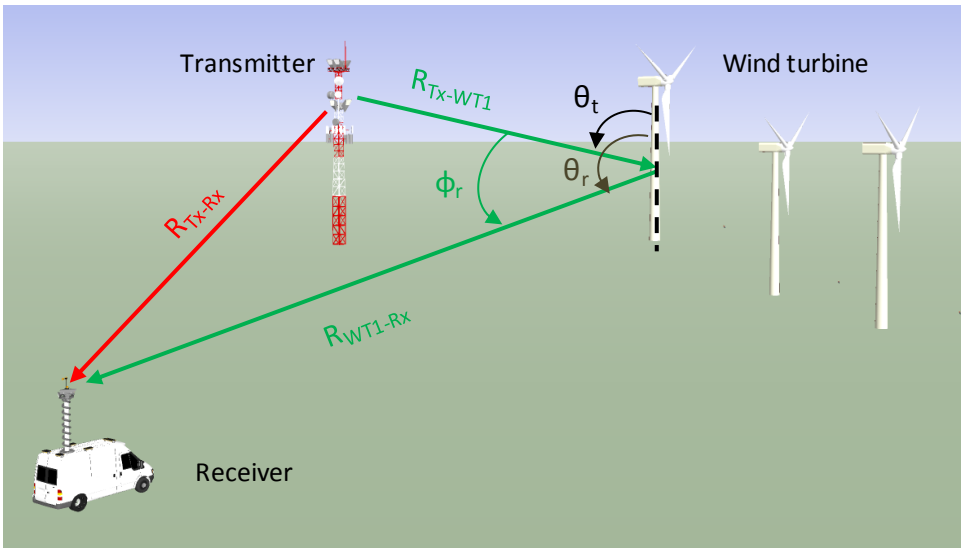

Number of paths

The number of paths is on a first approach, the total number of wind turbines of the wind farm, plus a static path corresponding to the signal from the transmitter. Depending on the results obtained for their delays and amplitudes, as explained in the following subsections, the number of paths may be reduced.

Relative delays of the paths

For each wind turbine, the relative delay τ_i (s) of the scattered signal is calculated as a function of the distance difference between the direct path (transmitter-receiver) and the path of the scattered signal (transmitter-wind turbine-receiver) according to equation (B-1).

$$\tau_i = \frac{\left(R_{Tx-WT_i} + R_{WT_i-Rx} - R_{Tx-Rx}\right)}{c} \tag{B-1}$$

where:

$R_{Tx\text{-}WTi}$: transmit antenna to *i*-th wind turbine distance (m)

$R_{WTi\text{-}Rx}$: *i*-th wind turbine to receive antenna distance (m)

$R_{Tx\text{-}Rx}$: transmit antenna to receive antenna distance (m)

c: speed of light (m/s).

Mean amplitude of the paths

The static path with relative delay zero (i.e. the direct transmitter to receiver path) is taken as a reference, in such a way that its mean amplitude is 0 dB. Then the mean relative amplitude of each time-varying path is given by the power ratio between the power of the signal scattered from the corresponding wind turbine $P_{Tx\text{-}WTi\text{-}Rx}$ and the power of the direct signal from the transmitter $P_{Tx\text{-}Rx}$.

The direct power from the transmitter in the reception location, $P_{Tx\text{-}Rx}$, is calculated as a function of the transmitter to receiver distance $R_{Tx\text{-}Rx}$, the transmitter to receiver gain of the transmission radiation pattern $G_{Tx\text{-}Rx}$, the gain of the receiver radiation pattern $G_{Rx\text{-}Tx}$ and the wavelength λ, including the corresponding additional propagation losses L_{prop} (such as diffraction losses due to terrain features), as shown in equation (B-2).

$$P_{Tx-Rx} = \frac{P_t G_{Tx-Rx} G_{Rx-Tx} \lambda^2 L_{prop}}{\left(4\pi\right)^2 R_{Tx-Rx}^2} \tag{B-2}$$

where:

P_t: maximum transmitter power (W)

$G_{Tx\text{-}Rx}$: transmit antenna gain in the direction of the receive antenna (dimensionless)

$G_{Rx\text{-}Tx}$: receive antenna maximum gain (dimensionless)

L_{prop}: propagation losses (dimensionless)

$R_{Tx\text{-}Rx}$: transmit antenna to receive antenna distance (m)

λ: wavelength (m).

For each wind turbine, the power of the scattered signal in the receiver location $P_{Tx\text{-}WTi\text{-}Rx}$ is calculated using the bistatic radar equation, according to equation (B-3).

$$P_{Tx-WT_i-Rx} = \frac{P_t G_{Tx-WT_i} G_{Rx-WT_i} \lambda^2 \sigma_i}{(4\pi)^3 R_{Tx-WT_i}^2 R_{WT_i-Rx}^2} \quad \text{(B-3)}$$

where:

P_t: maximum transmitter power (W)

$G_{Tx\text{-}WTi}$: transmit antenna gain toward the wind turbine *i* (dimensionless)

$G_{Rx\text{-}WTi}$: receive antenna gain toward the wind turbine *i* (dimensionless)

σ_i: bistatic radar cross section (RCS) of the mast in the receiver direction (m^2)

$R_{Tx\text{-}WTi}$: transmit antenna to *i*-th wind turbine distance (m)

$R_{WTi\text{-}Rx}$: *i*-th wind turbine to receive antenna distance (m)

λ: wavelength (m).

The RCS of the mast in the receiver direction σ_i (m^2) is obtained as:

$$\sigma_i(\phi_r, \theta_t) = krL_{nf}^2 \sqrt{\frac{1+\cos\phi_r}{2}} \sin\theta_t \quad \text{(B-4)}$$

where:

k: wave number $k = 2\pi/\lambda$ (m^{-1})

r: tower radius (m)

σ_i: bistatic radar cross section (RCS) of the mast in the receiver direction (m^2)

ϕ_r: receive antenna angular position in the horizontal plane, measured at the wind turbine under consideration with respect to the transmit antenna location (see Fig. B-20)

θ_t: transmit antenna angular position in the vertical plane measured at the wind turbine under consideration from the vertical plane (see Fig. B-20)

λ: wavelength (m).

For the distances where the effect of the turbines may be of consideration, far field condition in the context of signal scattering is not usually fulfilled, since normally.

$$R_{Tx-WTi} < \frac{2L^2}{\lambda} \quad \text{(B-5)}$$

where:

$R_{Tx\text{-}WTi}$: transmit antenna to *i*-th wind turbine distance (m)

L: tower length (m)[7].

In such cases, near field effects of signal scattering can be included by considering a near field tower length L_{nf} (m), given by:

[7] If the mast is a truncated right circular cone, the mast radius *r* is calculated as the mean radius of the cone, and the mast length *L* is the length of the slanted surface of the truncated cone.

$$L_{nf} = \sqrt{\frac{\lambda R_{Tx-WTi}}{2}} \tag{B-6}$$

where:

$R_{Tx\text{-}WTi}$: transmit antenna to *i*-th wind turbine distance (m)

λ: wavelength (m).

The relative position of the transmit antenna, the wind turbine and the receive antenna is calculated (taking as a reference the half-height point of the mast) as a function of the incidence angle in the vertical plane (θ_t) as well as the receive antenna angles in the horizontal and vertical planes (ϕ_r, θ_r). Note that the considered coordinate system does not depend on the blade position or orientation, as it is referenced to the horizontal position of the transmit antenna ($\phi_t = 0°$), as shown in Fig. B-20.

FIGURE B-20

Coordinate system for the scattering model.

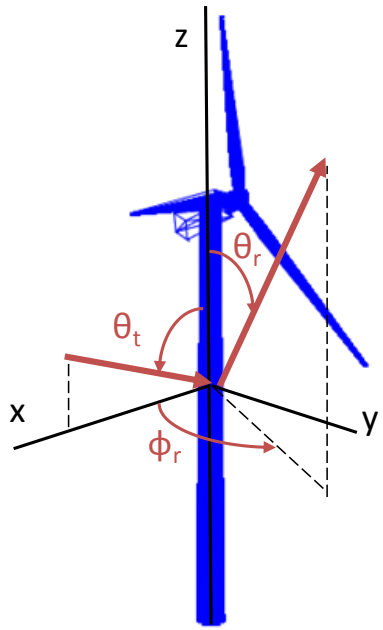

The application limits of these angular positions are:

$-120° < \phi_r < 120°$, which defines the bistatic angle range in the horizontal plane that limits the backscattering region (i.e. forward scattering occurs in the region ±60° behind the wind turbine),

$70° < \theta_t < 110°$ and $160° - \theta_t < \theta_r < 200° - \theta_t$, which impose a vertical limit related to the physical optics theory, where the accuracy of RCS estimations err by wider margins as the direction of observation moves farther away from the specular direction.

It should be noted that the scattering model is valid when at least a significant part of the mast is illuminated by the transmitted signal. Therefore, the transmit antenna radiation pattern should be analysed and, in case that condition is fulfilled, it is recommended to take the maximum gain of the section of the radiation pattern that impinges on the mast for the parameter $G_{Tx\text{-}WTi}$.

As for the receive antenna gain, it should be considered that the antenna will normally be oriented towards the transmitter and thus, broadly speaking, $G_{Rx\text{-}WTi}$ will be lower than the maximum gain of

the radiation pattern of the receiver. Characteristics of directivity and polarization of antennas for the reception of television broadcasting can be found in Recommendation ITU-R BT.419.

The mean amplitude of each path is given by the ratio of both powers expressed in dB, as given by equation (B-7):

$$P_i = 10\log\left(\frac{P_{Tx-WTi-Rx}}{P_{Tx-Rx}}\right) \tag{B-7}$$

Paths with power ratios lower than –45 dB shall be omitted.

Doppler Spectra

For the characterization of the Doppler spectra, three representative cases of empirical Power Spectral Densities (PSDs) are provided, in order to characterize potential situations of high, medium and low degree of time variability, which correspond to different rotation rates and rotor orientations. These Doppler spectra are adapted to each reception location by means of the maximum bistatic Doppler frequency f_{B_max} (Hz),which depends on the relative position of the transmit antenna, the wind turbine and the receive antenna ϕ_r, the maximum rotation frequency of the wind turbine ω_{max} (rad/s) and the blade length l, according to equation (B-8).

$$f_{B\_\max} = \frac{2\omega_{\max} l}{\lambda}\cos\left(\phi_r \,/\, 2\right) \tag{B-8}$$

To account for the different wind conditions that will probably be faced for a certain reception location, it is recommended that all the PSDs provided in Table B-3 are analysed for the system under study. In this way, the user of the channel model can obtain an overview of the different situations that may be encountered without the need for accurate estimations of specific wind directions or wind speeds. If a worst case estimation is desired, "high variability" should be used in the calculations.

TABLE B-3

Doppler PSDs for the channel model (expressed in dB/Hz)

High variability
$S_{high}(f) = \begin{cases} 19.7\exp\left(4.5 \cdot f \,/\, f_{B\_\max}\right) - 38.0 & -0.9 \cdot f_{B\_\max} \le f < 0 \\ \delta(f) & f = 0 \\ 21.4\exp\left(-4.8 \cdot f \,/\, f_{B\_\max}\right) - 38.1 & 0 < f \le 0.9 \cdot f_{B\_\max} \end{cases}$
Medium variability
$S_{medium}(f) = \begin{cases} 22.0\exp(6.1 \cdot f \,/\, f_{B\_\max}) - 30.4 & -0.7 \cdot f_{B\_\max} \le f < 0 \\ \delta(f) & f = 0 \\ 25.1\exp(-8.7 \cdot f \,/\, f_{B\_\max}) - 29.5 & 0 < f \le 0.6 \cdot f_{B\_\max} \end{cases}$
Low variability
$S_{low}(f) = \begin{cases} 22.9\exp(17.9 \cdot f \,/\, f_{B\_\max}) - 24.9 & -0.3 \cdot f_{B\_\max} \le f < 0 \\ \delta(f) & f = 0 \\ 23.2\exp(-17.6 \cdot f \,/\, f_{B\_\max}) - 25.0 & 0 < f \le 0.3 \cdot f_{B\_\max} \end{cases}$

Attachment 3.2
to
Part B

Wind farm scattering model

1 Introduction

Several scattering models are found in the literature to account for the effect of a wind turbine on a signal transmitted in the UHF band, including the simplified models of Recommendation ITU-R BT.805 and Recommendation ITU-R BT.1893-0. However, these theoretical models suffer from several limitations: they are only based on the signal scattered by the blades and do not account for the contribution of the mast, they are based on worst case assumptions with respect to the blade position and composition, and they do not model signal scattering in the vertical plane. Furthermore, the empirical evaluation of these scattering models reported proves that they fail to provide accurate estimations of the signal scattered by modern wind turbines.

What is more, simulations of the radar cross section (RCS) pattern of a wind turbine based on the physical optics theory show that the mast contribution is significantly higher than the contribution of the other components of the wind turbine in the directions where the RCS values are highest [14]. For this reason, the scattering model to be proposed is based on the signal scattered by the mast, which is represented by the RCS of a circular cylinder.

Moreover, the cases of impact in the UHF band occur for quite short distances between transmitters and wind turbines. Under these circumstances, the far field condition required to apply the RCS concept, which is relative to the transmitter to scattering object distance, is not fulfilled. Therefore, near field effects must be taken into account and included in the scattering model.

2 Theoretical basis of the proposed scattering model

2.1 Bistatic RCS of a circular cylinder

The proposed model is based on the work published by Siegel et al. in [15], where RCS patterns of different surfaces of revolution based on physical optics approximations are given. The RCS pattern of an elliptic cylinder is obtained as a function of its dimensions and the angular positions of the transmitter and receiver in both the vertical and the horizontal planes (θ_t,ϕ_t and ϕ_r, θ_r respectively).

Some simplifications can be made to the proposed expression to adapt it for circular cylinders and avoid indeterminate forms for some combinations of angular positions, obtaining equation (B-9) [13].

$$\sigma(\phi_r,\theta_r,\theta_t) = 2k\pi L^2 \sqrt{\frac{1+\cos\phi_r}{2}} \cdot \frac{\sin\theta_t^2}{\sin\theta_t + \sin\theta_r} \cdot \mathrm{sinc}^2\left(\frac{kL\left(\cos\theta_t + \cos\theta_r\right)}{2}\right) \tag{B-9}$$

where $k = 2\pi/\lambda$, λ is the wavelength, r is the cylinder radius and L is the cylinder length. According to the physical optics theory, the accuracy of RCS estimations err by wider margins as the direction of observation moves farther away from the specular direction. In order to define the application limits of equation (B-9), the characteristics of the shapes corresponding to the horizontal and vertical planes of the cylinder have been considered. For the horizontal plane, the limit established for a sphere is used, in such a way that $-120^\circ < \phi_r < 120^\circ$. For the vertical plane, a flat plate can be taken as a reference, for which the physical optics theory performs quite well in predicting the returns in the region at within 20 degrees to either side of normal incidence, i.e. $70^\circ < \theta_t < 110^\circ$.

Considering a similar margin for the bistatic case, the receiver angular position should be 20º to either side of the specular direction ($\theta_r = 180º - \theta_t$), in such a way that $160° - \theta_t < \theta_r < 200° - \theta_t$.

2.2 Near field effects

The formal definition of radar cross section states that the distance between the radar and the object must become infinite in order to eliminate any distance dependence in the RCS characteristics, i.e. far field condition in the context of signal scattering must be fulfilled. However, the cases of impact in the UHF band occur for quite shorter distances between transmit antennas and wind turbines. Therefore, near field effects in the context of signal scattering must be taken into account and included in the scattering model.

According to [16], the near field effect for monostatic reception results in a RCS reduction which can be equivalent to consider a *near field size* instead of the real size of the object. This *near field size* L_{nf} is calculated according to equation (B-10), where R is the transmitter to object distance and λ is the wavelength.

$$L_{nf} = \sqrt{\frac{\lambda R}{2}} \tag{B-10}$$

Nonetheless, under near field condition, apart from the reduction in monostatic RCS, some additional effects on the scattering pattern are observed. The *filling of nulls* with decreasing distances in the scattering pattern is the first symptom; second, the *increment* in the amplitudes of the *sidelobes* of the pattern; and finally, the above-mentioned *reduction* in the amplitude of the *main lobe* of the object's pattern. Taking into account these effects, the scattering pattern of the cylinder in the vertical plane will lose the directivity typical of the sinc function. Therefore, in near field conditions, the RCS value corresponding to the specular direction can be used for wider angular positions.

3 Wind farm scattering model

The proposal for applying near field effects to the scattering model is to estimate the RCS value of the *near field size*L_{nf} corresponding to the specular direction in the vertical plane, and use it within the application limits established by the physical optics theory in this plane.

Table B-4 shows the proposed Wind farm model to characterize signal scattering by a wind turbine in the UHF band, including its limits of application.

TABLE B-4

Wind farm Scattering model

<table>
<tr><td colspan="3">Near field condition $R_{Tx-WTi} < \frac{2L^2}{\lambda}$, being $R_{Tx\text{-}WTi}$ the transmit antenna to wind turbine distance and L the mast length</td></tr>
<tr><td colspan="3">$\sigma_i(\phi_r,\theta_t) = krL_{nf}{}^2\sqrt{\frac{1+\cos\phi_r}{2}}\sin\theta_t$

being $k = 2\pi/\lambda$, λ the transmission wavelength, r the mast radius ϕ_r the receive antenna angular position in the horizontal plane measured at the wind turbine under consideration from the direction of the transmit antenna, θ_t the transmitter angular position in the vertical plane measured at the wind turbine under consideration from the vertical plane and $L_{nf} = \sqrt{\frac{\lambda R_{Tx-WTi}}{2}}$</td></tr>
<tr><td colspan="3">Application limits</td></tr>
<tr><td>$70° < \theta_t < 110°$</td><td>$-120° < \phi_r < 120°$</td><td>$160° - \theta_t < \theta_r < 200° - \theta_t$</td></tr>
</table>

The scattering contribution from the blades is included as a time variability factor that is described in Attachment 3.3.

Attachment 3.3
to
Part B

Wind farm Doppler spectra model

1 Doppler power spectral density characterization

The time variability of the channel is normally represented by Doppler models. To obtain the Doppler model for this particular case, the starting point has been the empirical data obtained from a measurement campaign in the surroundings of a wind farm in Spain, as described in Attachment 2.

The common feature of all the estimated PSDs is the main component at 0 Hz, and decreasing power spectral densities for higher frequencies. In order to account for these special variability features of the scattering signals due to the rotating blades, a new exponential model is proposed [17]. This model is composed of a Dirac delta for the zero Doppler frequency, and side components of decreasing power spectral density for the lowest and highest frequencies, according to equation (B-11).

$$S(f) = \begin{cases} a\exp(bf) - c & f_{min} \le f < 0 \\ \delta(f) & f = 0 \\ d\exp(-ef) - g & 0 < f \le f_{max} \end{cases} \quad \text{(B-11)}$$

where *S(f)* is the PSD expressed in dB/Hz, *a*, *b*, *c*, *d*, *e* and *g* are positive constants, *f* stands for frequency (Hz), $\delta(0)$=0 dB/Hz and f_{min} and f_{max} are the minimum and maximum observable Doppler shifts respectively.

The Doppler spectrum of the signal scattered by a wind turbine depends on the relative locations of transmit antenna-wind turbine-receive antenna, the rotor orientation with respect to transmit antenna and receive antenna, and the blades rotational speed. Considering that both the rotor orientation and the blades rotational speed are dependent on the wind conditions, different levels of channel variability will be faced for a certain reception location in case of changing weather conditions. For this reason, a set of representative Doppler spectra cases corresponding to the different levels of variability that will be faced in a fixed reception location has been selected for the proposed channel model. These Doppler spectra are shown in Table B-3 (Attachment 3.1).

The selected Doppler PSDs are referenced to the maximum bistatic Doppler frequency shift f_{B_max}. This parameter is calculated for a certain reception location as a function of the bistatic angular separation transmitter-wind turbine-receiver ϕ_r, the maximum rotation rae of the wind turbine ω_{max} and the blade length l equation (B-12).

$$f_{B\_max} = \frac{2\omega_{max} l}{\lambda} \cos\left(\phi_r / 2\right) \tag{B-12}$$

Therefore, the proposed spectra are adapted to each particular reception location by means of the calculation of f_{B_max}, which allows the estimation of new situations of time variability due to different working frequencies, wind turbine dimensions and relative locations of transmit antenna-wind turbine-receive antenna transmitter-wind turbine-receiver.

To account for the different wind conditions that will probably be faced for a certain reception location, it is recommended that the three PSDs provided in Table B-3 are considered in the channel model. In this way, the user of the channel model can obtain an overview of the different situations that may be encountered without the need for accurate estimations of wind directions or wind speeds.

Attachment 4
to
Part B

Wind turbines impact to terrestrial DTV services in the UHF band

1 Introduction

The preliminary results about the wind turbines impact to terrestrial DTV services obtained by the University of the Basque Country (UPV/EHU) were included both in Recommendation ITU-R BT.1893-0 and Report ITU-R BT.2142-1. However, as stated in Report ITU-R BT.2142-1, further work was needed in order to analyse the influence of the time-varying multipath interference from the wind turbines on the DVB-T reception quality, considering not only the multipath level but also the relative delays and the dynamics of the scattered signals.

A simplified method has been developed in order to obtain the potential increment in the *C/N* threshold ratio of the DVB-T system as a function of the propagation channel characteristics.

2 Summary of contributions to Recommendation ITU-R BT.1893

In most of the situations where the impact of the wind farm to DTV reception quality was analysed, the threshold carrier-to-noise ratios (*C/N*) obtained were similar to the threshold *C/N* ratios expected in environments in the absence of wind farms. More precisely, the DVB-T reception quality does not seem to be affected in the forward scattering region of the wind turbines for the cases considered and the limits assumed for this study.

In the backscattering region, by contrast, increases in the *C/N* threshold ratio may be experienced, depending both on the multipath level due to signal scattering from the wind turbines, and the time variability of these scattered signals as blades rotate. In order to characterize the multipath channel in the backscattering region further and relate these characteristics to the obtained *C/N* threshold ratios, two parameters have been defined in Attachment 4.1, *multipath energy* and *mean standard deviation*. These parameters can be calculated from measurements or applying the channel model defined in Attachment 3.

As a function of these parameters, an estimation of the potential increment in the *C/N* threshold ratio with respect to the theoretical threshold for a Ricean channel can be obtained as explained in Attachment 4.1.

This study concludes that dynamic multipath from wind turbines may cause DTTB reception problems, especially in case of non LoS to the transmitter but LoS to the wind farm. This condition of non LoS to the transmitter should be furtherly analysed.

The obtained results may be used as simple guidelines in order to estimate the potential degradation caused by a wind farm on a DVB-T service.

Attachment 4.1
to
Part B

Empirical Evaluation of the Impact of Wind Turbines on DVB-T Reception Quality

1 Introduction

This Attachment presents some empirical threshold carrier-to-noise (*C*/*N*) ratios in the area of influence of a wind farm, in order to assess the potential impact of the scattered time-varying signals from wind turbines on the DVB-T services in the UHF band.

The bit error rate (BER) as a function of *C/N* is the most important figure of merit for any digital transmission system. More precisely, the corresponding BER after Viterbi decoding is used to determine the threshold of quasi error free condition (QEF reception is considered when BER after Viterbi is equal to 2×10^{-4}). For the DVB-T configuration used in Spain (8 MHz channel, 8K mode, 64-QAM modulation and 2/3 code rate), the system has a theoretical threshold *C*/*N* figure of 16.7 dB for a Gaussian channel, 17.3 dB for a Ricean channel and 20.3 dB for a Rayleigh channel [19]. These theoretical thresholds are based upon perfect channel estimation (without considering phase noise) and ideal receiver implementation, and thus in practical situations the *C/N* requirement for demodulation is increased by some dB. For fixed antenna reception, a Ricean channel multipath profile will generally be experienced.

2 Methodology

The measurements of BER as a function of *C/N* were taken in thirty nine different reception locations placed between 2 and 13 km away from the transmitter, under normal operation of the wind farm. 25 of the reception locations correspond to backscattering from the wind turbines, while the other 14 correspond to forward scattering.

The DVB-T professional receiver, controlled by a software tool, generates different levels of additive noise in order to obtain the threshold *C/N* ratio for QEF reception condition. In addition to this, the DVB-T signal was recorded as explained in Attachment 2.1 to PART B for further relating the multipath level obtained from the channel impulse response to the threshold *C/N* ratio estimated by the DVB-T professional receiver.

The measurements corresponding to backscattering signals were carried out at each reception location pointing the antenna at different directions. The first measurement was recorded pointing the receive antenna towards the transmit antenna, and for successive measurements the antenna was misaimed in steps of 15º in azimuth. When the receive antenna is not pointing towards the transmit antenna, the multipath level of the received signal is expected to vary and therefore the influence of the amplitude of the echoes from the wind turbines in the reception quality can be evaluated. Altogether, 160 different situations are analysed.

The measurements corresponding to the forward scattering signals were carried out in locations where the transmit antenna, one or more turbines and the receive antenna are lined-up, with the receiver antenna pointing towards the transmit antenna. In total, 56 different situations of signals scattered in the forward region were measured [18].

3 Analysis of the propagation channel

The type of propagation channel encountered in the vicinity of the wind farm depends on the scattering region where the receiver is located, i.e. on the relative position of transmit antenna-wind turbine-receive antenna.

3.1 Backscatteringregion

In the *backscatteringregion* of the wind turbines, the channel impulse response at the measurement system will be composed of the direct path and a series of attenuated, time delayed, and phase shifted replicas caused by signal scattering on the wind turbines.

The *backscattering region*, where the proposed model is applicable, is comprised within the interval $-120° < \phi_r < 120°$, (i.e. forward scattering occurs in the region ±60° behind the wind turbine).

As an example, Fig. B-21 shows 200 consecutive channel impulse responses corresponding to a reception condition where the *C/N* threshold for BER equal to 2×10^{-4} is 19 dB, and Fig. B-22 shows the same graph for a reception condition where the *C/N* threshold is 24.5 dB. The scattered signals from the wind turbines of "Wind Farm I" are indicated as WT 1 to WT 5.

FIGURE B-21

DVB-T channel impulse responses during 800 consecutive symbols (*C*/*N* threshold = 19 dB)

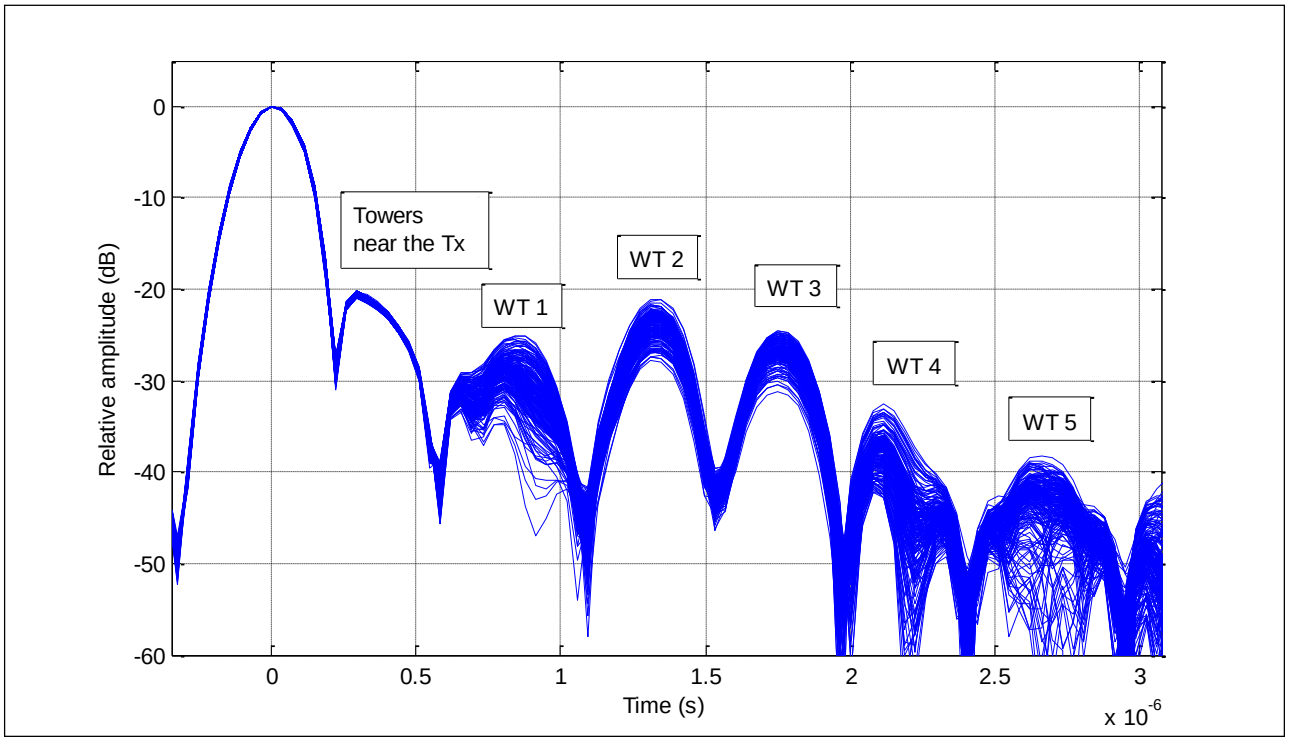

FIGURE B-22

DVB-T channel impulse responses during 800 consecutive symbols (*C*/*N* threshold = 24.5 dB)

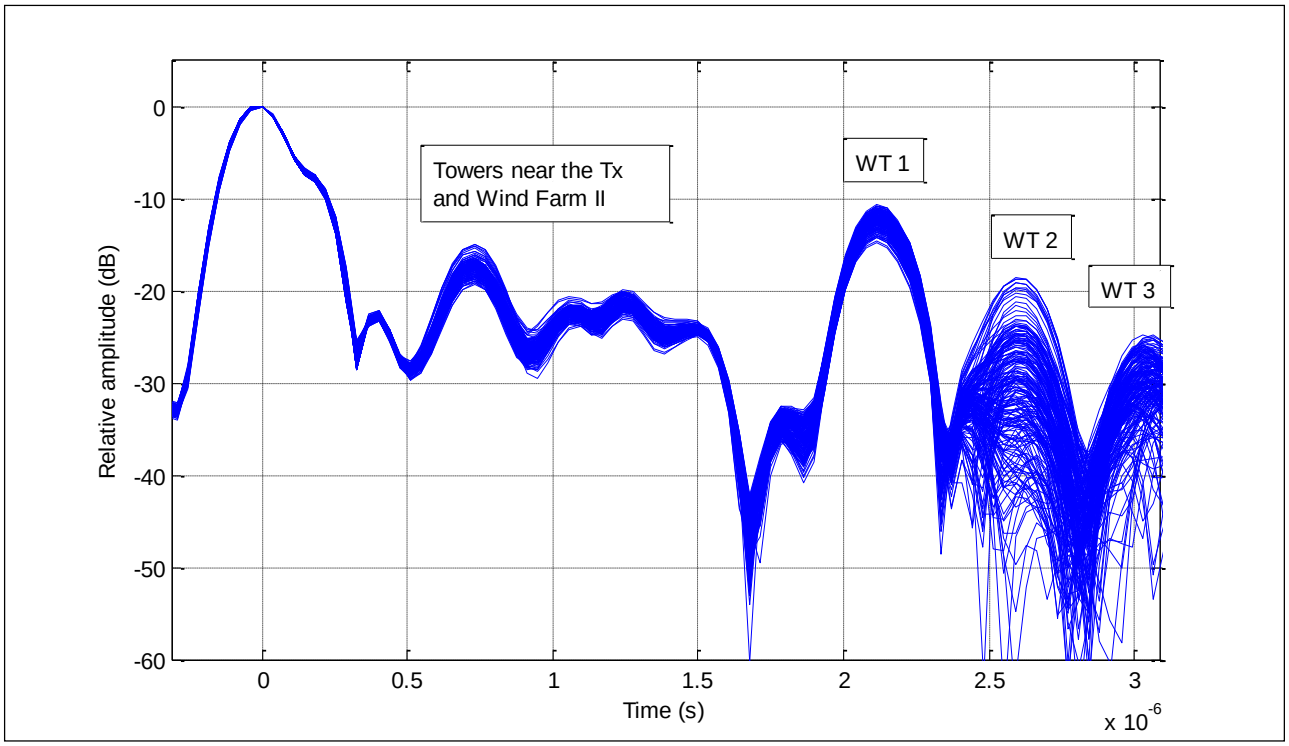

The scattered signals from "Wind Farm II" and the other telecommunication towers near to the DTTB transmitters are also indicated in the Figures. As it is shown in the Figure, the increase in the *C/N* threshold corresponds to back-scattered signals of higher amplitude

Therefore, it is necessary to characterize the multipath channel in the backscattering region for further relating these characteristics to the obtained threshold *C/N* ratios. The characterization should not only consider the amplitude of the multiple paths but also their time variability. To do so, two parameters have been defined: *multipath energy* and *mean standard deviation* [19].

The first parameter takes into account the mean level of the multipath due to signal scattering on wind turbines. Thus, it considers both the multipath number and the mean amplitudes of these paths. To do so, the *multipath energy* of the channel, P_{mult}, is defined as the sum of the mean normalized received power from each wind turbine. The mean value of each path is calculated as a representative central value of the path because the scattering signals vary as blades rotate. Therefore, the *multipath energy* of the impulse response is given by equation (B-13).

$$P_{mult} = \sum_{i=1}^{N} mean\left(P\left(\tau_i, t\right)\right) \tag{B-13}$$

where:

i = 1 and *i* = *N*: indices of the first and last paths above a threshold level of –45 dB with respect to the direct path

$P(\tau_i,t)$: time-varying received power from path *i* normalized with respect to the main path.

The mean standard deviation, std_{mean}, is calculated as the mean of the standard deviations of the time varying signals scattered by each wind turbine in a certain measurement.

Hence, it provides a measure of the time variability of the channel impulse response during the recording time. The mean standard deviation is given by equation (B-14).

$$std_{mean} = \frac{\sum_{i=1}^{N} std_i}{N} \tag{B-14}$$

where:

i = 1 and *i* = *N*: indices of the first and last paths above a threshold level of –45 dB with respect to the direct path

std_i: standard deviation of the time varying normalized received power from path *i* (dB).

3.2 Forward scattering region

The *forward scattering region* (the *backscattering region* is comprised within the interval $-120° < \phi_r < 120°$ so the forward scattering occurs in the region ±60° behind the wind turbine).

corresponds to locations where the transmit antenna one or more turbines and the receive antenna are lined-up. In these situations, the relative delays of the scattered signals tend to zero. In general, the forward scattering from a target is stronger than the backscattering, but is nearly out of phase with the incident field. Consequently, the forward scatter is generally subtracted from the incident field, thereby creating a shadow region of reduced intensity behind the target.

Figure B-23 shows 200 consecutive channel impulse responses corresponding to a reception condition in the forward scattering of the wind turbines of Wind Farm I.

As forward scattered signals have a delay close to zero, it can be observed that the signals scattered by the wind turbines of Wind Farm I are overlapped with the direct signal from the transmit antenna, and there is no significant multipath due to backscattered signals.

FIGURE B-23

DVB-T channel impulse responses during 800 consecutive symbols (Forward scattering)

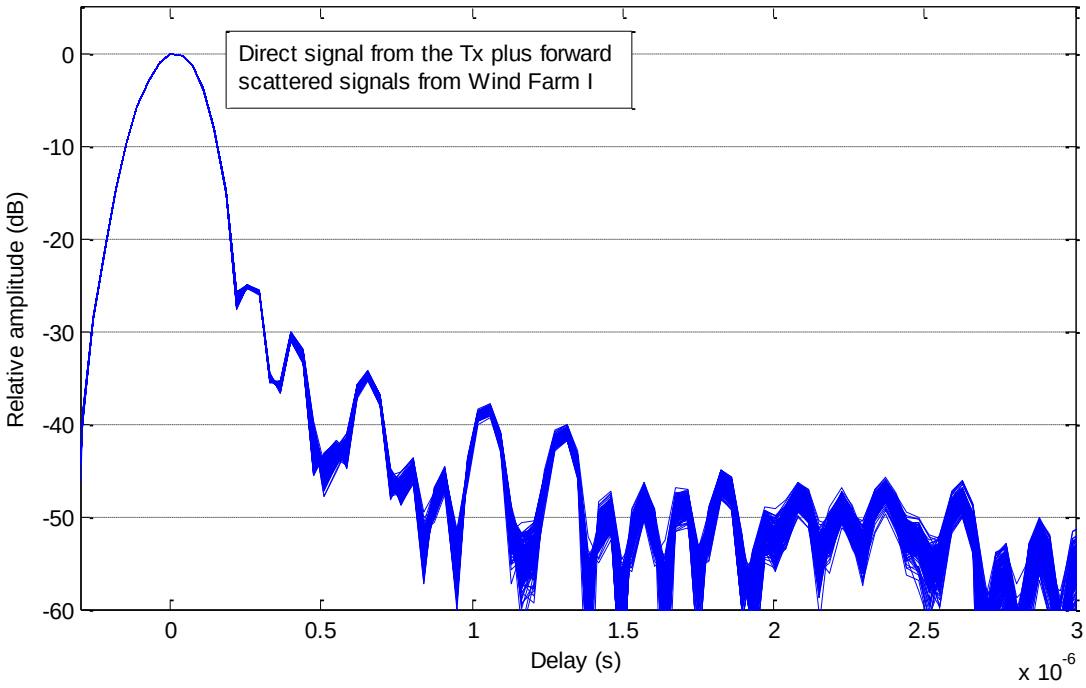

4 Results and discussion

This section exposes and analyses the obtained results focused on the DVB-T service quality.

4.1 Backscattering

Figure B-24 shows the bit error rate (BER) as a function of *C/N* for the different situations measured in the backscattering region of the wind turbines. Obtained results can be divided in two different groups. It can be observed that the main part of the measurements (75 %) feature a threshold *C/N* ratio below 19.3 dB, that is, the theoretical threshold for a Ricean channel considering a margin of about 2 dB (corresponding to the receiver implementation losses and the use through a practical RF transmission system) [12]. As a significant result, it can be concluded that those *C/N* threshold ratios are similar to those expected in environments with absence of wind farms.

FIGURE B-24

Backward scattering: BER after Viterbi as a function of *C/N* ratio

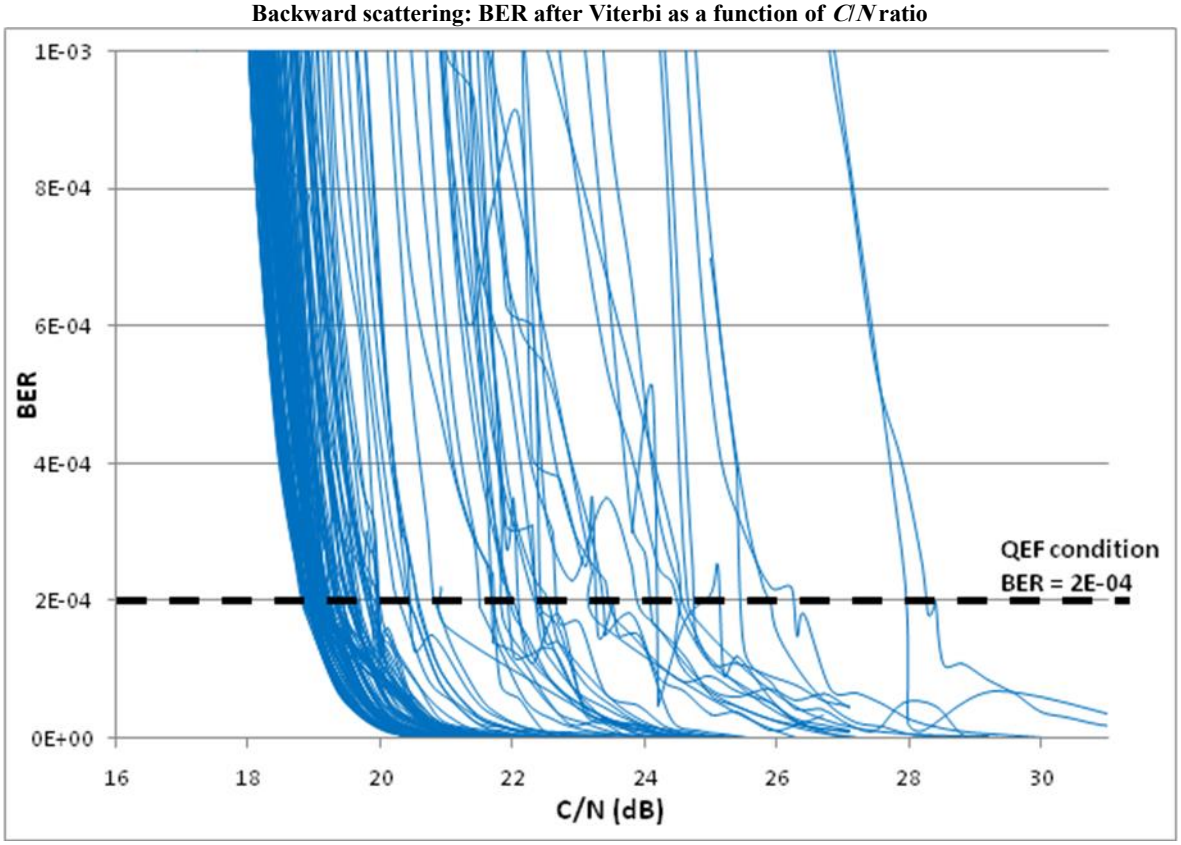

However, there is a group of measurements that show *C/N* threshold ratios higher than 19.3 dB and up to 28 dB. These measurements correspond to situations where the scattered signals from the wind turbines degrade the DVB-T reception quality, increasing the theoretical *C/N* threshold ratio.

In order to represent the *C/N* threshold ratios measured in the backscattering region as a function of the characteristics of the multipath channel, Fig. B-25 shows the required *C/N* ratios with respect to *multipath energy* (expressed in dB). The size of the bubbles is determined by the values of the *mean standard deviation* of each measurement (expressed in dB). The bubbles are also depicted from light grey to black as a function of the mean standard deviation to provide a clearer representation.

FIGURE B-25

Backscattering region. Required *C/N* ratios as a function of the characteristics of the multipath channel [18]

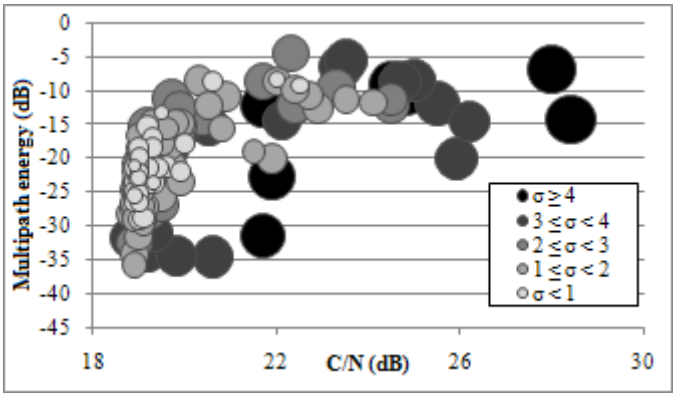

As it can be observed in the Figure, there is a clear correlation between the increasing *C/N* ratios and the *multipath energy*. Moreover, measurements with the same level of *multipath energy* feature a higher *C/N* threshold ratio when the *mean standard deviation* is also higher.

As a significant result, all the measurements with *multipath energy* values higher than –15 dB have a *C/N* threshold ratio equal or higher than 19.3 dB, independently of their *mean standard deviation*. By contrast, Recommendation ITU-R BT.1893-0 states that the effects of the wind turbines are reduced during periods when the wind turbines are not rotating.

For measurements with *multipath energy* values lower than –15 dB, the most significant increments over the theoretical threshold of 19.3 dB are obtained for the highest values of *mean standard deviation*. Moreover, all the measurements with *multipath energy* values lower than –25 dB and *mean standard deviation* values below 2 dB provide *C/N* ratios close to 19.3 dB.

Table B-5 summarizes the maximum increments in the *C/N* threshold ratios with respect to the Ricean *C/N* threshold as a function of *multipath energy*.

TABLE B-5

Maximum increment of the *C/N* thresholds over the theoretical Ricean *C/N* threshold

Multipath energy	**Maximum increment of the *C/N* threshold over the theoretical Ricean *C/N* threshold**
$P_{mult} \geq$ –15 dB	9.1 dB
–15 dB> $P_{mult} \geq$ –25 dB	6.6 dB
–25 dB> $P_{mult} \geq$ –35 dB	2.4 dB
$P_{mult} <$ –35 dB	0 dB

4.2 Forward scattering region

Figure B-26 shows the bit error rate (BER) as a function of threshold *C/N* for the different situations measured in the forward scattering region of the wind turbines. It can be observed that all the measurements feature threshold *C/N* ratios in a narrow margin around the theoretical threshold of 19.4 dB for a Gaussian channel. Therefore, for all the different situations measured, including several orientations of the wind turbines with respect to the wind direction (and therefore with respect to the transmit antenna-receive antenna path), the effect of the forward scattering seems to be negligible.

FIGURE B-26

Forward scattering: BER after Viterbi as a function of *C*/*N*

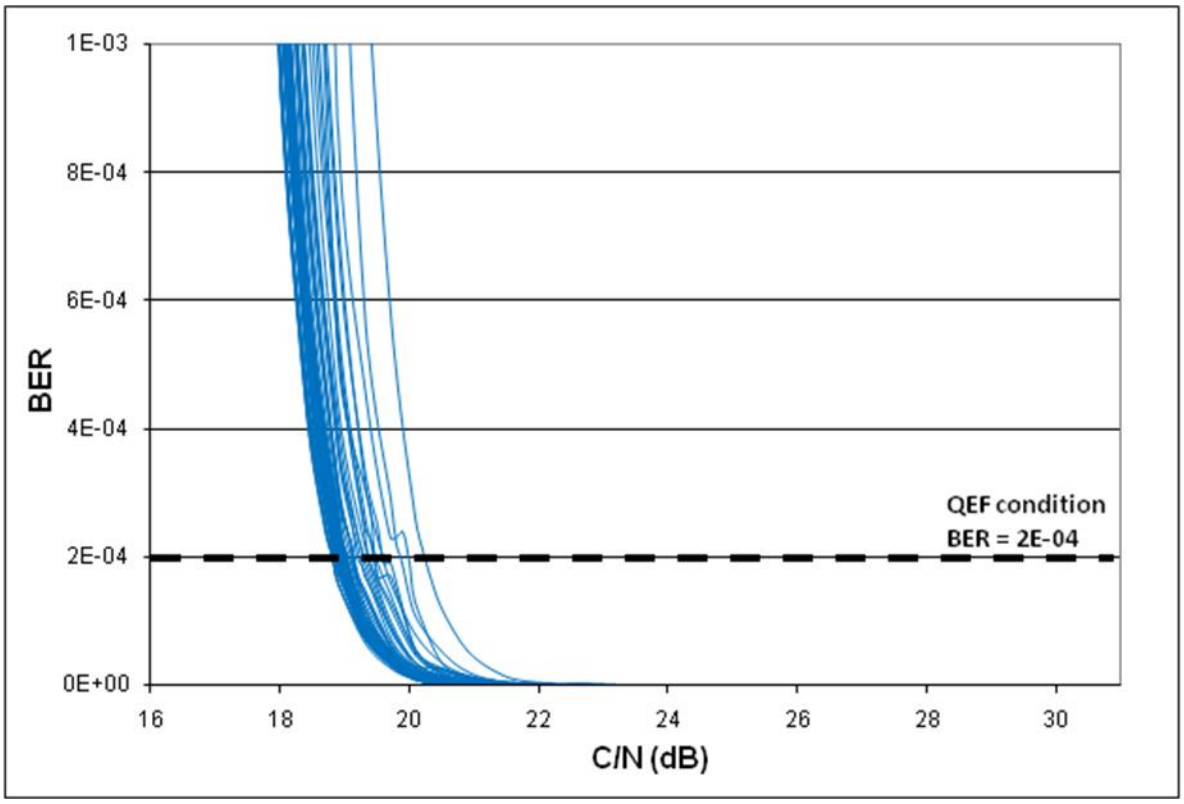

5 Conclusions

In most of the situations where the impact of a wind farm to DVB-T reception quality was analysed, the threshold *C*/*N* ratios obtained were similar to those expected in environments with the absence of wind farms. More precisely, the DVB-T reception quality does not seem to be affected in the forward scattering region of the wind turbines, for the cases considered. In the case of the backscattering region, in those situations where the scattered signals from wind turbines are significant in amplitude and variability, the threshold *C*/*N* ratio necessary for QEF condition is higher.

There is an increasing tendency of the threshold *C*/*N* ratio with the amplitude of the echoes of the time-varying multipath due to wind turbines. Reception areas where the dynamic multipath level is above –35 dB may experience increments in the *C*/*N* threshold ratios for QEF condition up to 8 dB as a function of the time variability of the scattered signals.

It should be mentioned that, in the area where the trials were carried out, multipath levels above –25 dB are not usual when pointing the receive antenna towards the transmit antenna, so it is unlikely that the multipath level will be severe enough to cause disruption to the DVB-T reception in most part of the analysed area. In a general case, the use of an omnidirectional antenna will cause higher levels of multipath energy to be detected in the receiver.

These results may be used as simple guidelines in order to estimate the potential degradation caused by a wind farm on a DVB-T service.

Attachment 5
to
Part B

Example of use

1 Adaptation of the channel model to a particular reception condition

The parameters of the TSR channel model have to be adapted to each reception location of the coverage area of a transmitter potentially affected by a wind farm. To do so, a digital terrain database can be used to divide the coverage area into small grids of a given accuracy. For each of the centre locations of these grids, the parameters of the channel model for those specific conditions can be obtained, as explained in the following section. This process is easily implementable in planning tools, and provides a fast overview of the potential degradation due to the wind farm.

It should be noted that the channel model is independent of the television standard, and as such, it can be used to estimate the potential impact of a wind farm on any television broadcasting service provided in the UHF band, as explained in § 2.

1.1 Number of paths

The number of paths is given by the number of wind turbines that compose the wind farm (named 1 to 3 in Fig. B-27), plus a static path corresponding to the transmitter (named 0 in Fig. B-27).

FIGURE B-27

Graphical representation of the number of paths

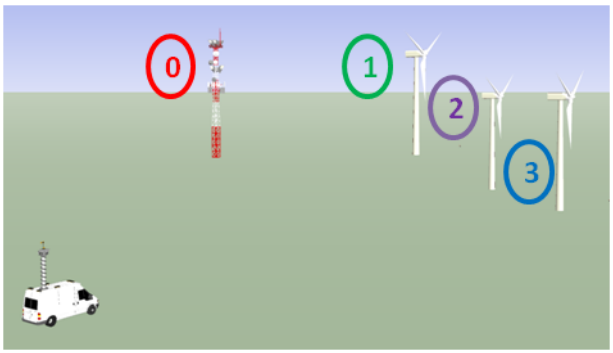

1.2 Relative delays of the paths

The signal from the transmitter is taken as the reference for calculating the relative delays of each multipath component, in such a way that each of the remaining delays are calculated according to Eq. (B-1) in Attachment 3.1.

FIGURE B-28

Graphical representation of the data required to calculate the relative delays of the paths

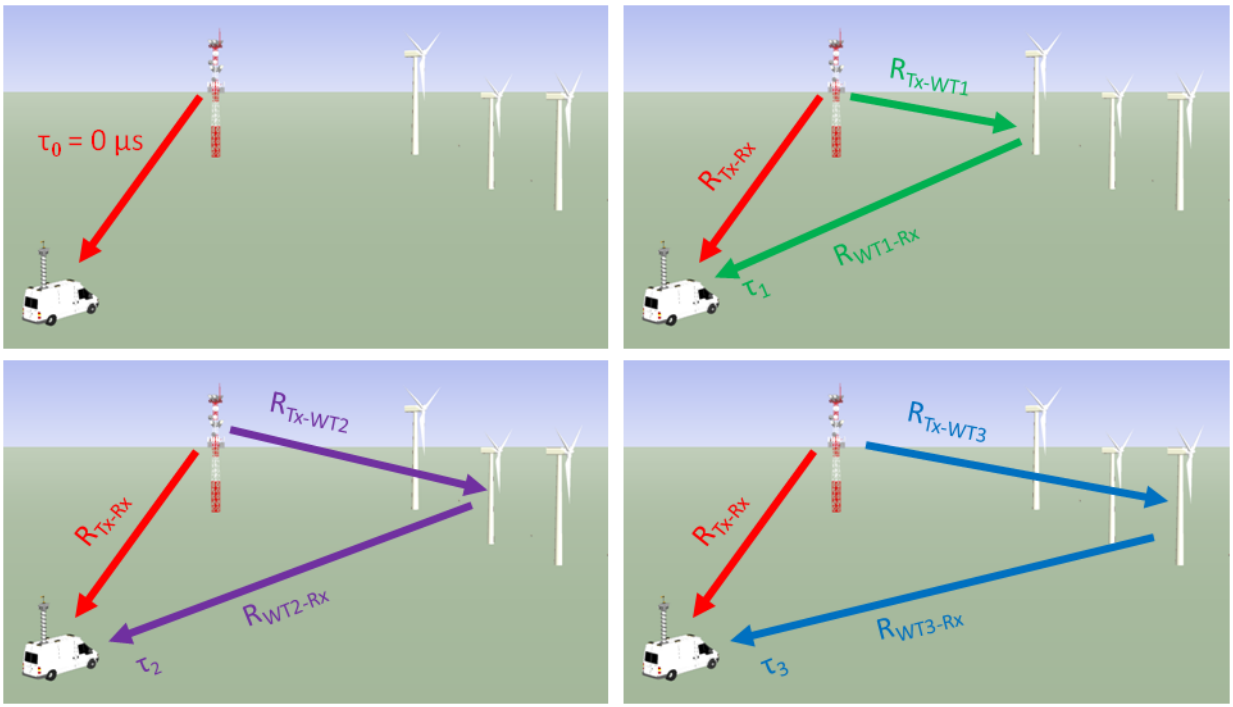

1.3 Mean amplitude of the paths

The mean amplitude of the path corresponding to the direct signal from the transmit antenna is also taken as the power reference (0 dB). Hence, the mean amplitude of the remaining multipath components is given by the ratio, measured in the reception location and expressed in dB, between the power of the signal scattered from the corresponding wind turbine $P_{Tx\text{-}WTi\text{-}Rx}$ and the power of the direct signal from the transmit antenna $P_{Tx\text{-}Rx}$.

FIGURE B-29

Graphical representation of the data required to calculate the relative amplitude of the paths

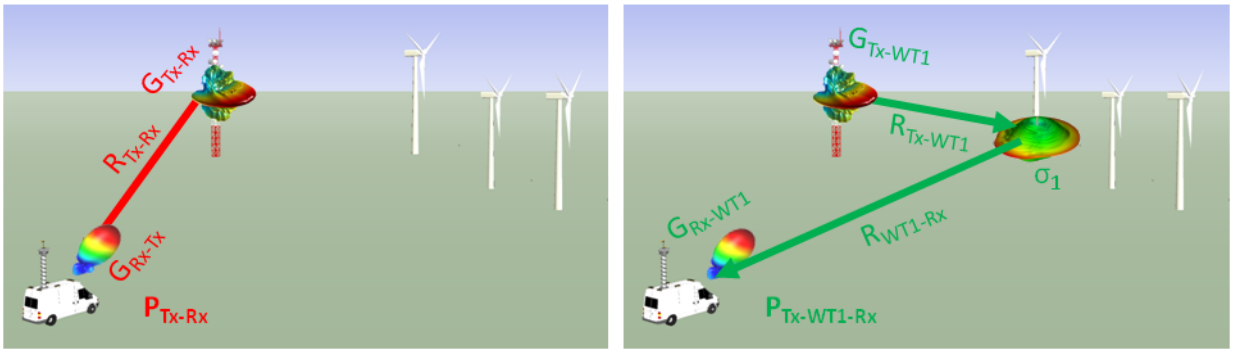

The direct signal from the transmit antenna is calculated as indicated in Eq. (B-2) in Attachment 3.1.

For each wind turbine, the power of the scattered signal $P_{Tx\text{-}WTi\text{-}Rx}$ is calculated as indicated in Eq. (B-3) in Attachment 3.1. To do so, the radar cross section of the mast in the receiver direction needs to be calculated as shown in Eq. (B-4) in Attachment 3.1.

This RCS depends on the relative position of the transmit antenna, the wind turbine and the receive antenna, as shown in Fig. B-30.

FIGURE B-30

Relative position Tx-WT-Rx to calculate the RCS of the mast in the receive antenna direction

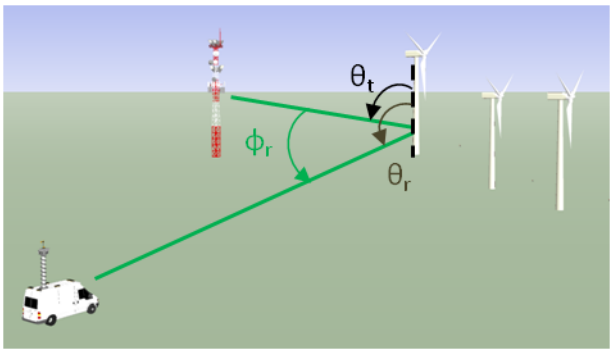

Finally, the mean amplitude of each path is normalized with respect to the power of the direct signal from the transmit antenna, as given by Eq. (B-7) in Attachment 3.1.

1.4 Doppler spectra

For the characterization of the Doppler spectra, representative PSDs corresponding to different levels of variability have been defined. These cases characterize increasing levels of variability due to different rotation rates and orientations of the wind turbine with respect to the transmit antenna and the receive antenna.

These Doppler spectra need to be suited to each reception location of new cases under study by calculating the corresponding maximum bistatic Doppler frequency f_{B_max}, which will depend on the relative position of the transmit antenna, the wind turbine and the receive antenna, the transmission wavelength, the maximum rotation rate, and the blade length (see Eq. (B-8) in Attachment 3.1). This way, the Doppler spectra of Table B-3 in Attachment 3.1 are to be adapted to the particular conditions of the new case under study by means of the specific value of f_{B_max}.

To account for the different wind conditions that will probably be faced for a certain reception location, it is recommended that the three PSDs provided in Table B-3 are considered in the channel model. In this way, the user of the channel model can obtain an overview of the different situations that may be encountered without the need for accurate estimations of wind directions or wind speeds.

2 Estimation of the impact on DTV services

Once the channel model has been adapted, the most complete way to estimate the impact on a certain service is to develop some simulations of the effect of the resulting time-varying channel model on the corresponding reception threshold. This implies obtaining a realization of the channel model, i.e. obtaining the successive channel impulse responses that characterize the signal propagation in the presence of a wind farm. The complex time-varying paths that correspond to the signal scattering from each wind turbine can be obtained generating a set of white Gaussian processes, whose power spectral densities are shaped by a shaping filter whose amplitude transfer function is $H(f) = \sqrt{S(f)}$, where *S(f)* is the Doppler power spectrum. The resulting filter must have a normalized power of 1, so that the individual path gains have to be properly scaled to account for the different powers of the taps according to the calculated mean amplitude.

For the specific case of DVB-T, a simplified method to estimate the potential degradation due to a wind farm is described in the following subsection.

2.1 Impact on DVB-T

The potential increment in the CNR threshold for Quasi Error Free (QEF) reception with respect to the typical Ricean channel used for the planning of fixed broadcast services can be estimated as proposed in Attachment 4. To do so, both empirical scattered signals or the estimated complex tap-gain processes obtained as mentioned above, can be used to calculate the *multipath energy* and the *mean standard deviation* as indicated in Eq. (B-13) and (B-14). Based on the obtained parameters, the maximum increment of the CNR thresholds over the theoretical Ricean CNR threshold can be predicted according to the results presented in Fig. B-26 and Table B-5 from Attachment 4.1.

PART C

Results of studies in Italy

The effect of the scattering of digital television signals from a wind turbine

Attachment 1
to
Part C

Example of use

1 Wind turbine impairment evaluation: the Lagopesole case

The demand of green power plant is continuously increasing and wind farms are one of the most important. Unfortunately sometimes the place chosen for the installation of a new wind farm (a wind farm is a place having several wind turbines) is very close to sites with radiocommunication systems like Air Traffic Control radars, weather and maritime radars, aeronautical radio navigation systems, such as VOR and ILS, radio astronomy, fixed radio links and broadcasting services. The elements of the wind turbines and their dynamics can interact radio signal through the diffraction of the transmitted/received radiocommunication signal. Such interaction can reduce the *C/N* margin or can create impairments on the radiocommunication signal synchronous with the rotation of the blades.

In the past, Rai Way had built a transmitting site placed near the city of Sassano situated in Basilicata (Italy). The name of the transmitting site is Lagopesole. Lagopesole transmitter broadcasts the Rai 1 multiplex which contains four video programmes, RaiUno, RaiDue, RaiTre, RaiNews24 and three audio programmes, RadioUno, RadioDue and RadioTre.

Recently a private company requested to the local Administration the permission to build a small wind farm composed by 4 wind turbines. The location of the wind turbines and the broadcasting transmitter are shown in the following Fig. C-1.

FIGURE C-1

Aerial view of the wind farm and Lagopesole transmitter station

The company in charge to build the wind farm provided the coordinates of the wind turbines and their characteristics. The wind turbines are identified as T0593286, T0593274, T0584057 and T0593297.

Rai Way provided the characteristics of the transmitting station reported into Table C-1.

TABLE C-1

DVB-T service characteristics

Lagopesole transmitting station	
Coordinates	Lat: 40° 48' 22" Long: 15° 46' 27"
Tower height	30 m
Antenna height	25 m
Transmission frequency	538 MHz (CH 29)
Maximum ERP (real)	97 W
Radiating system	3 × 3 panels 8 dipoles (0°-180°-270°)

Due to the short distances between the transmitter site and the locations selected for the wind turbines, it has been considered appropriate to analyse the relative heights of the transmitting antennas and of the wind turbines. In this analysis, altimetry data and the tilt of the radiating system have been considered.

Figure C-2 shows the relative heights of the wind turbines and of the transmission antennas, considering the terrain profile and the tilt of the radiating system (tilt of maximum gain and lower limit of the –3 dB beamwidth).

FIGURE C-2

Height of transmitter antennas and wind turbines, terrain profile and tilt of the radiating system for turbines T0593286, T0593274, T0584057 and T0593297 (from left to right and top to bottom)

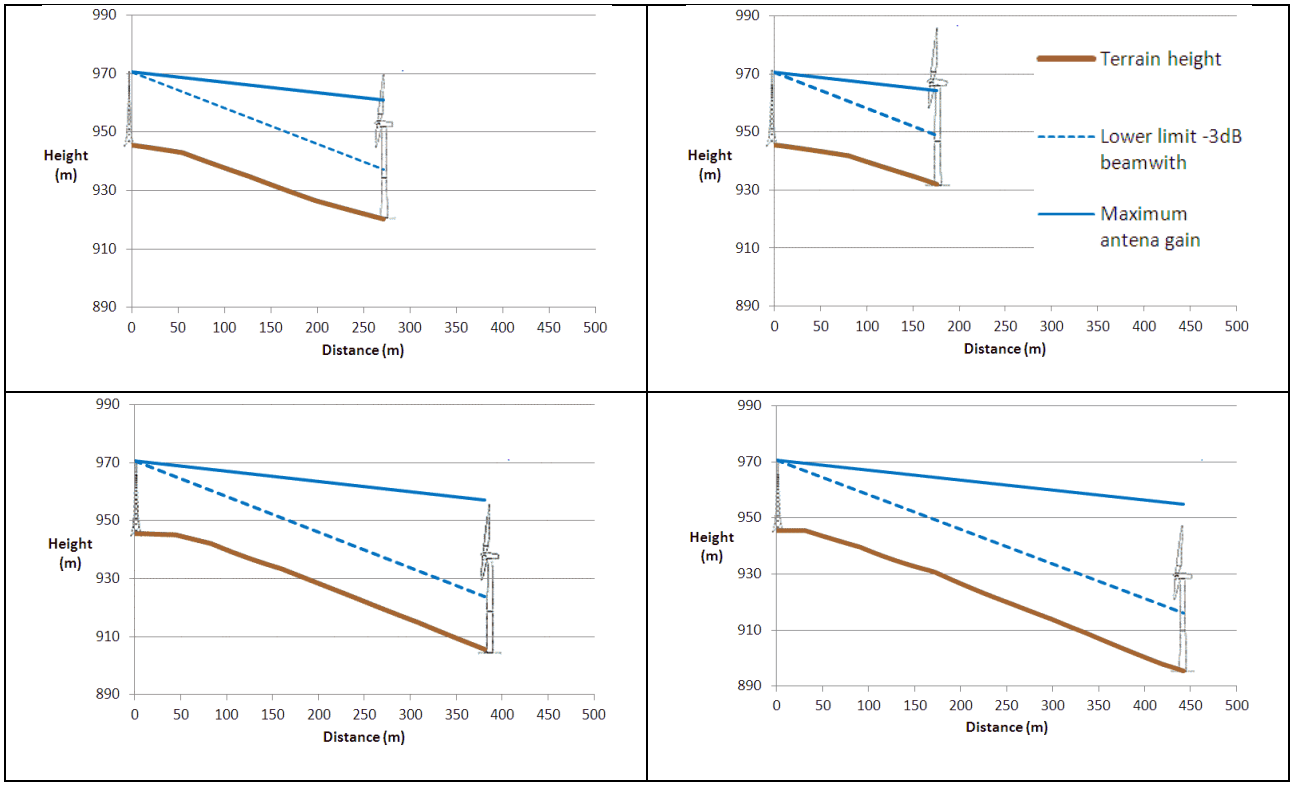

Rai Way developed a measurement system based onto Recommendation ITU-R BT.1735 in which the real coverage of a broadcasting transmitter is evaluated. A set of measurement points, reported in Table C-2, characterise the coverage of the Lagopesole transmitter.

TABLE C-2

MEASUREMENT POINT	LON	LAT	HEIGHT (asl)	FIELD STRENGHT	POL	MER
1	154407	404816	770	79	V	37,6
2	154435	404652	928	81	V	34,3
3	154451	404749	751	80	V	38,0
4	154510	404830	792	80	V	37,5
5	154510	404945	778	74	V	35,5
6	154530	404715	757	82	V	38,3
7	154530	404715	757	85	V	38,7
8	154530	404847	793	90	V	39,4
9	154540	404622	914	82	V	37,9
10	154540	404622	914	82	V	37,7
11	154610	404652	801	82	V	37,7
12	154610	404803	887	97	V	39,3
13	154633	404930	780	89	V	39,2
14	154640	404845	846	89	V	39,2
15	154657	404703	835	84	V	38,4
16	154701	404842	904	83	V	27,8

In two points the measurements have been repeated twice in different days in a week. It is notable that the field strengths measured at the fixed height of 10 mt agl is ever more than 25 dB higher than the minimum median field strength planned for the band IV (RLP 90%). The measure of MER is ever very high with the exception in the point 16 where it is less than 30 dB.

The possible impairments of wind turbines have been evaluated for each measurement point and for all the coverage area. Particular attention has been given to the measurement point 16 where the MER measured is worse than the others points.

Figure C-3 represents the map of the measurement points and the transmitter location.

FIGURE C-3

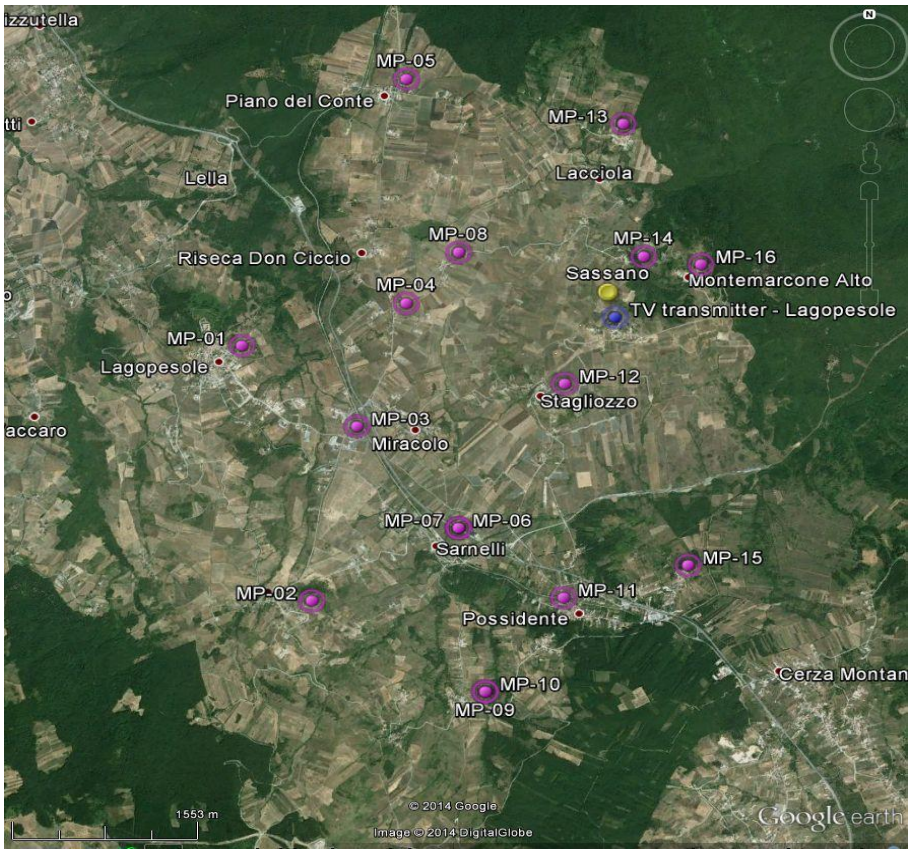

The analysis of the possible impairments has been provided in cooperation with the University of the Basque Country. Figure C-4 shows the whole area involved with the indications where degradation of *C/N* can be expected. The applied method is the one recommended into Recommendation ITU-R BT.1893.

FIGURE C-4

Impairment evaluated in accordance with Recommendation ITU-R BT.1893

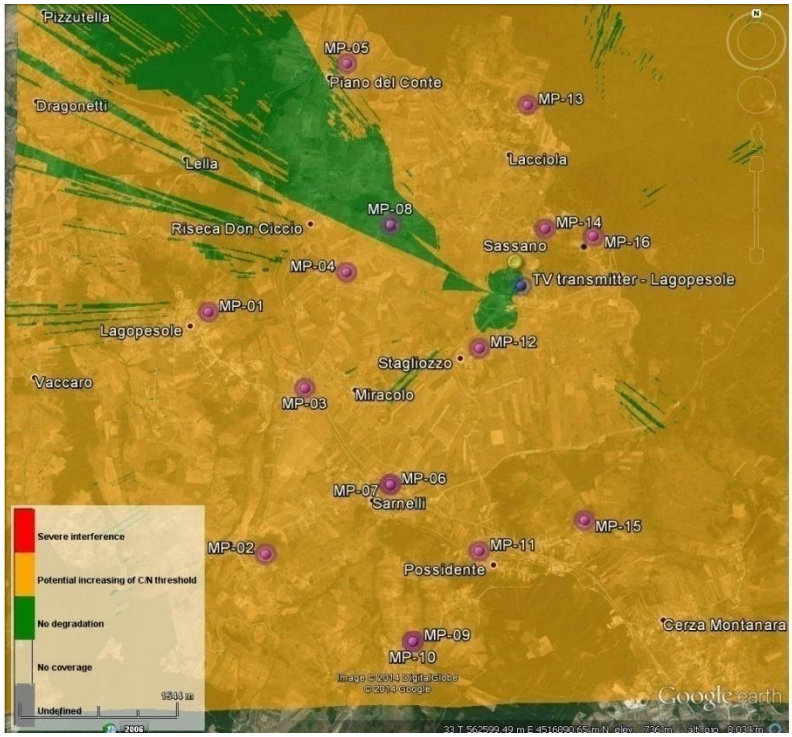

No severe interferences are expected. In the most critical point, where MER is lower than in the other points, the detailed analysis is reported in the Table C-3.

TABLE C-3

Detailed analysis of the point 16, Montemarcone Alto

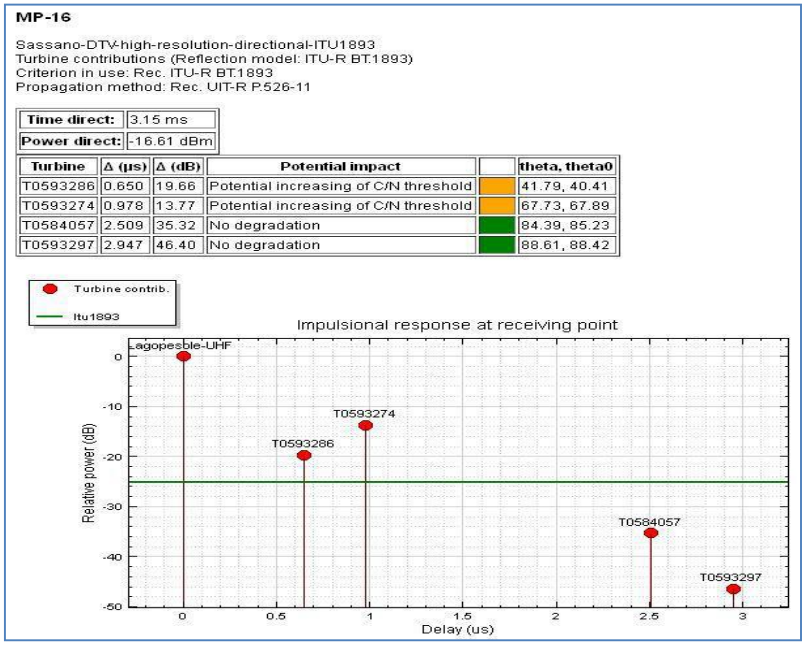

Similar analysis have been conducted utilising the method called Wind farm. The obtained results confirm that, at least, two wind turbines can cause impairments in the measurement point 16, Montemarcone Alto.

The following Table C-4 includes the whole evaluation made with both methods, BT.1893 Part 1 and Part 2 Wind farm, in which in the row there are the measurement points and in the column there are the single turbine.

TABLE C-4

Frame of the interferences (double xx means greater degradation of the C/N)

							ITU BT.1893				TSR			
MEASUREMENT POINT	LON	LAT	HEIGHT (asl)	FIELD STRENGHT	POL	MER	T0593286	T0593274	T0584057	T0593297	T0593286	T0593274	T0584057	T0593297
1	154407	404816	770	79	V	37,6	x	x					x	
2	154435	404652	928	81	V	34,3	x	x				x	x	
3	154451	404749	751	80	V	38,0	x	x					x	
4	154510	404830	792	80	V	37,5	x						x	
5	154510	404945	778	74	V	35,5		x			x			x
6	154530	404715	757	82	V	38,3	x	x				x	x	
7	154530	404715	757	85	V	38,7	x	x				x	x	
8	154530	404847	793	90	V	39,4					x		x	x
9	154540	404622	914	82	V	37,9	x	x	x	x		xx	xx	
10	154540	404622	914	82	V	37,7	x	x	x	x		xx	xx	
11	154610	404652	801	82	V	37,7	x	x		x	x	x	x	
12	154610	404803	887	97	V	39,3		x			x	x	x	
13	154633	404930	780	89	V	39,2		x	x		x	x		x
14	154640	404845	846	89	V	39,2	x	x			x	x		x
15	154657	404703	835	84	V	38,4	x	x			x	x	x	x
16	154701	404842	904	83	V	27,8	x	x			x	x	x	x

On the base of the expected degradation of *C/N* and considering the measured MER, Rai Way asked the company in charge for the construction of the wind farm to consider the possibility to limit some movements such as Yaw and Pitch. The company didn't accept the proposal and it has been agreed to build only two wind turbines instead of four.

Moreover, Rai Way decided to install near Montermarcone Alto a measurement system, called ASAP, able to continuously record same parameters such as Field Strength, MER, BER, impulse response. The objective is to compare the situation before, during and after the construction of the wind farm for a period of time as long as one year.

PART D

References

[1] "*TCX3000 RF recorder/player operation manual*", ADIVIC, Febr. 2008 (available in http://www.adivic.com).

[2] "Digital Broadcast Analysis Software" (available in http://www.arbitrary.es)

[3] VAN KATS, P.J. and PAGER, 0.P.E., "*Reflections of Electromagnetic Waves By Large Wind Turbines and their Impact on UHF Broadcast Reception*", Report 511 TM/84, British Library, 1984.

[4] EATON, J.L. BLACK, R.I. and TAYLOR, G.H., "*Interference to television reception from large wind turbines*", BBC Research Department, Engineering Division, March 1983.

[5] WRIGHT, D.T., 1992/7, "*Effects of wind turbines on UHF television reception*", BBC Research Department Report, 1999.

[6] SENGUPTA, D.L. and SENIOR, T.B.A., "*Electromagnetic Interference to Television Reception Caused by Horizontal Axis Windmills*", Proceedings of the IEEE, Vol. 67, No. 8, August 1979.

[7] SENGUPTA, D.L. and SENIOR, T.B.A., "*Wind Turbine Generator Siting Handbook*", Technical Report No.2, University of Michigan, December 1979.

[8] SPERA, D.A. and SENGUPTA, D.L., "*Equations for Estimating the Strength of TV Signals Scattered by Wind Turbines*", NASA Contractor Report 194468, May 1994.

[9] BURTON, T., SHARPE, D., JENKINS, N. and BOSSANYI, E., "*Wind Energy Handbook*", Ed. John Wiley & Sons, 2001.

[10] ETSI EN 300 744 V1.6.1, "*Digital Video Broadcasting (DVB); Framing structure, channel coding and modulation for digital terrestrial television*", 2008.

[11] DE LA VEGA, D. *et al.*, "*Use of the channel impulse response of the DVB-T Service for the Evaluation of the Reflected Signals of Wind Farms*" I²MTC 2008 – IEEE International Instrumentation and Measurement Technology Conference, May 2008.

[12] Australian Broadcasting Authority, "*Digital Terrestrial Television Broadcasting Planning Handbook – Including Technical And General Assumptions*", April 2002 (ISBN 0 642 27064 3).

[13] I. Angulo *et al.*, "*A Measurement-based Multipath Channel Model for Signal Propagation in Presence of Wind Farms in the UHF Band*", IEEE Transactions on Communications, accepted for publication

[14] I. Angulo, D. de la Vega, *et al.*, "*Analysis of the mast contribution to the scattering pattern of wind turbines in the UHF band*", Proceedings of the 5th European Conference on Antennas and Propagation (EUCAP), pp. 707-711, 11-15 April 2011

[15] K.M. Siegel, H.A. Alperin *et al.*, "*Bistatic Radar Cross Sections of Surfaces of Revolution*", Journal of Applied Physics, Vol. 26, N. 3, March 1955

[16] E. Van Lil *et al.*, "*Computations of Radar Returns of Wind Turbines*", Proceedings of the 3rd European Conference on Antennas and Propagation, EUCAP 2009, pp. S19P16:1-S19P16:5, Berlin, 23-27 March 2009

[17] I. Angulo *et al.*, "*Empirical Doppler Characterization of Signals Scattered by Wind Turbines in the UHF Band under Near Field Condition*", Intern. Journal of Antennas and Propag., vol. 2012, Article ID 252689.

[18] I. Angulo, D. de la Vega, O. Grande, N. Cau, U. Gil, Y. Wu, D. Guerra, P. Angueira, "*Empirical Evaluation of the Impact of Wind Turbines on DVB-T Reception Quality*", IEEE Transactions on Broadcasting, vol. 58, no. 1, pp. 1-9, March 2012.

[19] International Telecommunication Union, "*Multipath propagation and parameterization and its characteristics*", Recommendation ITU-R P.1407-4, 2009.